

AD-A261 481



WL-TR-92-2114

ORGANIC ELECTROLYTES FOR SODIUM  
BATTERIES



DR B VESTERGAARD

THE TECHNICAL UNIVERSITY OF DENMARK  
CHEMISTRY DEPARTMENT A  
BUILDING 207  
2800 LYNGBY DENMARK

SEP 92

FINAL REPORT FOR 04/01/90-03/31/92

APPROVED FOR PUBLIC RELEASE; DISTRIBUTION IS UNLIMITED.

93-03924



132P8

DTIC  
ELECTE  
FEB 25 1993  
E D

AERO PROPULSION AND POWER DIRECTORATE  
WRIGHT LABORATORY  
AIR FORCE MATERIEL COMMAND  
WRIGHT PATTERSON AFB OH 45433-6563


98 2 24 048


## NOTICE


When Government drawings, specifications, or other data are used for any purpose other than in connection with a definitely Government-related procurement, the United States Government incurs no responsibility or any obligation whatsoever. The fact that the government may have formulated or in any way supplied the said drawings, specifications, or other data, is not to be regarded by implication, or otherwise in any manner construed, as licensing the holder, or any other person or corporation; or as conveying any rights or permission to manufacture, use, or sell any patented invention that may in any way be related thereto.

This report is releasable to the National Technical Information Service (NTIS). At NTIS, it will be available to the general public, including foreign nations.

This technical report has been reviewed and is approved for publication.

  
DAVID M. RYAN  
Project Engineer

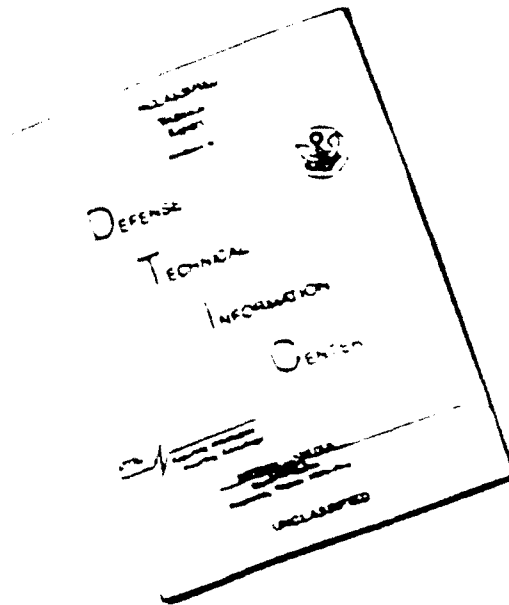
  
RICHARD A. MARSH  
Section Chief  
Battery Electrochemistry  
Power Technology Branch

  
WILLIAM U. BORGER  
Chief, Aerospace Power Division  
Aero Propulsion & Power Directorate

If your address has changed, if you wish to be removed from our mailing list, or if the addressee is no longer employed by your organization please notify WL/POOS-2, WPAFB, OH 45433-6563 to help us maintain a current mailing list.

Copies of this report should not be returned unless return is required by security considerations, contractual obligations, or notice on a specific document.

# DISCLAIMER NOTICE



THIS DOCUMENT IS BEST  
QUALITY AVAILABLE. THE COPY  
FURNISHED TO DTIC CONTAINED  
A SIGNIFICANT NUMBER OF  
PAGES WHICH DO NOT  
REPRODUCE LEGIBLY.

REPORT DOCUMENTATION PAGE			Form Approved OMB No. 0704 0188	
<small>Public reporting burden for this collection of information is estimated to average 1 hour per response, including the time for reviewing instructions, searching existing data sources, gathering and maintaining the data needed, and completing and reviewing this collection of information. Send comments regarding this burden estimate or any other aspect of this collection of information, including suggestions for reducing this burden, to Washington Headquarters Services, Directorate for Information Operations and Reports, 1215 Jefferson Davis Highway, Suite 1204, Arlington, VA 22202-4302, and to the Office of Management and Budget, Paperwork Reduction Project (0704-0188), Washington, DC 20503.</small>				
1. AGENCY USE ONLY (Leave blank)	2. REPORT DATE SEP 92	3. REPORT TYPE AND DATES COVERED FINAL 04/01/90--03/31/92		
4. TITLE AND SUBTITLE ORGANIC ELECTROLYTES FOR SODIUM BATTERIES		5. FUNDING NUMBERS C AFOSR -90- -023 PE 62203 PR 3145 TA 22 WU 33		
6. AUTHOR B VESTERGAARD				
7. PERFORMING ORGANIZATION NAME(S) AND ADDRESS(ES) THE TECHNICAL UNIVERSITY OF DENMARK CHEMISTRY DEPARTMENT A BUILDING 207 2800 LYNGBY DENMARK		8. PERFORMING ORGANIZATION REPORT NUMBER		
9. SPONSORING OR PERFORMING ORGANIZATION NAME(S) AND ADDRESS(ES) AERO-PROPULSION AND POWER DIRECTORATE WRIGHT LABORATORY AIR FORCE MATERIEL COMMAND WL/POOS, Attn: RYAN 513-2557770 WPAFB OH 45433-6563		10. SPONSORING MONITORING AGENCY REPORT NUMBER WL-TR-92-2114		
11. SUPPLEMENTARY NOTES MONITORING AGENCY: EUROPEAN OFFICE OF AEROSPACE RESEARCH AND DEVELOPMENT PSC 802 BOX 14 FPO AE 09499-0200				
12a. <del>CLASSIFIED</del> FOR PUBLIC RELEASE; DISTRIBUTION IS UNLIMITED.			12b. DISTRIBUTION CODE	
13. ABSTRACT (Maximum 200 words)  The preparation of several triazolium chloride derivatives has been performed. This includes 1-ethyl-4-methyl-1,2,4-triazolium chloride (1e4m124tcl), 1,4-dimethyl-1,2,4-triazolium chloride (14dm124tcl), 1,2-dimethyl-1,2,3-triazolium chloride (12dm123tcl), 1-methyl-3-paramethoxy-benzyl-1,2,3-triazolium chloride (1m3pmb123tcl). Other nitrogen containing ring systems like 1,2-dimethyl-pyrazolium chloride (12dmpcl), 3-methyl-thiazolium chloride (3mtzcl) and 1-methyl-3-ethyl-imidazolium chloride (MEICl) have also been synthesized. Finally, an attempt to prepare 1,4-dimethyl-tetrazolium chloride (14dmtcl) has been done with partly success. Along with the preparation procedures for the above mentioned chloride salts, we also report the recrystallization procedures and the melting point or decomposition temperature for the salts. Addition of AlCl <sub>3</sub> to the organic chloride salts above have been performed and the reactions are reported. The conductivity of 14dm124tcl:AlCl <sub>3</sub> and the 1m3pmb123tcl:AlCl <sub>3</sub> are given and compared with the MEICl:AlCl <sub>3</sub> system. Conductivities of the pure salts of the MEICl, 14dm124tcl, 1e4m124tcl and 3mtzcl are also given. Voltammograms of small amounts (< 3 mole %) of 14dm124tcl in NaCl:AlCl <sub>3</sub> melts at 160-170°C have been performed and indicated that 14dm124tcl acted as a reversible anode in these or similar melts. AC-impedance measurements of sodium in basic MEICl:AlCl <sub>3</sub> melts have been done and the results are reported, together with AC-impedance measurements of Neosepta <sup>®</sup> an- or cation exchange membranes. Battery experiments with Na/Nasicon/FeCl <sub>3</sub> :MEICl:AlCl <sub>3</sub> /Mo have shown a reduction of Fe <sup>3+</sup> to Fe <sup>2+</sup> by the electrolyte. A 100% utilization of the remaining 2/3 of the capacity was possible.				
14. SUBJECT TERMS SODIUM; PASSIVATION OF SODIUM IN ROOM TEMPERATURE MEICl:AlCl <sub>3</sub> MELTS. CONDUCTIVITY OF 1,4-DIMETHYL-1,2,4- TRIAZOLIUM CHLORIDE:AlCl <sub>3</sub> MELTS.			15. NUMBER OF PAGES 133	
			16. PRICE CODE	
17. SECURITY CLASSIFICATION OF REPORT UNCLASSIFIED	18. SECURITY CLASSIFICATION OF THIS PAGE UNCLASSIFIED	19. SECURITY CLASSIFICATION OF ABSTRACT UNCLASSIFIED	20. LIMITATION OF ABSTRACT UL	

## Table of contents.

page

Table of contents .....	iii
List of Tables .....	v
List of Figures .....	vi
List of Formula Structures, formula names and abbreviations ..	ix
List of chemicals .....	x
1.0 Introduction .....	1
1.1 MEICl:AlCl <sub>3</sub> .....	2
1.2 MOPAC .....	2
1.3 Batteries .....	3
2.0 Experimental .....	6
2.1 Preparation of trimethyloxonium tetrafluoroborate .....	6
2.2 Standardization of NaOH .....	8
2.3 Preparation of 1-ethyl-4-methyl-1,2,4-triazolium chloride and 1,4-dimethyl-1,2,4-triazolium chloride ...	8
2.3.1 Preparation of 1,2,4-triazole sodium salt .....	8
2.3.2 Preparation of 1-ethyl (or methyl)-1,2,4-triazole ..	9
2.3.3 Preparation of 1-ethyl-4-methyl-1,2,4-triazolium tetrafluoroborate .....	11
2.3.4 Ion exchange of BF <sub>4</sub> <sup>-</sup> with Cl <sup>-</sup> .....	11
2.4 Preparation of 1,2-dimethyl-1,2,3-triazolium chloride .	12
2.4.1 Preparation of 2-methyl-1,2,3-triazolium-1-oxid ....	13
2.4.2 Preparation of 2-methyl-1,2,3-triazole .....	15
2.4.3 Preparation of 1,2-dimethyl-1,2,3-triazolium tetrafluoroborate .....	15
2.4.4 Anion exchange of BF <sub>4</sub> <sup>-</sup> with Cl <sup>-</sup> .....	16
2.5 Preparation of 1,2-dimethyl-pyrazolium chloride .....	16
2.5.1 Deprotonation of pyrazole .....	16
2.5.2 Methylation of the pyrazolium anion.....	17
2.5.3 Quaternization of the 1-methyl-pyrazole .....	17
2.5.4 Anion exchange of BF <sub>4</sub> <sup>-</sup> with Cl <sup>-</sup> .....	17
2.6 Preparation of 1-methyl-3-paramethoxybenzyl-1,2,3- triazolium chloride .....	18
2.6.1 Preparation of paramethoxybenzyl-1,2,3-triazole ....	18
2.6.2 Quaternization of 1-pmb-1,2,3-triazole .....	20
2.6.3 Anion exchange of the tosylate ion with Cl <sup>-</sup> .....	20
2.7 Preparation of 3-methyl-thiazolium chloride .....	20
2.7.1 Preparation of the 1,3-thiazole .....	21
2.7.2 Alkylation of the thiazole ring .....	22
2.8 Preparation of 1-methyl-3-ethyl-imidazolium chloride ..	23
2.9 Preparation of 1,4-dimethyl-tetrazolium chloride .....	23
2.10 Other experimental techniques .....	25
3.0 Results and discussion .....	30
3.1 Stability of the organic compounds .....	30
3.2 Reactivity with aluminum chloride .....	33
3.3 Conductivity measurements .....	36
3.3.1 MEICl:AlCl <sub>3</sub> .....	36

# Table of contents.

	page
3.3.2 1-methyl-3-paramethoxybenzyl-1,2,3-triazolium chloride-AlCl <sub>3</sub> .....	37
3.3.3 1,4-dimethyl-1,2,4-triazolium chloride-AlCl <sub>3</sub> .....	38
3.3.4 Specific conductivity of the pure salts .....	42
3.4 Voltammetric investigations of 14dm124tcl .....	44
3.5 Test Batteries .....	51
3.5.1 Separators .....	51
3.5.2 Special test cells. Nasicon .....	52
3.5.2.1 Neosepta <sup>R</sup> membrane .....	54
3.5.2.2 AC-impedance measurements .....	56
3.5.2.2.1 Conclusion .....	62
3.5.2.3 Na/MEICl:AlCl <sub>3</sub> /Na .....	63
3.5.2.3.1 Reactions between sodium and MEICl:AlCl <sub>3</sub> ....	68
3.5.2.3.2 Conclusion .....	68
3.5.3 Unsuccessful test cells .....	71
3.5.3.1 Na/Nasicon/MEICl:AlCl <sub>3</sub> /Ni <sub>3</sub> S <sub>2</sub> and Na/Beta"-alumina/MEICl:AlCl <sub>3</sub> /Ni -.....	71
3.5.3.2 Na/Nasicon/FeCl <sub>3</sub> :1m3pmb123tcl:AlCl <sub>3</sub> /Mo .....	72
3.5.3.3 Na/FeCl <sub>3</sub> :MEICl:AlCl <sub>3</sub> /C-felt/W .....	73
3.5.3.3.1 Conclusion .....	75
3.5.3.4 Na/CuCl <sub>2</sub> :MEICl:AlCl <sub>3</sub> /Stainless steel mesh (NaCu-1) and Na/MEICl:AlCl <sub>3</sub> /CuS (NaCuS-1) .....	76
3.5.3.4.1 Conclusion .....	79
3.5.3.5 Na/MEICl:AlCl <sub>3</sub> /FeS .....	81
3.5.3.5.1 Conclusion .....	82
3.5.3.6 Na/MEICl:AlCl <sub>3</sub> /V <sub>2</sub> O <sub>5</sub> .....	82
3.5.3.7 Na/MEICl:AlCl <sub>3</sub> /Al (NaAl-3) .....	83
3.5.3.7.1 Conclusion .....	84
3.5.3.8 Al/MEICl:AlCl <sub>3</sub> /FeS (FeS-38) .....	86
3.5.3.8.1 Conclusion .....	87
3.5.3.9 Al/NaCl:MEICl:AlCl <sub>3</sub> /TiS <sub>2</sub> (TiS-1) .....	88
3.5.4 Partly successful test cells .....	89
3.5.4.1 Na/Nasicon/MEICl:AlCl <sub>3</sub> /Al .....	89
3.5.4.1.1 Conclusion .....	89
3.5.4.2 Na/Nasicon/FeCl <sub>3</sub> :MEICl:AlCl <sub>3</sub> /Mo or stainless steel (NaFe-13 & NaFe-14) .....	95
3.5.4.2.1 Na/Nasicon/FeCl <sub>3</sub> :MEICl:AlCl <sub>3</sub> /Mo .....	96
3.5.4.2.2 Na/Nasicon/FeCl <sub>3</sub> :MEICl:AlCl <sub>3</sub> /W .....	98
3.5.4.2.3 Na/Nasicon/FeCl <sub>3</sub> :MEICl:AlCl <sub>3</sub> /Mo or s. steel (NaFe-19, NaFe-20) .....	100
3.5.4.2.4 Na/Nasicon/FeCl <sub>3</sub> :MEICl:AlCl <sub>3</sub> /stainl. steel , flat cell design, NaFe-23) .....	106
3.5.4.2.5 Conclusion .....	108
3.5.4.2.6 Appendix A, NaFe-19 & NaFe-20 .....	111
4.0 Conclusion .....	114
5.0 References .....	115

### List of Tables.

Vapor pressures of gasses at certain temperatures.	2.3.2.1
MOPAC Calculations for some selected organic cations.	3.1.1
Reactions between organic salt/aluminum chloride.	3.2.1
The MEICl:AlCl <sub>3</sub> system.	3.3.1.1
Least-Squares-Fitted Parameters for specific conductivities of 1-m-3-pmb-1,2,3-tCl:AlCl <sub>3</sub> according to (equation 3.3.2.1) with $t_0 = 80^\circ\text{C}$ .	3.3.2.1
Specific conductivity of 1,4-dimethyl-1,2,4-triazolium chloride:AlCl <sub>3</sub> .	3.3.3.1
Least-Squares-Fitted Parameters for Specific Conductivities of 1,4-dimethyl-1,2,4-triazolium chloride:AlCl <sub>3</sub> according to (equation 3.3.2.1) with $t_0 = 80^\circ\text{C}$ .	3.3.3.2
Overall cell resistance in the Na/Nasicon/NaCl:MEICl:AlCl <sub>3</sub> /Nasicon/Na cell at $125^\circ\text{C}$ with different compositions of the electrolyte.	3.5.2.1
Estimated conductivities of Neosepta <sup>R</sup> membranes.	3.5.2.2.1
Overall cell resistance in the Na/MEICl:AlCl <sub>3</sub> /Na cell at room temperature.	3.5.2.3.1
Sodium behavior towards MEICl:AlCl <sub>3</sub> melts.	3.5.2.3.1.1
Standard potential of copper couples in AlCl <sub>3</sub> :BuPyCl melts versus aluminum in acidic 2:1 (molar) AlCl <sub>3</sub> BuPyCl melt.	3.5.3.4.1
Na/Nasicon/MEICl:AlCl <sub>3</sub> /Al (NaAl-1) voltage and resistance after different discharge currents.	3.5.4.1.1
Overall cell resistance in the NaAl-1 cell at $125^\circ\text{C}$ .	3.5.4.1.2
Charge/discharge performance of the Na/Nasicon/MEICl:AlCl <sub>3</sub> /Al (NaAl-2) cell at $125^\circ\text{C}$ .	3.5.4.1.3
Na/Nasicon/MEICl:AlCl <sub>3</sub> :FeCl <sub>3</sub> /Mo (NaFe-13). Voltage and resistance vs. discharge (1 mA) and different charge currents.	3.5.4.2.1.1
Charge needed to reach 5.0V during a $0.5\text{mA}/\text{cm}^2$ charging process for NaFe-19 and NaFe-20.	3.5.4.2.3.1
Voltages during discharge/charge for NaFe-23.	3.5.4.2.4.1
Overview of the total resistance in NaFe-19 and NaFe-23 immediately after discharge.	3.5.4.2.5.1
Cell resistance and Na/FeCl <sub>2</sub> plateau in the NaFe-19 cell.	3.5.4.2.5.2

## List of Figures.

Typical discharge/charge curves for the Al/MEtCl:AlCl <sub>3</sub> :FeCl <sub>3</sub> /RVC system in an acidic methyl-ethyl-imidazolium:aluminum chloride room temperature melt.	1.3.1
Idealized open circuit voltage plateaus of Na/beta-alumina/NaAlCl <sub>4</sub> /FeCl <sub>2</sub> (Fe-matrix) at 250°C compared with the Na/beta-alumina/NaAlCl <sub>4</sub> /NiCl <sub>2</sub> (Fe-matrix) system.	1.3.2
Condensing of dimethyl ether.	2.1.1
Set-up for preparation of trimethyloxonium tetrafluoroborate	2.1.2
Preparation of 1,2,4-triazole sodium salt.	2.3.1.1
Preparation of 1-ethyl-1,2,4-triazole.	2.3.2.1
Preparation of 1-ethyl-4-methyl-1,2,4-triazolium tetrafluoroborate	2.3.3.1
Preparation of 1-ethyl-4-methyl-1,2,4-triazolium chloride.	2.3.4.1
2-methyl-1,2,3-triazolium-1-oxid.	2.4.1.1
2-methyl-1,2,3-triazole.	2.4.2.1
Schematic overview of reactions involved in preparation of paramethoxybenzylazide.	2.6.1.1
Conversion of paramethoxybenzylazide into 1-paramethoxybenzyl(pmb)-1,2,3-triazole.	2.6.1.2
Schematic diagram of preparation of 3-methyl-thiazolium chloride.	2.7.1.1
Formation of 1-methyl-3-ethyl-imidazolium chloride	2.8.1
3-compartment Pyrex cell.	2.10.1
Flat cell design.	2.10.2
Witeq battery cell design for Na/Nasicon tube batteries.	2.10.3
Conductivity of 1-m-3-pmb-1,2,3-tcl:AlCl <sub>3</sub> (X <sub>AlCl<sub>3</sub></sub> = 0.55).	3.3.2.1
Specific conductivity of 1,4-dimethyl-1,2,4-triazolium chloride:AlCl <sub>3</sub> .	3.3.3.1
Specific conductivity of 14dm124tcl:AlCl <sub>3</sub> (X <sub>AlCl<sub>3</sub></sub> = 0.50) vs. temperature.	3.3.3.2
Specific conductivity of 1-methyl-3-ethyl-imidazolium chloride vs. temperature.	3.3.4.1
Specific conductivity of 3-methyl-thiazolium chloride vs. temperature.	3.3.4.2
Specific conductivity of 1,4-dimethyl-1,2,4-triazolium chloride vs. temperature.	3.3.4.3
Specific conductivity of 1-ethyl-4-methyl-1,2,4-triazolium chloride vs. temperature.	3.3.4.4
CV with working tungsten electrode at 169°C(NaCl:AlCl <sub>3</sub> :14dm124tcl).	3.4.1
CV with working tungsten electrode at 169°C(NaCl:AlCl <sub>3</sub> :14dm124tcl).	3.4.2
CV with working tungsten electrode at 169°C(NaCl:AlCl <sub>3</sub> :14dm124tcl).	3.4.3
CV with working tungsten electrode at 165°C(NaCl:AlCl <sub>3</sub> :14dm124tcl).	3.4.4
CV with working tungsten electrode at 170°C(NaCl:AlCl <sub>3</sub> :14dm124tcl).	3.4.5
Working tungsten electrode at different temperatures (NaCl:AlCl <sub>3</sub> :14dm124tcl).	3.4.6
CV with working tungsten (W) or aluminum (Al) electrode at 165°C (NaCl:AlCl <sub>3</sub> :14dm124tcl).	3.4.7
General formula of Neosepta <sup>R</sup> cation (hydrogen) exchange membranes.	3.5.1
Charge/discharge vs. electrolyte composition and current for the Na/Nasicon/NaCl:MEtCl:AlCl <sub>3</sub> /Nasicon/Na cell at 125°C.	3.5.2.1



## List of Figures.

Metal housing for the NaK cell in the argon glove box.	3.5.2.1.1
Charge/discharge of the NaK/CMX/NaK cell (NaK-1).	3.5.2.1.2
The AC-impedance cell design.	3.5.2.2.1
AC-impedance measurements for the dry CMX cation membrane.	3.5.2.2.2
AC-impedance measurements of the ACS anion membrane in a basic MEICl:AlCl <sub>3</sub> (X <sub>AlCl<sub>3</sub></sub> =0.41) melt.	3.5.2.2.3
AC-impedance measurements of the ACS anion membrane in a basic MEICl:AlCl <sub>3</sub> (X <sub>AlCl<sub>3</sub></sub> =0.41) melt.	3.5.2.2.4
AC-impedance measurements of the AMH anion membrane in a basic MEICl:AlCl <sub>3</sub> (X <sub>AlCl<sub>3</sub></sub> =0.41) melt.	3.5.2.2.5
AC-impedance measurements of the AMH anion membrane in a basic MEICl:AlCl <sub>3</sub> (X <sub>AlCl<sub>3</sub></sub> =0.41) melt.	3.5.2.2.6
Glass beaker cell design for AC-impedance measurements.	3.5.2.3.1
AC-impedance measurements of Na/MEICl:AlCl <sub>3</sub> /Na in a basic MEICl:AlCl <sub>3</sub> (X <sub>AlCl<sub>3</sub></sub> =0.41) melt.	3.5.2.3.2
AC-impedance measurements of Na/MEICl:AlCl <sub>3</sub> /Na in a basic MEICl:AlCl <sub>3</sub> (X <sub>AlCl<sub>3</sub></sub> =0.41) melt.	3.5.2.3.3
AC-impedance measurements of Na/MEICl:AlCl <sub>3</sub> /Na in a basic MEICl:AlCl <sub>3</sub> (X <sub>AlCl<sub>3</sub></sub> =0.41) melt.	3.5.2.3.4
AC-impedance measurements of Na/MEICl:AlCl <sub>3</sub> /Na in a basic MEICl:AlCl <sub>3</sub> (X <sub>AlCl<sub>3</sub></sub> =0.41) melt.	3.5.2.3.5
Set-up for impedance measurements.	3.5.2.3.6
Charge/discharge in the Na/MEICl:AlCl <sub>3</sub> /Na cell with a basic MEICl:AlCl <sub>3</sub> (X <sub>AlCl<sub>3</sub></sub> =0.41) melt.	3.5.2.3.7
Voltage vs. current in the Na/MEICl:AlCl <sub>3</sub> /Na cell with a basic MEICl:AlCl <sub>3</sub> (X <sub>AlCl<sub>3</sub></sub> =0.41) melt.	3.5.2.3.8
Self discharge of the NaFeC-2 cell, showing that at least three equilibrium constants are involved in the discharge mechanism.	3.5.3.3.1
Accelerated charge curve for the NaFeC-2 cell.	3.5.3.3.2
Charge/self discharge curve for NaCuS-1 at room temperature.	3.5.3.4.1
Charge/self discharge curve for NaFeS-22 at room temperature.	3.5.3.5.1
Charge curve for NaAl-3 at room temperature.	3.5.3.7.1
Voltage/charge current for the NaAl-3 battery at room temperature.	3.5.3.7.2
OCV of the Al/MEICl:AlCl <sub>3</sub> /FeS cell discharged with 0.020 and 0.015 mA/cm <sup>2</sup> cathodic current densities.	3.5.3.8.1
OCV of the Al/NaCl:MEICl:AlCl <sub>3</sub> /TiS <sub>2</sub> cell discharged with 0.001 and 0.01 mA/cm <sup>2</sup> cathodic current densities.	3.5.3.9.1
Discharge of the Na/Nasicon/MEICl:AlCl <sub>3</sub> /Al (NaAl-1) cell.	3.5.4.1.1
Voltage vs. current in the Na/Nasicon/MEICl:AlCl <sub>3</sub> /Nasicon/Na (NaAl-1) cell with a acidic MEICl:AlCl <sub>3</sub> (X <sub>AlCl<sub>3</sub></sub> =0.60) melt.	3.5.4.1.2

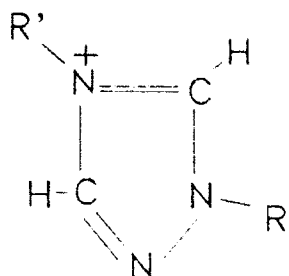
# List of Figures.

Charge/discharge (2 mA) performance of cycle 10 for the Na/Nasicon/MEICl:AlCl <sub>3</sub> /Al (iNaAl-2) cell at 125°C.	3.5.4.1.3
Discharge of Na/Nasicon/MEICl:AlCl <sub>3</sub> :FeCl <sub>3</sub> /Mo (NaFe-13) at 125°C.	3.5.4.2.1.1
Discharge of Na/Nasicon/MEICl:AlCl <sub>3</sub> :FeCl <sub>3</sub> /Mo (NaFe-17) at 125°C.	3.5.4.2.2.1
Second discharge/charge cycle for NaFe-19 & NaFe-20 cells at 125°C.	3.5.4.2.3.1
Third discharge/charge cycle for NaFe-19 & NaFe-20 at 125°C.	3.5.4.2.3.2
Fourth discharge/charge cycle for NaFe-19 & NaFe-20 at 125°C.	3.5.4.2.3.3
OCV curves for NaFe-19 and NaFe-20 (steel) after cycles 4.	3.5.4.2.3.4
Voltage oscillation of the NaFe-19 cell during charge in cycle 3.	3.5.4.2.3.5
Discharge/charge cycles for NaFe-23 at 125°C.	3.5.4.2.4.1
Voltage vs. current of the Na/Nasicon/FeCl <sub>3</sub> :MEICl:AlCl <sub>3</sub> /Mo (NaFe-19) cell. Cycle no. 2 at the Na/FeCl <sub>2</sub> plateau.	3.5.4.2.5.1

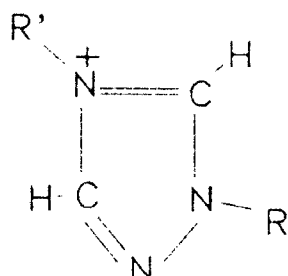
Accession For	
NTIS CRA&I	<input checked="" type="checkbox"/>
DTIC TAB	<input checked="" type="checkbox"/>
Unannounced	<input type="checkbox"/>
Justification .....	
By .....	
Distribution /	
Availability Codes	
Dist	Avail and/or Special
A-1	

TO QUALITY INSPECTOR

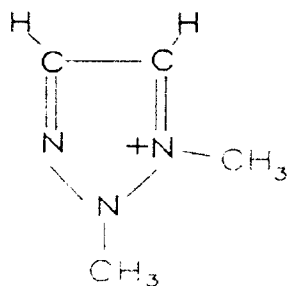
Formula cation structures, formula names and formula salt abbreviations utilized in this report.



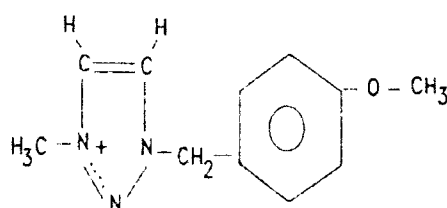
R,R' = Methyl.  
1,4-dimethyl-1,2,4-triazolium cation.  
(14dm124tcl).



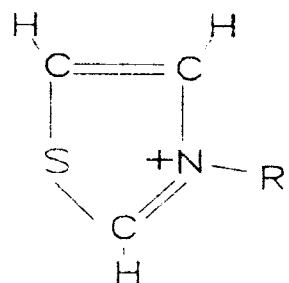
R = Ethyl, R' = Methyl.  
1-ethyl-4-methyl-1,2,4-triazolium cation.  
(1e4m124tcl).



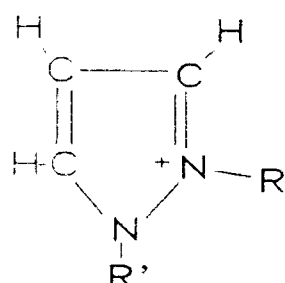
1,2-dimethyl-1,2,3-triazolium cation.  
(12dm123tcl).



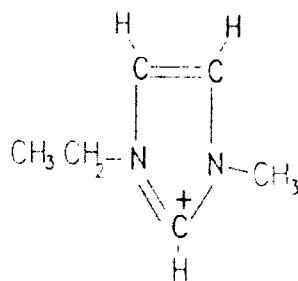
1-methyl-3-(4-methoxybenzyl)-1,2,3-triazolium cation.  
(1m3pmb123tcl).



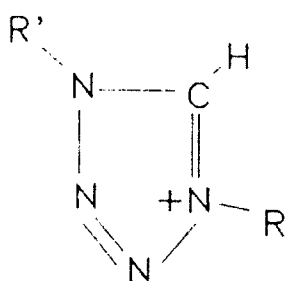
R = Methyl.  
3-methyl-thiazolium cation.  
(3mtzcl)



R,R' = Methyl.  
1,2-dimethyl-pyrazolium cation.  
(12dmpcl)



1-methyl-3-ethyl-imidazolium cation.  
(MEICl).



R,R' = Methyl.  
1,4-dimethyl-tetrazolium cation.  
(14dmtecl).

# List of Chemicals.

<u>Chemical structure/name</u>	<u>molar weight</u>	<u>Chemical company, purity</u>
CH <sub>3</sub> CN (acetonitrile)	41.05	Merck, liChrosolv <sup>®</sup> , 99.8 %
C <sub>4</sub> H <sub>2</sub> O <sub>4</sub> (acetylenedicarboxylic acid)	114.06	Fluka, 99 %
Al (aluminum)	26.98	, 99.99 %
CH <sub>3</sub> OC <sub>6</sub> H <sub>4</sub> CHO (anisaldehyde)	136.15	DTH, Organic Institute.
NH <sub>3</sub> (ammonia anhydrous)	17.03	Dansk ilt og brint.
NH <sub>4</sub> Cl (ammonium chloride)	53.49	Merck, 99.8 %
H <sub>3</sub> NCS <sub>2</sub> NH <sub>3</sub> (ammonium dithiocarbonate)	110.19	DTH, CDA.
HN <sub>4</sub> CNH <sub>2</sub> ·H <sub>2</sub> O (5-aminotetrazole mono hydrate)	103.08	DTH, CDA.
BaO (barium oxide anhydrous)	153.34	BDH, nr. 279523N.
BF <sub>3</sub> ·O(C <sub>2</sub> H <sub>5</sub> ) <sub>2</sub> (boron trifluoride etherate)	141.93	Aldrich, nr. 32018-8.
CS <sub>2</sub> (carbon disulfide)	76.14	Merck, 99.9 %
CH <sub>2</sub> ClCHO (chloroacetaldehyde)	78.50	Aldrich, 50 % aqueous sol.
C <sub>2</sub> H <sub>5</sub> Cl (chloroethane)	64.52	Aldrich, 99.7 %
CuCl <sub>2</sub> ·2H <sub>2</sub> O (Cupric chloride)	170.47	Heraeus, 99 %
CuSO <sub>4</sub> ·5H <sub>2</sub> O (cupric sulfate pentahydrate)	249.68	BDH, A.R.
CuS (Cupric sulfide)	95.61	, 99.9 %
CH <sub>2</sub> Cl <sub>2</sub> (dichloromethane)	84.93	DTH, Organic Institute.
NH <sub>2</sub> :(NH) <sub>2</sub> NHCN (dicyandiamide)	84.08	Riedel-de-Häen, 99 %
(HOCH <sub>2</sub> CH <sub>2</sub> ) <sub>2</sub> O (diethylene glycol)	106.12	DTH, Organic Institute.
(CH <sub>3</sub> CH <sub>2</sub> ) <sub>2</sub> O (diethylether)	74.12	DTH, Organic Institute.
(CH <sub>3</sub> ) <sub>2</sub> O (dimethyl ether)	46.07	DTH, Organic Institute.
HCON(CH <sub>3</sub> ) <sub>2</sub> (dimethyl formamide)	73.10	Riedel-de-Häen, 99 %
(CH <sub>3</sub> O) <sub>2</sub> SO <sub>2</sub> (dimethyl sulfate)	126.13	Fluka.
C <sub>3</sub> H <sub>5</sub> ClO (epichlorohydrine, 1-chlor-2,3-epoxypropane)	92.53	DTH, Organic Institute.
CH <sub>3</sub> CH <sub>2</sub> OH (ethanol)	46.07	DTH, (99 % or 96 %).
CH <sub>3</sub> COOC <sub>2</sub> H <sub>5</sub> (ethyl acetate)	88.11	Merck, z.a.
CH <sub>3</sub> CH <sub>2</sub> I (ethyl iodide)	155.97	Sigma, nr. 14259.
1-e-4-m-1,2,4-triazolium-BF <sub>4</sub> (C <sub>5</sub> N <sub>3</sub> H <sub>10</sub> BF <sub>4</sub> )	198.96	DTH, CLA
1-e-4-m-1,2,4-triazolium-Cl(C <sub>5</sub> N <sub>3</sub> H <sub>10</sub> Cl)	147.61	DTH, CDA.
1-ethyl-1,2,4-triazole (C <sub>4</sub> N <sub>3</sub> H <sub>7</sub> )	97.12	DTH, CDA
4-ethyl-1,2,4-triazole (C <sub>4</sub> N <sub>3</sub> H <sub>7</sub> )	97.12	DTH, CDA
FeCl <sub>3</sub> ·6H <sub>2</sub> O (iron trichloride)	270.30	Merck, 99.8 %
FeS (iron sulfide)	87.91	, 99.9 %
HCHO (formaldehyde)	30.03	Fluka.
C <sub>2</sub> H <sub>2</sub> O <sub>2</sub> (glyoxal)	58.04	Fluka.
HCl (hydrochloric acid anhydrous)	36.46	Merck, 37 % w/w.
NH <sub>2</sub> OH·HCl (hydroxylamine hydrochloride)	69.49	Sigma, 99 %
H <sub>3</sub> PO <sub>2</sub> (hypophosphorous acid)	66.00	Aldrich, 50 % w/w sol.
MgSO <sub>4</sub> (magnesium sulfate anhydrous)	120.36	Fluka, 99 %
CH <sub>3</sub> OH (methanol)	32.04	BP Chemicals AB, 99.9 %
NH <sub>2</sub> CS <sub>2</sub> CH <sub>3</sub> (methyl dithiocarbamate)	107.19	DTH, CDA.
CH <sub>3</sub> NNNH <sub>2</sub> (methylhydrazine)	46.07	Aldrich, 98 %
C <sub>4</sub> N <sub>2</sub> H <sub>6</sub> (1-methyl-imidazole)	82.11	Aldrich, 99 %
CH <sub>3</sub> I (methyl iodide)	141.94	Aldrich, 99 %
(CH <sub>3</sub> ) <sub>2</sub> N <sub>4</sub> CH-Cl (1-m-4-m-tetrazolium-chloride)	134.57	DTH, CDA.
(CH <sub>3</sub> ) <sub>2</sub> N <sub>4</sub> CH-BF <sub>4</sub> (1-m-4-m-tetrazolium-tetrafluoroborate)	185.92	DTH, CDA.
1-m-2-m-1,2,3-triazolium-BF <sub>4</sub> (C <sub>4</sub> N <sub>3</sub> H <sub>8</sub> BF <sub>4</sub> )	184.93	DTH, CDA.
1-m-2-m-1,2,3-triazolium-Cl(C <sub>4</sub> N <sub>3</sub> H <sub>8</sub> Cl)	133.58	DTH, CDA.
1-m-4-m-1,2,4-triazolium-Cl(C <sub>4</sub> N <sub>3</sub> H <sub>8</sub> Cl)	133.58	DTH, CDA.
1-m-4-m-1,2,4-triazolium-BF <sub>4</sub> (C <sub>4</sub> N <sub>3</sub> H <sub>8</sub> BF <sub>4</sub> )	184.93	DTH, CDA.
1-m-3-pmb-1,2,3-t-tosylate (CH <sub>3</sub> C <sub>2</sub> H <sub>2</sub> N <sub>3</sub> CH <sub>2</sub> C <sub>6</sub> H <sub>4</sub> OCH <sub>3</sub> )	375.44	DTH, CDA.
SO <sub>3</sub> C <sub>6</sub> H <sub>4</sub> CH <sub>3</sub>		
C <sub>3</sub> N <sub>2</sub> CH <sub>6</sub> (methyl-pyrazole)	82.11	DTH, CDA.

<u>Chemical structure/name</u>	<u>molar weight</u>	<u>Chemical company, purity</u>
$\text{HN}_4\text{CH}_3$ (1-methyl-tetrazole)	84.08	DTH, CDA.
$\text{CH}_3\text{C}_6\text{H}_4\text{SO}_2\text{OCH}_3$ (methyl 4-toluensulfonate)	186.23	DTH, Organic Institute.
2-methyl-1,2,3-triazole ( $\text{C}_3\text{N}_3\text{H}_5$ )	83.09	DTH, CDA.
1-methyl-1,2,4-triazole ( $\text{C}_3\text{N}_3\text{H}_5$ )	83.09	DTH, CDA.
2-methyl-1,2,3-triazolium-1-oxid ( $\text{C}_3\text{N}_3\text{H}_5\text{O}$ )	99.09	DTH, CDA.
Mo (Molybdenum)	95.94	Buch & Holm, 99%.
$\text{N}_2$ (nitrogen)	28.01	Dansk ilt og brint.
$\text{CH}_3\text{NO}_2$ (nitromethane)	61.04	Fischer Scient. Comp. 99.9%.
$\text{CH}_3\text{OC}_6\text{H}_4\text{CH}_2\text{OH}$ (paramethoxybenzyl alcohol)	138.17	DTH, CDA.
$\text{CH}_3\text{OC}_6\text{H}_4\text{CH}_2\text{N}_3$ (paramethoxybenzylazide)	163.18	DTH, CDA.
$\text{CH}_3\text{OC}_6\text{H}_4\text{CH}_2\text{Cl}$ (paramethoxybenzyl chloride)	156.61	DTH, CDA.
$\text{CH}_3\text{OC}_6\text{H}_4\text{C}_2\text{N}_3\text{H}_2$ (paramethoxybenzyl-1,2,3-triazole)	175.19	DTH, CDA.
$\text{P}_2\text{O}_5$ (phosphorus pentaoxide)	141.94	Ferak, rein.
$\text{PCl}_3$ (phosphorus trichloride)	137.33	DTH, Organic Institute.
$\text{K}_2\text{CO}_3$ (potassium carbonate anhydrous)	138.21	Merck, 99%.
KCl (potassium chloride)	74.55	Riedel-de-Häen, 99.5%
$\text{KHC}_8\text{H}_4\text{O}_4$ (potassium hydrogen phthalate)	204.22	Merck, z.s.
KOH (potassium hydroxide)	56.11	Merck, z.s.
$\text{C}_6\text{H}_5\text{C}_3\text{H}_7$ (propylbenzene)	120.20	DTH, Organic Institute.
$\text{C}_3\text{N}_2\text{H}_4$ (pyrazole)	68.08	Aldrich, 98%
$\text{C}_3\text{N}_2\text{H}_3\text{Na}$ (pyrazole sodium salt)	90.06	DTH, CDA.
$\text{C}_5\text{H}_5\text{N}$ (pyridine)	79.10	Aldrich, 99%, A.C.S.
Na (sodium)	22.99	Merck, 99.98%.
$\text{NaN}_3$ (sodiumazide)	65.01	Merck, 99%, z.s.
$\text{Na}_2\text{CO}_3$ (sodium carbonate)	105.99	Merck, 99.5%, z.s.
NaCl (sodium chloride)	58.44	Merck, 99.5%.
NaOH (sodium hydroxide)	40.00	DTH (33%).
$\text{NaNO}_2$ (sodium nitrite)	69.00	Riedel-de-Häen.
$\text{H}_2\text{SO}_4$ (sulfuric acid)	98.07	DTH, Organic Institute.
$\text{C}_4\text{H}_8\text{O}$ (tetrahydrofuran, THF)	72.11	Ferak, 99%
$\text{HN}_4\text{CH}$ (tetrazole)	70.05	DTH, CDA.
$\text{NaN}_4\text{CH}$ (tetrazole sodium salt)	92.04	DTH, CDA.
1,2,4-triazole ( $\text{C}_2\text{N}_3\text{H}_3$ )	69.07	Alfa, 98%.
1,2,4-triazole sodium salt ( $\text{C}_2\text{N}_3\text{H}_2\text{Na}$ )	91.05	DTH, Organic Institute.
$(\text{CH}_3)_3\text{OBF}_4$ (trimethyloxonium-BF <sub>4</sub> )	147.91	DTH, Organic Institute.

DTH: The Technical University of Denmark.

Dansk ilt og brint: Danish company for production of pure gasses.

CDA: Chemical Department A.

e: Ethyl group.

m: Methyl group.

pmb: Paramethoxybenzyl.

t: Triazolium.

This final report for the project "Organic Electrolytes for Sodium Batteries" contains a summary of earlier given status reports in connection with the project.

The aim of the investigations was to develop new room temperature molten salts electrolytes mainly with radical substituted heterocyclic organic chlorides (see p. 8) mixed with aluminum chloride.

The new electrolytes should have an ionic conductivity comparable with  $\text{MEICl}:\text{AlCl}_3$  or better.

A computer model program MOPAC (Molecular Orbital Package) (ref. 1, 2) was to be included to calculate theoretically reduction potentials for a variety of organic cations (ref. 3). Furthermore, MOPAC could be utilized to predict the electron densities, and then give a prediction of the stability of the organic cation.

It has been shown by Osteryoung and Gale (ref. 4) that the organic cation 1-butyl-pyridinium ( $\text{C}_4\text{H}_9\text{C}_5\text{H}_5\text{N}$ ) in basic melts (molar fraction of  $\text{AlCl}_3$  less than 0.5,  $X_{\text{AlCl}_3} < 0.5$ ) spontaneously was reduced by elemental (metallic) aluminum. Unsaturated double bonds contiguous to the hetero atom in heterocyclic compounds are more reactive than those in the benzene ring and they are usually the easiest to reduce, because attack is taking place at positions of low electron density (ref. 5).

Deposition/stripping of aluminum in basic  $\text{MEICl}:\text{AlCl}_3$  would realize a significant voltage gain of 1.4 V compared to aluminum in acidic melts (ref. 6). Unfortunately, the reduction of the organic  $\text{MEI}^+$  cation takes place before the deposition of aluminum in basic  $\text{MEICl}:\text{AlCl}_3$  melts. By voltammetry, we hoped to find an enhanced electrochemical window for some of the new organic compounds.

Finally, sodium was to be tested as suitable anode for room temperature molten salts batteries. Eventually aluminum or other suitable anode materials could be utilized. Impedance measurements were included to determine the stability of sodium in the organic melts. The stability has visually been demonstrated earlier (ref. 7, 8).

## 1.1

### MEICl:AlCl<sub>3</sub>.

Ionic liquids formed by mixing 1-methyl-3-ethyl-imidazolium chloride with AlCl<sub>3</sub> are of interest as electrolytes for batteries, because these liquids are nonaqueous media with relatively high conductance at and below room temperature (ref. 9, 10, 11, 12). Furthermore these melts can be utilized as solvents for studying ionic complexes and also may serve as catalytic solvents for Friedel-Crafts reactions (ref. 13, 14). Stripping and deposition of aluminum occur reversibly in acidic melts. The rates of deposition can be high (25 mA/cm<sup>2</sup>) and the efficiency > 99% (ref. 15). In basic melts only oxidation of aluminum has been noted to occur, and Wilkes et al. (ref 6, 16) have shown that the reduction of aluminum was not promoted by elevated temperatures (up to 181°C), nor by utilizing mixed haloaluminates of AlCl<sub>3</sub>/AlBr<sub>3</sub>, nor by introduction of LiCl, BF<sub>3</sub> or MgCl<sub>2</sub> to the basic MEICl:AlCl<sub>3</sub> melts. The reduction of the methyl-ethyl-imidazolium cation was observed at a potential about 0.8 V cathodic of that at which the aluminum oxidation in the melt occurred. By the reduction of the organic cation an orange color is formed in the melt (ref. 17, 18).

## 1.2

### MOPAC.

Computational chemistry can be divided into 3 major categories: molecular mechanism, semiempirical, ab initio/Gaussian methods. Macromolecules are best studied by molecular mechanism and electronic properties of small molecules are most accurately calculated using ab initio methods. In between lie the semiempirical methods, of which MNDO (Modified Neglect of Diatomic Overlap) (ref. 19), MINDO/3 (Modified INDO) (ref. 20) and AM1 (Austin Model 1) (ref. 21), are the most popular (ref. 2) (INDO:Intermediate Neglect of Differential Overlap (ref. 22)).

In reference 2, J.J.P. Stewart has given an excellent description of MOPAC: 'MOPAC is a general-purpose, semiempirical molecular orbital program for study of chemical reactions involving molecules, ions, and linear polymers'. By the help of MOPAC it should be possible to calculate many chemical quantities, i.e.:

atomic charge, dipole moments, electron density, entropy, heat capacity, heat of formation, ionization potentials, molecular geometries, unit cell lengths, vibrational frequencies etc. (ref. 2).

LUMO (Lowest Unoccupied Molecule Orbital) energies were utilized to calculate the reduction potentials of the organic cations.

### 1.3 Batteries.

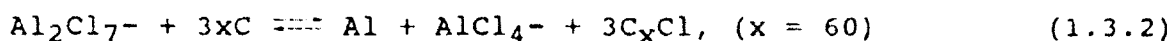
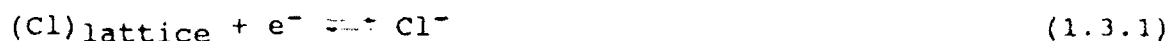
Al/melt/FeS<sub>2</sub> batteries have been investigated with NaCl:AlCl<sub>3</sub> melts at 170-250°C with a considerable capacity decline of 0.1-1.0 % per cycle due to the dissolution of the FeS<sub>2</sub> into the electrolyte. The solubility of FeS<sub>2</sub> in the electrolyte increases considerably with temperature (ref. 23). It is therefore desirable to operate at lower temperatures. Takomi and Koura (ref. 23) found that the Al/melt/FeS<sub>2</sub> system with an 2:1 AlCl<sub>3</sub>:BPC (butyl-pyridinium-chloride) melt, should be operated between 100 and 150°C, because below 100°C a considerable polarization on the positive FeS<sub>2</sub> electrode takes place. The performance of the BPC cells was not as good (even at 170°C) as for the Al/NaCl:AlCl<sub>3</sub>/FeS<sub>2</sub> basic system, probably because the conductivity of the organic-inorganic electrolyte was lower than for the common inorganic NaCl:AlCl<sub>3</sub> basic melt (ref. 23). The conductivity of the organic melt could be improved by adding MCl (M= Na, Li) to the electrolyte, and it could be shown that basic melts (below 50 mole % AlCl<sub>3</sub>) had a larger capacity and a higher cell voltage than the acidic melts. By working with basic cells having 9-17 mole% BPC and various compositions of AlCl<sub>3</sub>:MCl, Takomi and Koura have shown that the AlCl<sub>3</sub>:MCl:BPC electrolyte is superior to the common AlCl<sub>3</sub>:BPC for use in Al/melt/FeS<sub>2</sub> batteries. The Open Circuit Voltages (OCV) for the cells were around 1.5-1.6V (100-150°C).

Al/melt, Cl<sub>2</sub>/Carbon cells with different organic/inorganic mixtures have been investigated by P.R. Gifford and J.B. Palmisano (ref. 24) in an acidic (1.5:1) AlCl<sub>3</sub>:1,2-dimethyl-3-propylimidazolium chloride melt. The positive electrode was graphite, which acts as an intercalation electrode for the dissolved chlorine gas, thus avoiding the need for a separator. However, some self discharge was observed, and



after several weeks the unloaded cell capacity has declined to slightly over 50 % of the theoretical discharge amount. The average discharge voltage for current densities of 1-10 mA/(g graphite) was 1.7 V at room temperature, and the average chlorine:graphite ratio was 1:60 (C<sub>60</sub>Cl) at that temperature.

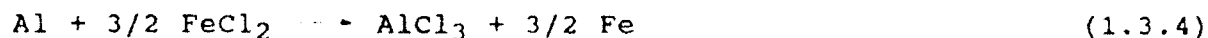
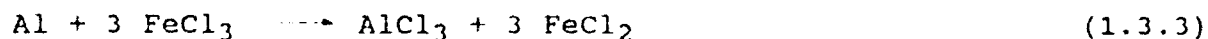
The proposed cell reactions are (equation 1.3.2 being the overall reaction) :



Studies of Fe(II) and Fe(III) in an AlCl<sub>3</sub>:BPC room temperature electrolytes have been done by Osteryoung et al. (ref. 25) and by Hussey et al. (ref. 26).

They have found that the Fe(II)-Fe(III) electron transfer process becomes irreversible in acidic melts, but the process is reversible in the basic melt. The equilibrium potential increased with the acidity of the melt. Hussey et al. (ref. 26) found that acidic melts were slightly unstable towards Fe(III) and were oxidized with a maximum rate of 0.5 mole Fe(III)/hour (50°C), while the basic melt was completely stable towards Fe(III).

Al/melt, FeCl<sub>3</sub>/RVC batteries with MEICl:AlCl<sub>3</sub> melts have been investigated by Donahue et al. (ref. 18, 27). The overall electrochemical process is described below, and the calculated standard cell voltage of reaction 1.3.3 and 1.3.4 was 1.85 V and 0.75 V, respectively (ref. 18, 27):



The OCV of a Al/melt, FeCl<sub>3</sub>/RVC room temperature cell in a 'common' (not specified) acidic electrolyte was measured to be 1.9 V, which is slightly higher than the calculated value (ref. 18).

Typical discharge (5 mA = 1.25 mA/cm<sup>2</sup> cathodic) and charge (2.5 mA = 0.65 mA/cm<sup>2</sup> cathodic) curves are shown in Figure 1.3.1. It was found that the Al anode was surrounded by Fe flakes after discharge.

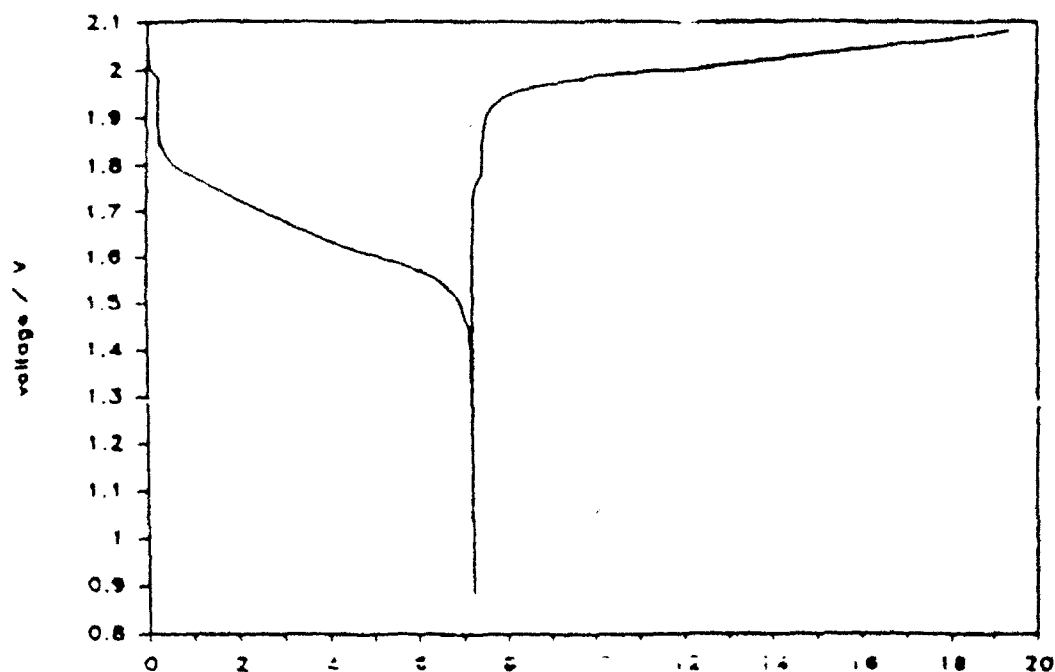


Figure 1.3.1.

Typical discharge/charge curves for the Al/MEICl:AlCl<sub>3</sub>:FeCl<sub>3</sub>/RVC system in an acidic methyl-ethyl-imidazolium:aluminum chloride room temperature melt. (ref. 18).

It was found that the positive reactants (FeCl<sub>3</sub>, CuCl<sub>2</sub>) was almost insoluble in acidic melts, but very soluble in basic melts. In order to avoid self discharge in the basic electrolytes the melts were saturated with the positive reactants (ref. 18).

Na/separator/melt/FeCl<sub>2</sub>(Fe-matrix) 'ZEBRA' cells have been extensively studied by Bones et al. (ref. 28, 29, 30) with beta-alumina as a separator, basic NaAlCl<sub>4</sub> as the electrolyte and the working temperature around 250°C. The idealized open circuit voltage plateaus for those cells are illustrated in Figure 1.3.2.

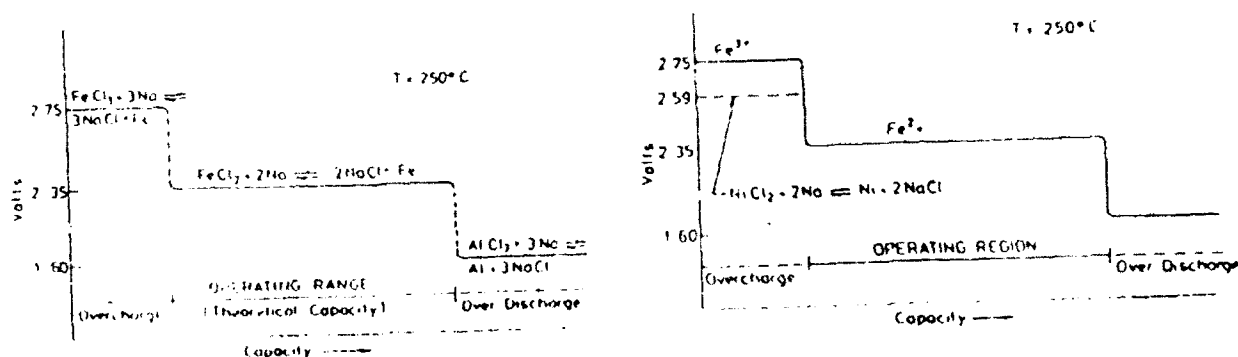


Figure 1.3.2.

Idealized open circuit voltage plateaus of Na/beta-alumina/NaAlCl<sub>4</sub>/FeCl<sub>2</sub>(Fe-matrix) at 250°C compared with the Na/beta-alumina/NaAlCl<sub>4</sub>/NiCl<sub>2</sub>(Fe-matrix) system (ref. 28).

It was not desirable to overcharge the cells and then reach the  $\text{Fe}^{3+}$  plateau, because the cell resistance increased due to poisoning of the beta-alumina ceramic by the soluble  $\text{Fe}^{3+}$  ion. In contrast the  $\text{FeCl}_2$  was insoluble in the NaCl saturated  $\text{NaAlCl}_4$  electrolyte (ref. 30).

During the charge/discharge operations from Fe to  $\text{FeCl}_2$  in a basic  $\text{NaAlCl}_4$ , an intermediate sodium-iron-chloride structure  $\text{Na}_6\text{FeCl}_8$  is formed. This intermediate phase appeared after 25% of charge and was seen by a 0.012 V change in the plateaus. However, in acidic melts it is unlikely that there should be any intermediate plateaus.

## 2.0 Experimental.

Chapter 2.1 to 2.9 contains the organic preparation procedures while chapter 2.10 contains other experimental techniques.

### 2.1 Preparation of trimethyloxonium tetrafluoroborate. (ref. 31).

Dimethyl ether (360 mL) was condensed in a 500 mL round bottom flask with a reflux cooler and a  $\text{P}_2\text{O}_5$  drying tube (see Figure 2.1.1). The round bottom and the reflux aggregate was cooled with dry ice ( $\text{CO}_2$ ) and isopropyl alcohol.

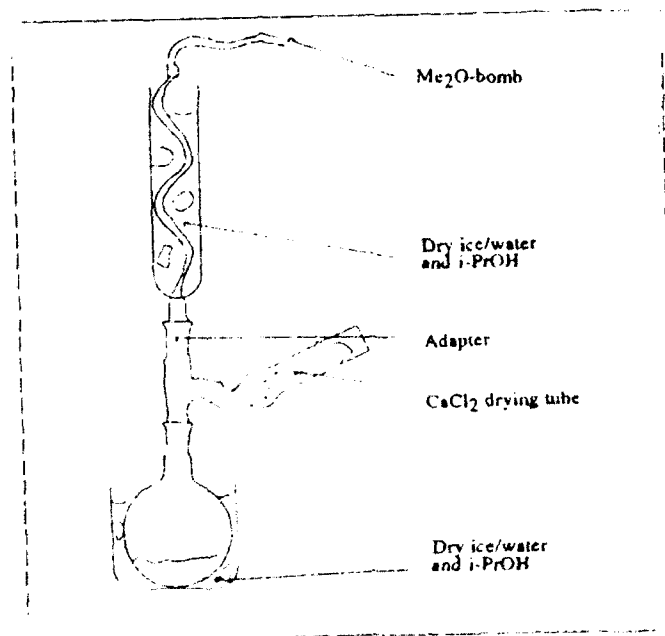
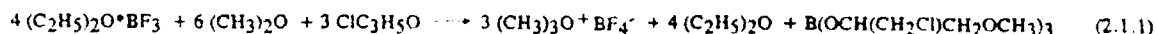


Figure 2.1.1.  
Condensing of dimethyl ether.  
(ref. 32).

To a 2 L three necked round bottom flask with reflux aggregate and mechanical stirring was added 290 mL  $\text{CH}_2\text{Cl}_2$  and 163 mL (1.32 mole) boron trifluoride etherate ( $\text{BF}_3 \cdot \text{O}(\text{C}_2\text{H}_5)_2$ ) (Fw 141.93, mp - 58°C, bp 126°C).

The cooled dimethyl ether (360 mL) was distilled through a hose to the three necked round bottom. When all dimethyl ether has been added the hose was replaced with a dropping funnel with a pressure equalizing connection. 115 mL (1.46 mole) epichlorohydrin ( $\text{C}_3\text{H}_5\text{ClO}$ ) was added in a period of 30 minutes with vigorous stirring and reflux (see Figure 2.1.2).

After further 3 h, the stirring was stopped and the solvent was removed utilizing a filter-stick. Washing was done with 2-400 mL  $\text{CH}_2\text{Cl}_2$ , addition of dry diethyl ether (400 mL) and then transferred to a 500 mL round bottom flask. The ether was removed utilizing a filter-stick and the remanence was dried at 0.1 mmHg. The expected reaction is given in equation 2.1.1 (ref. 31):



Yield 73% (142 g) trimethyloxonium tetrafluoroborate, white crystals, m.p. not measured, (ref. 31: 180°C decomposition). Brown crystals were obtained when the product was exposed to water, and boron acid was formed.

Storage: Cool dry room (-23°C) or ampule.

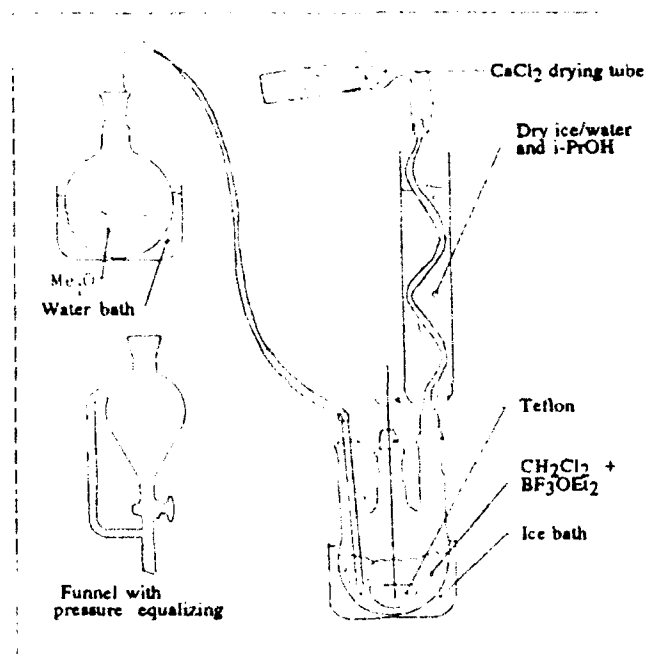


Figure 2.1.2.

Set-up for preparation of trimethyloxonium tetrafluoroborate.

## 2.2

### Standardization of NaOH (ref. 33).

Potassium Hydrogen Phthalate ( $\text{KHC}_8\text{H}_4\text{O}_4$ ) is a nonhygroscopic crystalline solid useful for standardization of bases with phenolphthalein as indicator (colorless - red). 50 mL concentrated NaOH was filled into a 500 mL volumetric flask and diluted to the mark with deionized water. 3.3697 g KHP was weighed into a conical flask and dissolved in 150 mL deionized water. 4 drops of phenolphthalein was added and the solution was titrated with the diluted NaOH solution utilizing a 25 mL buret.

## 2.3

### Preparation of 1-ethyl-4-methyl-1,2,4-triazolium chloride and 1,4-dimethyl-1,2,4-triazolium chloride.

The preparation took place in 4 steps as outlined below.

#### 2.3.1 Preparation of 1,2,4-triazole sodium salt (ref. 34, 35).

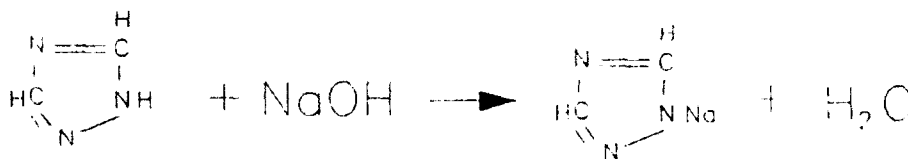


Figure 2.3.1.1

Preparation of 1,2,4-triazole sodium salt.

A standard 30 % (w/w) NaOH titrated solution was weighed into a round bottom flask with stopper. An equivalent amount of 1,2,4-triazole was added.

The mixture was heated (heating container, 110-120°C) and refluxed until a water clear homogeneous solution was reached (approx. 30 minutes). Cooling (white precipitate), and removing of the water took place by vacuum rotary evaporation (approx. 1-2 mmHg) firstly at room temperature and then at 70°C until a dry-looking cake was formed. Finally, the temperature was increased to 200°C (oil bath), still under the 1-2 mmHg vacuum (2-3 hours). Nitrogen was added and the vacuum pump was stopped. Then, by cooling a white precipitate of triazole sodium salt was obtained. Yield close to 100%.

### 2.3.2 Preparation of 1-ethyl (or methyl)-1,2,4-triazole.

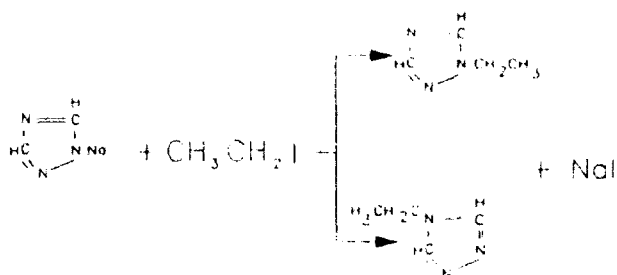


Figure 2.3.2.1.

Preparation of 1-ethyl-1,2,4-triazole.

\* Utilize  $\text{CH}_3\text{I}$  instead of  $\text{C}_2\text{H}_5\text{I}$  for the dimethyl synthesis.

Utilizing a round bottom flask, the triazole sodium salt was dissolved in acetonitrile (4.3 mL  $\text{CH}_3\text{CN}$  / 10 millimole triazole sodium salt). Stirring was done for 20-30 minutes and then it was cooled to approx.  $-25^\circ\text{C}$  (Acetone/dry ice bath). An equivalent amount of ethyl iodide (preferently through a rubber septum using an accurate syringe) was added and the round bottom was closed by a rubber stopper!

The bottom was left with stirring until room temperature was reached (the dry ice has melted). Then the solution was heated (with stopper) to  $80^\circ\text{C}$  for 3 hours\*.

After cooling to room temperature the acetonitrile was vacuum evaporated and a precipitate of NaI and 1-ethyl-triazole/4-ethyl-triazole was obtained. By adding dichloromethane (5 to 6 times the volume of solid) NaI was kept precipitated and the triazole product was dissolved. NaI was removed by filtration and was washed with  $\text{CH}_2\text{Cl}_2$ .  $\text{CH}_2\text{Cl}_2$  was removed by vacuum evaporation, and the final solution was yellow and viscous.

The final solution with the triazole product was vacuum distilled while stirring:

1-ethyl-1,2,4-triazole ( $65-67^\circ\text{C}$ , 10 mmHg), ( $77-79^\circ\text{C}$ , 22 mmHg).

(1-methyl-1,2,4-triazole ( $63-64^\circ\text{C}$ , 15 mmHg) ).

\* Due to the closed system the stopper was in between shortly removed.

The distilled solution was water clear. The remanence was brownish due to NaI and 4-ethyl-1,2,4-triazole.

Note:

A better procedure could be to do the preparations in a sealed Pyrex ampule instead.

The vapor pressure of ethyl iodide at 80°C will be approx. 1 atmosphere (see Table 2.3.2.1). The medium wall Pyrex ampules ( $\phi_{outer} = 30$  mm,  $\phi_{inner} = 24$  mm, height = 18-20 mm) should be able to stand for at least 12 atmospheres internal working pressure (ref. 36).

The vapor pressure for the ethyl iodide is of course lower than for ethyl chloride, and we have successfully used ethyl chloride in sealed Pyrex ampules at 80°C when making 1-methyl-3-ethyl-imidazolium chloride (see chapter 2.8, preparation of MEICl).

The vapor pressure for the acetonitrile is even lower than for the ethyl iodide.

Table 2.3.2.1.

Vapor pressures of gasses at certain temperatures (ref. 37).

mmHg	10	40	100	400	760
	°C	°C	°C	°C	°C
CH <sub>3</sub> F	- 131.6	- 119.1	- 109.0	- 89.5	----
CH <sub>3</sub> Cl	- 92.4	- 76.0	- 63.0	- 38.0	- 24.0
CH <sub>3</sub> Br	- 72.8	- 54.2	- 39.4	- 11.9	3.6
CH <sub>3</sub> I	- 45.8	- 24.2	- 7.0	25.3	42.4
C <sub>2</sub> H <sub>5</sub> F	- 97.7	- 81.8	- 69.3	- 45.3	- 32.0
C <sub>2</sub> H <sub>5</sub> Cl	- 65.8	- 47.0	- 32.0	- 3.9	12.3
C <sub>2</sub> H <sub>5</sub> Br	- 47.5	- 26.7	- 10.0	21.0	38.4
C <sub>2</sub> H <sub>5</sub> I	- 24.3	- 0.9	18.0	52.3	72.4
CH <sub>3</sub> CN	- 16.3	7.7	27.0	62.5	81.8
CH <sub>2</sub> Cl <sub>2</sub>	- 43.3	- 22.3	- 6.3	24.1	40.7
CH <sub>3</sub> NO <sub>2</sub>	2.8	27.5	46.6	82.0	101.2

### 2.3.3 Preparation of 1-ethyl-4-methyl-1,2,4-triazoliumtetrafluoroborate.

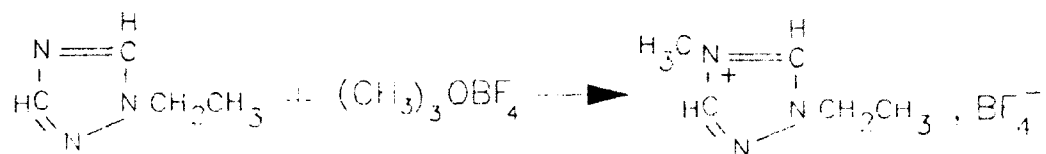


Figure 2.3.3.1.

Preparation of 1-ethyl-4-methyl-1,2,4-triazolium tetrafluoroborate.

1-ethyl-1,2,4-triazole was dissolved in nitromethane (200 mL/mole triazole) in a conical flask while stirring. An equivalent trimethylsilyloxoniumtetrafluoroborate was added quickly in small amounts. The reaction time was 2 hours under constant stirring and at room temperature.

By adding diethylether (4 times the volume of nitromethane), 1-ethyl-4-methyl-1,2,4-triazoliumtetrafluoroborate was precipitated, most often as an oil. The ether was decanted, and the oil was washed 2-3 times with ether. (The precipitate was white crystals in case of the 1-methyl-4-methyl-1,2,4-triazoliumtetrafluoroborate preparation). It was difficult to precipitate the 1-ethyl-4-methyl-triazoliumtetrafluoroborate, and the preparation was continued with the water clear oil. Excess of ether was removed by vacuum evaporation.

### 2.3.4 Ion exchange of $\text{BF}_4^-$ with $\text{Cl}^-$ .

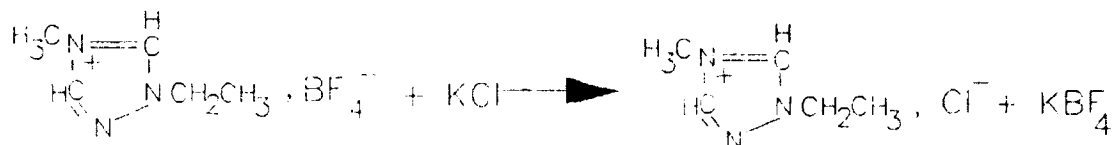


Figure 2.3.4.1.

Preparation of 1-ethyl-4-methyl-1,2,4-triazolium chloride.

1-ethyl-4-methyl-triazoliumtetrafluoroborate was dissolved in boiling water (1 g utilized 0.5-0.8 ml water). By adding an equivalent



amount of a 5M KCl solution and then cooling with an ice bath,  $\text{KBF}_4$  was precipitated (very viscous) and removed by filtration (washing with cold water). The filtrate was vacuum evaporated at  $60^\circ\text{C}$  (water pump, 10-12 mmHg). The compound was dissolved in boiling dry ethanol (approx. 40 ml ethanol/mole compound) and the solution was hot filtered to remove any traces of  $\text{KBF}_4$ . The ethanol was vacuum evaporated at  $40-50^\circ\text{C}$  (water pump, 10-12 mmHg). Water was removed as an azeotrope with ethanol when dissolving 1 g of compound in 10 ml dry ethanol. The mixture was concentrated under vacuum. This procedure was repeated 3-4 times. The precipitate was now white crystals.

Recrystallization of the compound was done by dissolving in dry ethanol and recrystallization by addition of dry diethylether. The crystals were quite hygroscopic after the remaining ether was vacuum evaporated.

Storage: Covered (preventing light) sealed Pyrex ampules.

Melting points:

1-ethyl-4-methyl-1,2,4-triazolium chloride :  $85-90^\circ\text{C}$

1,4-dimethyl-1,2,4-triazolium chloride :  $103-104^\circ\text{C}$

#### 2.4 Preparations of 1,2-dimethyl-1,2,3-triazolium chloride.

(ref. 38, 39, 40).

The main preparative steps was:

2-methyl-1,2,3-triazolium-1-oxid  $\longrightarrow$  2-methyl-1,2,3-triazole  $\longrightarrow$   
1,2-dimethyl-1,2,3-triazolium tetrafluoroborate  $\longrightarrow$  1,2-dimethyl-  
1,2,3-triazolium chloride.

## 2.4.1

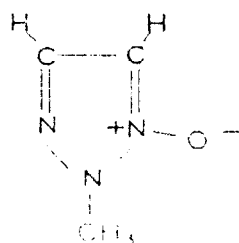
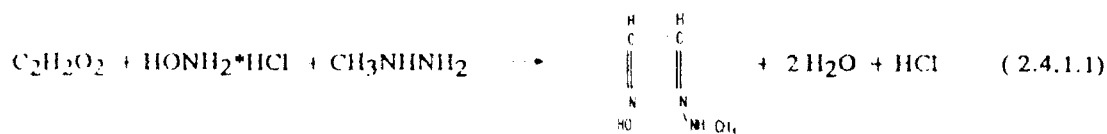
Preparation of 2-methyl-1,2,3-triazolium-1-oxid.

Figure 2.4.1.1

2-methyl-1,2,3-triazolium-1-oxid.

Hydroxylamine hydrochloride ( $\text{NH}_2\text{OH}\cdot\text{HCl}$ ) (52.2 g, 0.75 mole) was well ground with a little molar excess of sodium carbonate ( $\text{Na}_2\text{CO}_3$ ) (83.5 g, 0.75 mole). A mixture of an equal molar amount of glyoxal (40 % solution, 85.5 mL) ( $\text{C}_2\text{H}_2\text{O}_2$ ), corresponding to the hydroxylamine hydrochloride, and distilled water (275 mL) was made. During only 30 s the mixture was added into the 2 L conical flask. The amount of distilled water was approximately 3 times the amount of the glyoxal solution. While stirring, an equal molar amount of methylhydrazine (39.3 mL, 0.75 mole) mixed with methanol (60.7 mL) (the volume of methanol was 1.5 times the volume of methylhydrazine) was quickly introduced (10-15 seconds after the rate of  $\text{CO}_2$  evolution has decreased). Note that a high rate of  $\text{CO}_2$  evolution was seen at these steps (i.e. the 2 L flask size prevents the solution from slopping). While stirring for 30 minutes, methanol (2·100 mL) was used to wash the walls of the conical flask. The reaction forming the monooxime is written below:



The solution was now slightly yellow.

Sodium carbonate was utilized due to the very pH sensitive reaction.

The formation of the triazolium-1-oxid ring from the monooxime by oxidation was made with  $\text{CuSO}_4$  as additive. The procedure is mentioned in Finley's chemical abstract review book (ref. 41).

A light yellow mixture of cupric sulfate pentahydrate (500 g,  $\text{CuSO}_4 \cdot 5\text{H}_2\text{O}$ ), pyridine (500 mL,  $\text{C}_5\text{H}_5\text{N}$ ) and distilled water (300 mL) was dripped slowly to the solution while stirring vigoursly. A moderate reflux was obtained, due to heat evolution. After addition of the cupro solution the reflux and stirring was continued (30 minutes), utilizing a heating container to keep on the reflux. While still stirring the mixture was cooled with a water/ice bath and sulfuric acid (180 ml 96%  $\text{H}_2\text{SO}_4$ ) was added slowly. Introduction of concentrated  $\text{H}_2\text{SO}_4$  has been shown to give a more pure product (ref. 42). In this case a brownish compound was obtained, and it was filtered on a Büchner funnel with Hyflo Super Cel<sup>R</sup>\* (a kind of kieselguhr) as an additive agent to remove small particles of suspended matter. The water phase of the mother liquid was then continuously extracted with dichloromethane (500 mL  $\text{CH}_2\text{Cl}_2$ ) for 16 hours. The  $\text{CH}_2\text{Cl}_2$  phase was washed with 2 M NaOH (1.50 mL, 5.25 mL) and an almost colorless water phase was obtained. Every alkaline phase was washed again with  $\text{CH}_2\text{Cl}_2$  (2.25 mL). All the  $\text{CH}_2\text{Cl}_2$  phases was collected and dried with  $\text{MgSO}_4$ , filtered and rotary evaporated at room temperature.

The solid was recrystallized: Dissolved in absolute alcohol, treated with activated carbon, filtered and rotary evaporated again. Yield 39 g (52 %) of 2-methyl-1,2,3-triazolium-1-oxide (white crystals). Melting point 81.5-83°C.

It was observed that it is very important to use fresh glyoxal solutions, otherwise we obtained colored products and very low yields.

Hyflo Super Cel<sup>R</sup> : Produced by Johns-Manville, and can be bought by Fluka.

#### 2.4.2

#### Preparation of 2-methyl-1,2,3-triazole.

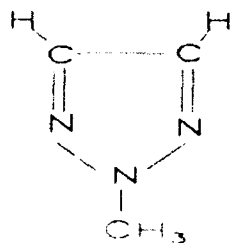


Figure 2.4.2.1.  
2-methyl-1,2,3-triazole.

Deoxygenation of the triazolium-oxid was done by  $\text{PCl}_3$  as described by Begtrup et al. (ref. 43, 44), and to control the exothermic process dichloromethane was utilized as solvent.

Phosphorus trichloride (65 mL, 0.74 mole) was slowly dripped (approx. 2 mL/min) through a funnel into a solution of 2-methyl-1,2,3-triazolium-1-oxid (31 g) and dichloromethane (30 mL). During the addition of  $\text{PCl}_3$  a constant reflux in the reaction flask was kept. The reflux was continued for one more hour utilizing a heating container. After cooling in water/ice bath we obtained a dark yellow-brown solution. To hydrolyse the solution (excess of  $\text{PCl}_3$  and  $\text{POCl}_3$ ), it was added to a covered glass beaker with ice/water (500 g). The temperature of the ice/water was kept below  $5^\circ\text{C}$ , being continuously stirred. Care must be taken, because the hydrolysis is a very exothermic reaction (ref. 42). After 1 hour, the water phase was extracted with  $\text{CH}_2\text{Cl}_2$  (5·100 mL). The dichloromethane phases was collected, dried with  $\text{MgSO}_4$  and filtered. The dichloromethane solution was distilled through a 30 cm packed and water cooled column ( $40^\circ\text{C}/760$  mmHg). Then propylbenzene (100 mL) was added (bp.  $157\text{--}159^\circ\text{C}$ ) and 2-methyl-1,2,3-triazole was evaporated ( $90\text{--}100^\circ\text{C}$ ). Yield 20.3 g (78 %, 0.24 mole). By adding the propylbenzene, we obtained a higher yield than without addition.

#### 2.4.3

#### Preparation of 1,2-dimethyl-1,2,3-triazolium tetrafluoroborate.

The 2-methyl-1,2,3-triazole (20.3 g) was dissolved in dry nitromethane (52 mL) and while stirring the addition of trimethylloxonium tetrafluoroborate (36.1 g, 0.24 mole) in small portions was performed. After stirring for 2 hours we had a colorless/milky solution. By addition of diethyl ether (220 mL) colorless crystals

were obtained, which were washed with diethyl ether (2.50 mL). The crystals were dried for 4 days over  $P_2O_5$  at 2 mmHg vacuum. Yield 41.1 g (91%).

2.4.4 Anion exchange of  $BF_4^-$  with  $Cl^-$ .  
(See also 2.3.4).

The 1,2-dimethyl-1,2,3-triazolium-tetrafluoroborate (41.1 g, 0.22 mole) was dissolved in boiling water (100 mL), and then cooled to room temperature. Addition of a KCl solution (0.22 mole, 16.6 g KCl, 40 mL water) and then cooling to  $<0^\circ C$  with ice/water/salt resulted in an exchange of  $BF_4^-$  with  $Cl^-$ . The solution was filtered, rotary evaporated and dissolved in boiling absolute alcohol (200 mL, azeotropic distillation). After a hot filter procedure, the remanence was cooled to  $0^\circ C$  and vacuum filtered. The remanence from this procedure was rotary evaporated, cooled and filtered again.

Totally, the crystals were recrystallized 3 times in absolute alcohol and finally dried for 2 days at 5 mmHg over  $P_2O_5$  as a drying agent.

Yield: 18.6 g (63 %), mp.  $191-193^\circ C$ .

In other experiments yields of 91.2 % with a melting point of  $219-220^\circ C$  has been reported (ref. 40), but the 1,2-dimethyl-1,2,3-triazolium chloride is probably not stable (presumable light sensitive).

2.5 Preparation of 1,2-dimethyl-pyrazolium chloride.

The preparation was done in 4 steps as seen below:

- 1) Deprotonation of the pyrazole.
- 2) Methylation of the pyrazolium anion (1-methyl-pyrazole).
- 3) Methylation of the 2.<sup>nd</sup> nitrogen atom (quaternization)  
(1,2-dimethyl-pyrazolium tetrafluoroborate).
- 4) Anion exchange of  $BF_4^-$  with  $Cl^-$ .

2.5.1 Deprotonation of pyrazole.

Pyrazole (34 g, 0.499 mole) and 8.99 M NaOH (55.5 mL, 0.499 mole) was placed in a round bottom flask with a stopper and heated (steam bath) until a clear yellow solution appeared. After cooling the water

was rotary evaporated and the remaining solid pyrazole sodium salt was dried (0.3 mmHg, 200°C, 20 minutes). The solid was cooled and kept under nitrogen until use. The mechanism of reaction is similar to Figure 2.3.1.1.

#### 2.5.2 Methylation of the pyrazolium anion.

CH<sub>2</sub>Cl<sub>2</sub> (215 mL) was added to the flask containing the pyrazole sodium salt, and the flask was cooled (-25°C) by a methanol/dry ice bath. CH<sub>3</sub>I (31 mL) was slowly added from a separating funnel, and the solution was stirred (magnetic stirrer). After the addition, the funnel was exchanged with a stopper. The solution was left stirring for 72 hours, while the temperature slowly increased to room temperature. In this way we obtained a yellow solution with a white precipitate of NaI. The solution was extracted with CH<sub>2</sub>Cl<sub>2</sub> (3·150 mL), filtered and the CH<sub>2</sub>Cl<sub>2</sub> was evaporated. 1-methyl-pyrazole was distilled at 126-128°C. It condensed as a colorless solution immediately after distillation, but became slightly yellow when exposed to daylight. Yield 26.33 g (0.32 mole, 64%).

#### 2.5.3 Quaternization of the 1-methyl-pyrazole. (1,2-dimethyl-pyrazolium tetrafluoroborate).

The quaternization of the 1-substituted pyrazole makes the ring more positive and sensitive towards nucleophilic attacks (ref. 40).

1-methyl-pyrazole (0.47 mole, 38.6 g) was dissolved in CH<sub>2</sub>Cl<sub>2</sub> (110 mL) and then cooled (ice/water). Trimethyl-oxonium-tetrafluoroborate (70 g, 0.47 mole) was added slowly while stirring. After 1 hour of stirring diethyl ether (400 mL) was added, and white crystals precipitated. After filtering and drying the yield was 95% 82 g (82 g, 0.45 mole). Mp. 55-56°C.

#### 2.5.4 Anion exchange of BF<sub>4</sub><sup>-</sup> with Cl<sup>-</sup>.

The procedure previously described was utilized, i.e. dissolving in water, addition of KCl, recrystallization in ethanol, etc.

Yield 84% (49.8 g, 0.38 mole). Mp. decomposes at 220-230°C.

Storage in the dark due to the light sensitivity of pyrazoles.

## 2.6

### Preparation of

#### 1-methyl-3-paramethoxybenzyl-1,2,3-triazolium chloride.

(ref. 45).

The preparation were performed in 3 steps:

- 1) Preparation of paramethoxybenzyl-1,2,3-triazole.
- 2) Quaternization of 1-pmb-1,2,3-triazole.
- 3) Anion exchange of the tosylate ion with  $\text{Cl}^-$ .

#### 2.6.1 Preparation of paramethoxybenzyl-1,2,3-triazole.

By a nucleophilic addition of formaldehyde to 4-methoxybenzaldehyde (anisaldehyde) in concentrated alkaline medium (NaOH) we conducted a Cannizzaro reaction\* forming paramethoxybenzyl (pmb) alcohol.

By nucleophilic substitution in concentrated acidic (HCl) solutions we obtained the paramethoxybenzyl chloride.

Utilizing dimethyl formamide (DMF,  $\text{HCON}(\text{CH}_3)_2$ ) as the solvent, the paramethoxybenzyl chloride was reacted with sodiumazide ( $\text{NaN}_3$ ) to give paramethoxybenzylazide (see Figure 2.6.1.1).

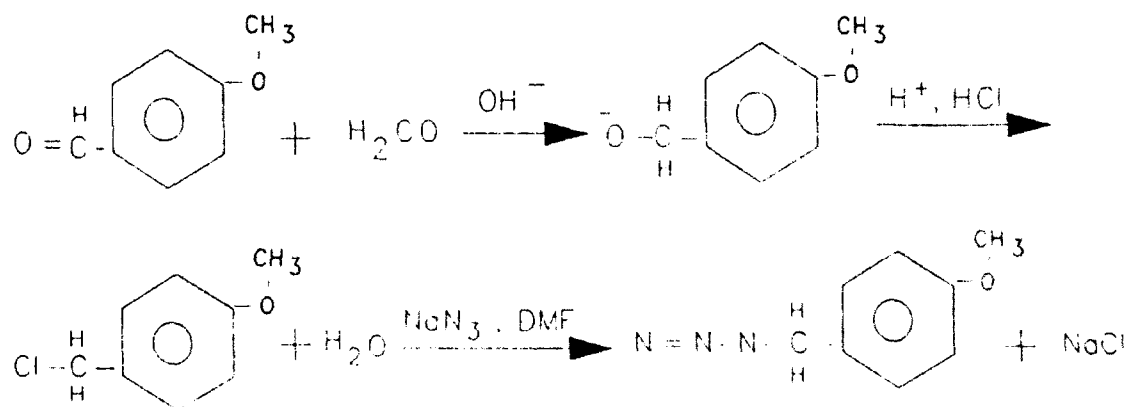


Figure 2.6.1.1

Schematic overview of reactions involved  
in preparation of paramethoxybenzylazide.

\* Cannizzaro reaction: In concentrated alkali, aldehydes containing no  $\alpha$ -hydrogens (eg. formaldehyde) undergo self-oxidation-and-reduction to give an alcohol and a salt (ref. 46).

To form rings from the 3 nitrogen atoms we utilized a 1,3 dipolar cyclic addition of acetylenedicarboxylic acid (HOCCCOOH) and then by decarboxylation we got the paramethoxybenzyl-1,2,3-triazole. This is given in Figure 2.6.1.2.

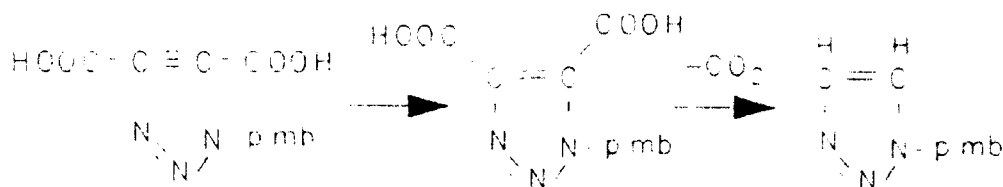


Figure 2.6.1.2  
Conversion of paramethoxybenzylazide into  
1-paramethoxybenzyl(pmb)-1,2,3-triazole.

The decarboxylation took place in diethyleneglycol with heat and reflux. 2 isomers are formed: the 1-pmb- and 2-pmb-1,2,3-triazole.

1-pmb-1,2,3-triazole-4,5-dicarboxylic acid (5 g) was dissolved in diethyleneglycol (20 mL) and heated to 200°C, with stirring and reflux. After 2 hours the solution was cooled and 1 M NaOH (20 mL) was added. Further reflux was performed, at 130-140°C for 1 hour. After cooling and addition of water (80 mL) the solution was extracted with CH<sub>2</sub>Cl<sub>2</sub> (3·15 mL). The total volume was reduced to half its value by evaporation, and it was washed/extracted with water (2·10 mL). The organic phase was dried with MgSO<sub>4</sub> and the CH<sub>2</sub>Cl<sub>2</sub> was rotary evaporated, leaving us with an yield of 70 % (2.4 g).

Recrystallization was done by boiling the crystals in diethyl ether (20 mL), then by cooling (-25°C) for at least 1 hour and lastly decanting the ether off. Repeating this procedure 3 times left us with the 1-pmb-1,2,3-triazole compound (47%, 1.6 g), mp. 92-94°C.

The 2-pmb-1,2,3-triazole was kept in the ether phase.



### 2.6.2

### Quaternization of 1-pmb-1,2,3-triazole.

Methyl-4-toluensulfonate was utilized to add a methyl group to the 1-pmb-1,2,3-triazole.

1-pmb-1,2,3-triazole (10 g) was mixed with 1.2 equivalent methyl toluenesulfonate (9.6 mL) utilizing an oil bath at 100°C and refluxing for 3 hours. We obtained a highly viscous compound (like sirup). After cooling, diethyl ether (50 mL) was added under stirring and then the ether was decanted off. After washing with diethyl ether (4·40 mL), the sirup was recrystallized in methanol (10 mL). Addition of diethyl ether (150 mL) was done to recover the salt, which was further washed with diethyl ether (4·40 mL). Yield 17.6 g of 1-methyl-3-pmb-1,2,3-triazolium tosylate (90%).

### 2.6.3

### Anion exchange of the tosylate ion with Cl<sup>-</sup>.

Amberlite IRA-400 ionexchanger<sup>R\*</sup> (700 mL) was added to a column and cleaned by elution with 2 M NaOH (1 L, 2-4 drop/second). Excess NaOH was removed with water until a neutral pH of the eluate was obtained. 2 M HCl (1 L) was dripped through the column to replace OH<sup>-</sup> with Cl<sup>-</sup>. Excess HCl was removed by water as for the NaOH case.

1-methyl-3-pmb-1,2,3-triazolium tosylate (0.05 mole) was dissolved in a little water and dripped through the column (1 drop/second). Totally the column was washed with 1.5 L of water. After rotary evaporation the yield was almost 100 %.

### 2.7

### Preparation of 3-methyl-thiazolium chloride.

(ref. 47).

The preparation took place in 2 steps:

- 1) Preparation of the 1,3-thiazole ring.
- 2) Alcylation of the thiazole ring.

\* Amberlite IRA-400: Strongly basic anion chloride exchanger - quaternary ammonium functionality, see for instance the Fluka<sup>R</sup> catalogue.

## 2.7.1

Preparation of the 1,3-thiazole.

(ref. 47, 48).

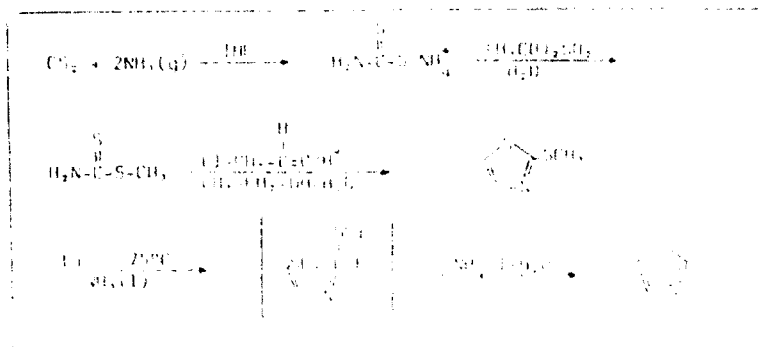


Figure 2.7.1.1

Schematic diagram of preparation of 3-methyl-thiazolium chloride.

Dry tetrahydrofuran (THF, 1500 mL) and dry  $\text{CS}_2$  (150 mL, 189 g, 2.49 mole) were mixed in a three necked conical flask.  $\text{NH}_3$  from a bomb (unknown flow) was flushed over the mixture and ammonium dithiocarbonate was formed ( $\text{H}_3\text{NCS}_2\text{NH}_3$ ). The temperature was kept between 40-45°C by cooling with ice. After 45 minutes the temperature dropped to 35°C and the ammonia flow was stopped. Excess of  $\text{NH}_3$  was evaporated by a water pump (20 minutes). By adding water (280 mL) and stirring vigorously the dithiocarbamate was dissolved, and we got 2 yellow phases. Dimethyl sulfate (282 g, 2.24 mole) was added from a funnel and the temperature was kept at 40-45°C (adjusting the speed of addition). Concentrated aqueous  $\text{NH}_3$  (40 mL) was introduced to the reaction mixture while continuously stirring for 15 minutes. The 2 phases were separated and the water phase was washed with diethyl ether (3.55 mL). The organic phases were dried at 50°C with  $\text{MgSO}_4$  and rotary evaporated. Further evaporation (to remove water, THF) was done with an oil pump (1-2 mmHg) for 12 hours. Yield 216 g (90 %) methyl dithiocarbamate.

The methyl dithiocarbamate (216 g, 2.02 mole), together with 96% ethanol (250 mL), 50 % Chloroacetaldehyde (346 g) and conc.  $\text{HCl}$  (5 mL) were added to a cooled 3 necked conical flask with thermometer and stopper. By stirring and a little heating (exothermic reaction) the temperature was brought to 80°C during a period of 45 minutes. The brownish solution was cooled to room temperature and most of the ethanol was rotary evaporated. By cooling with water/ice the temperature was kept between 0-20°C while 30 %  $\text{KOH}$  (300 mL) was added in small portions. We then obtained a yellow water phase at the top and a brownish oil at the bottom of the flask. The phases separated

slowly (over night). By extracting the water phase with dichloromethane (4.50 mL), drying with  $K_2CO_3$ , removing the dichloromethane by vacuum and finally perform a vacuum distillation ( $84^\circ C/11-13$  mmHg) we had got 149 g (58%) of 2-methylthio-1,3-thiazole. Mp.  $84^\circ C/11-13$  mmHg.

Anhydrous  $NH_3$  (600 mL) was transferred directly from a cylinder to a 3 necked conical flask (2 L). Then 52 g (0.4 mole) of 2-methylthio-1,3-thiazole, dissolved in dry ether (220 mL), was introduced. The mixture was cooled to  $-75^\circ C$  with  $N_2$  liquid, and  $N_2$  gas from a bomb was passed through the reaction flask and to the outlet. The outlet was removed and approx. 12 g (1.7 mole) of Li metal was introduced into the melt in small pieces keeping the temperature at  $-70 - -78^\circ C$ . The addition of Li was stopped when the solution became bluish (excess of lithium, i.e. stoichiometric coefficient of 4 (1.6 mole)). Powdered  $NH_4Cl$  (43 g, 0.8 mole) was added in small portions (totally, 15 minutes) and the temperature was maintained at  $-66$  to  $-73^\circ C$ . The cooling was stopped and  $NH_3$  was evaporated at 10 mmHg at room temperature, leaving a red solid. Introducing a  $10^\circ C$  solution of  $NH_4Cl$  (60 g, 300 mL) to the red solid, stirring and heating ( $30^\circ C$ ) for 45 minutes and then cooling to room temperature, left us with a brownish solution. Extracting by diethyl ether (10.50 mL), drying with  $K_2CO_3$ , evaporating the ether ( $80^\circ C$ ) from the yellow solution and finally a distillation of the 1,3-thiazole at  $115-117^\circ C$  gave a clear liquid product. Yield 19.3 g (58 %).

#### 2.7.2 Alkylation of the thiazole ring.

1,3-thiazole (47 g, 0.56 mole) was dissolved in nitromethane (121 mL) in an 1 L conical flask. The mixture was cooled to  $3^\circ C$ , and while stirring trimethyloxoniumtetrafluoroborate (83g, 0.56 mole) was added in small portions to keep the foam low (developing  $(CH_3)_2O$ ). The reaction time was 2 hours at room temperature. Introducing diethyl ether (511 mL) formed a lightbrown oil at the bottom of the conical flask. After separation of the two phases, the oil phase was washed with diethyl ether. Most of the nitromethane was evaporated with an oil pump. By NMR the remaining  $CH_3NO_2$  was determined and this resulted in a yield of 90% (94 g) of 3-methyl-thiazolium tetrafluoroborate.

By introducing KCl (37.5 g) dissolved in water (93 mL) and cooling (water/ice) white crystals of  $KBF_4$  were formed. The crystals were filtered and vacuum evaporated (oil pump, typical 1-2 mmHg) for 5 days. Yield 96 % (65.5 g). Recrystallization 2 times in nitromethane, 2 times in 96% alcohol and then washing with diethyl ether gave a 64% (43.7 g) yield of white crystals. The melting point for the 3-methyl-triazolium chloride was  $58-61^\circ C$ .

2.8 Preparation of 1-methyl-3-ethyl-imidazolium chloride.  
(ref. 15, 49, 50).

1-methyl-imidazole (Aldrich) (53 mL, 0.76 mole) was dried with BaO (5 g) and refluxed for 2 days at 220-230°C. The 1-methyl-imidazole was distilled (40-50°C) to another flask using a water vacuum pump (10 mmHg, determined by McLeod<sup>R</sup> instrument). 1-methyl-imidazole (30 mL, 0.376 mole) was introduced into a medium thick wall Pyrex ampule (3 mm) and cooled by ice/salt bath. Ethylchlorid (Aldrich) was utilized as received, transferred through a condenser (ice/salt) into a beaker (35 mL, 0.483 mole) and then introduced to the 1-methyl-imidazole. The ampule was carefully cooled by nitrogen and sealed off under vacuum ( $5 \cdot 10^{-2}$  mbar). The ampule was placed in a explosion secured rocking furnace. When the ampule has reached room temperature, the temperature was gradually raised by 10°C/2 hours until 50°C was reached. After 24 hours the temperature was raised to 60°C and after further 12 hours to 75°C. The reaction is illustrated below in Figure 2.8.1.

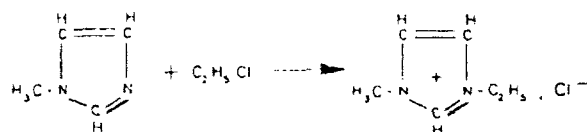


Figure 2.8.1

Formation of 1-methyl-3-ethyl-imidazolium chloride.

The rocking was continued for a total of 6 days. After cooling to room temperature, nice white crystals were isolated and dried under vacuum ( $5 \cdot 10^{-2}$  mbar) for a night, evaporating the excess ethylchloride. Yield 98(%) (54 g).

2.9 Preparation of 1,4-dimethyl-tetrazolium chloride.  
(ref. 51, 52).

The preparation took place in 6 steps:

5-aminotetrazole  $\rightarrow$  tetrazole  $\rightarrow$  tetrazole sodium salt  $\rightarrow$   
1-methyl-tetrazole  $\rightarrow$  1,4-dimethyl-tetrazolium-tetrafluoro-  
borate  $\rightarrow$  1,4-dimethyl-tetrazolium-chloride.

Dicyandiamide (16.8 g, 0.20 mole) was mixed with  $\text{NaN}_3$  (23.4 g, 0.36 mole) and water (40 ml) in a conical flask (300 ml). The mixture was heated and kept at 65-70°C and conc. aqueous HCl (30 ml) was introduced (20 minutes). The mixture was stirred for 6 hours at 65°C and 5-aminotetrazole was crystallizing. By cooling (0°C) for 1-2 hours crystals were precipitated, filtered and washed by ice water. Recrystallization was done in boiling water (37 mL) and the crystals were recovered by cooling and drying in air. Yield 75% (27.9 g, mp. 199°C) of 5-aminotetrazole-monohydrate.

A mixture of hypophosphoric acid (45 mL, 50 w/w %, 0.434 mole), water (197 mL) and aminotetrazole-monohydrate (40.52 g, 0.39 mole) was stirred in a beaker glass (1000 mL) forming an intermediate of the explosive diazonium salt (ref. 52).  $\text{NaNO}_2$  (27.14 g) dissolved in water (79 ml) was introduced while stirring, and the temperature was kept below 35°C by cooling (40 minutes). After complete reaction the stirring was continued for 1 extra hour.

pH was adjusted to 3.5 by adding NaOH (33%) and then the liquid was evaporated by 10 mmHg vacuum at 50°C (2-3 hours). The remaining yellow substance was extracted with an 1:1 mixture of ethanol:acetone and refluxed 10 minutes before decanting (1.195 mL, 1.97 mL, 5.20 mL). The ethanol:acetone mixture was evaporated and the yellow crystals were recrystallized in hot ethylacetate (10 minutes of reflux). The crystals were washed with the ethanol:acetone mixture (1.195 mL, 1.100 mL, 4.24 mL) and we ended up with white/yellow crystals of tetrazole (26.63 g, 97 %, mp. 139-145°C).

The tetrazole (7 g) was converted to the tetrazolium sodium salt by adding concentrated sodiumhydroxide (0.100 mole) in a conical flask (100 mL). After that, water was removed by rotary evaporation (20°C, oil pump 1 mmHg, 1 day), followed by slow heating to 200°C and further evaporation (15 minutes). Storage of the white/yellow crystals under  $\text{N}_2$ . Yield 100%, 9.2 g of tetrazole sodium salt.

Tetrazole sodium salt (9.79 g, 0.106 mole) was dissolved in 45 mL methanol under reflux (85°C) and stirring conditions in a three necked conical flask. Then we introduced 10.1 mL  $(\text{CH}_3)_2\text{SO}_4$  over 15 minutes, followed by a further reflux period (30 minutes). The methanol was then removed by distillation at 10 mmHg (room temperature). Finally, an extraction with 5.35 mL boiling  $\text{CH}_2\text{Cl}_2$  took place and a mixture of 1-methyl- or 2-methyl tetrazole was obtained (3:1, respectively).

Yield 76% (6.79 g). Separation of the products was done by distillation of the 2-methyl-tetrazole (1-methyl-tetrazole bp. > 200°C/1 mmHg, 2-methyl-tetrazole bp. 63°C/14-15 mmHg).

1-methyl-tetrazole (24.38 g, 0.290 mole) was dissolved in CH<sub>2</sub>Cl<sub>2</sub> (65 mL) using a water bath and stirring. Alkylation was done by introduction of (CH<sub>3</sub>)<sub>3</sub>BOF<sub>4</sub> (42.90 g, 0.290 mole), keeping the temperature constant at 35°C. After 1 hour, diethyl ether (50 mL) was introduced into the clear solution. Two phases separated, and the ether phase was removed by evaporation. An yield of 96% (51.8 g) was obtained.

Finally, anion exchange was performed as previously mentioned, using an equivalent amount of KCl solution.

#### 2.10 Other experimental techniques.

The preparation of anhydrous aluminum chloride by distillation and the drying of NaCl have been described previously (ref. 53).

MOPAC calculations were performed on a personal computer (IBM, PS/2, model 70, 386, 8 Mb Ram and OS/2 EE 1.3) if not otherwise stated. As Fortran compiler the 'MICROSOFT FORTRAN' version 5.0 was utilized.

Melting points were all obtained with a Gallenkamp (hot air) apparatus having an accuracy around ± 10%.

Conductivity measurements were performed in Pyrex H-cells described by Bjerrum and von Barner (ref. 54) with some insignificant changes. As electrodes we utilized tungsten wires (0.7 mm). As separator we utilized a capillary (d = 1-3 mm) with a length of 10 mm. The H-cell calibration was determined by means of 0.1 demal KCl solution as reported by Jones and Bradshaw (ref. 55). Silicone oil was chosen as the heating medium and the temperature was controlled by a direct digital controller REX-C4 (IMC401-E1) from RKC. Instrument Inc., Tokyo, Japan. The accuracy was ± 0.5°C. The measurements were all performed with a CDM-83 from Radiometer (Copenhagen, Denmark). The

frequency changes automatically dependent of the conductivity. The used conductivity ranges are listed below together with the respectively frequency and accuracy (percenties of readings): ( $[1.3 - 13 \mu\text{S}/\text{cm}]$ , 73 Hz,  $\pm 0.020\%$ ), ( $[13 - 130 \mu\text{S}/\text{cm}]$ , 536 Hz,  $\pm 0.75\%$  or at least  $\pm 3$  of first significant digit), ( $[1.3 - 13 \text{mS}/\text{cm}]$ , 4.69 KHz,  $\pm 2\%$  or at least  $\pm 3$  of first significant digit) and finally ( $[13 - 1300 \text{mS}/\text{cm}]$ , 50 KHz,  $\pm 2\%$  or at least  $\pm 3$  of first significant digit).

Cyclic voltammetry was performed in the H-type 3-compartment Pyrex cell (Fig. 2.10.1). A tungsten-wire working electrode ( $0.36 \text{ cm}^2$ ), a molybdenum-foil counter electrode and an aluminum reference electrode (in  $0.6 \text{ NaCl} - 0.4 \text{ AlCl}_3$  melt) were used. The electrochemical cell was sealed under 0.5 Atm. of Ar after each addition. The same silicone oil bath and temperature controller were used as for the conductivity measurements. Voltammetric measurements were carried out with a Schlumberger Model SI-1286 Electrochemical Interface. The CORRISOFT ERIC-2 System (ver. 1.14, Capcis March Limited, Manchester, England) programme was used to control the SI-1286.

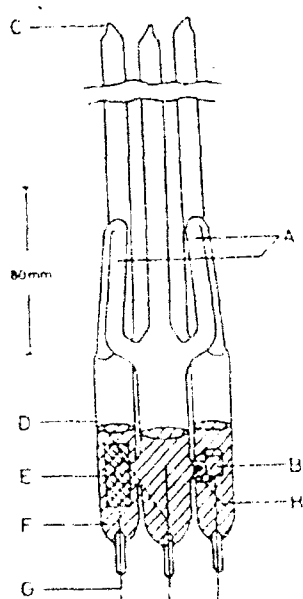


Figure 2.10.1.

3-compartment Pyrex cell (ref. 56).

A: Pressure equilibration tubes; B: Aluminum reference electrode C: Sealed cell; D: Tungsten working electrode; E: Molybdenum counter electrode; F: Electrolyte; G: Tungsten current collectors; H: Porous separator.

The Neosepta<sup>R</sup> membranes were received from Tokuyama Soda Co., Ltd. in Japan. The membranes were placed in a stirred 0.5 N sodium chloride solution at room temperature for 48 hours. They were then rinsed in distilled water and dried under vacuum for 24 hours at 40°C and 9 mm Hg. They were immediately transferred into the argon glove box, where they were kept until use.

All melt preparations for batteries, conductivities and cyclic voltammetry were performed in a Vacuum Atmosphere Corporation (HE-553) argon glove box with oxygen content less than 10 ppm and a dew point below -55°C.

Sodium was from Merck (Pro Analysis, 99.98%) and the aluminum rod was pure (99.99%). Sodium was freshly cut in the glove box, to obtain a shiny metallic surface. The aluminum was cleaned in a conc. acidic mixture of HNO<sub>3</sub>, H<sub>3</sub>PO<sub>4</sub> and H<sub>2</sub>SO<sub>4</sub> (ref. 57) and then in conc. NaOH.

The FeCl<sub>3</sub> was obtained from Merck (> 99.8% pure), and it was vacuum distilled (sublimed) at 305°C before use. The chloride content of the FeCl<sub>3</sub> has been determined by Volhard titration and found to be in agreement with the theoretical amount.

CuS and FeS was used as received, i.e. 99.9% pure. V<sub>2</sub>O<sub>5</sub> was a commercial product. The color was pink as expected. TiS<sub>2</sub> was utilized as received from the Ukrainian Institute of General and Inorganic Chemistry, Kiev.

The blue CuCl<sub>2</sub>·2H<sub>2</sub>O crystals from Heraeus (99% pure), was dried in a vacuum furnace at 110-130°C for 48 hours (crystals were then yellow-brown), and then transferred directly into the argon box, for use.

Mo was from a Danish company, Buch & Holm, and was approximately 99% pure. The Mo was rinsed in concentrated aqueous HCl for 5 minutes, washed with distilled water and dried before use. The stainless steel mesh (American Iron Standard Institute (AISI) type no. 1316) was from Nordisk Perforerings Fabrik a Danish company, and it was rinsed in ethanol and dried before use. The ceramic Nasicon tubes were produced at the Institute of Mineral Industry at the Technical University of Denmark. We dried the tubes in a vacuum furnace at 500°C for at least 24h, and then we oxidized the organic residues by



leading air over the ceramic tubes for approximately 1h, still keeping the temperature at 500°C. After this, the still hot tubes were transported into the argon box.

The  $\text{MEICl}:\text{AlCl}_3$  melt was prepared by adding small portions of  $\text{AlCl}_3$  to a glass beaker containing  $\text{MEICl}$  while stirring. Then the mixture of  $\text{MEICl}:\text{AlCl}_3$  was allowed to cool, before further addition of  $\text{AlCl}_3$ . This procedure prevented thermal decomposition of the  $\text{MEICl}$ . The melt was water clear as long as the composition was basic. In the acidic case our melts became slightly yellow.

$\text{FeCl}_3$  was put directly into the  $\text{MEICl}:\text{AlCl}_3$  melt, which turned yellow/brown immediately, leaving some undissolved  $\text{FeCl}_3$  at the bottom of the cell.

The  $\text{CuCl}_2$  also dissolved directly in the  $\text{MEICl}:\text{AlCl}_3$  which then became yellow.

Preparation and cleaning of the 50:50 atom percent sodium-potassium alloy has been described before (ref. 58).

Typical cell housings are illustrated below in Figure 2.10.2 and 2.10.3.

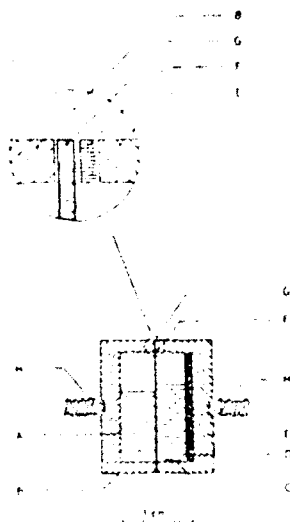


Figure 2.10.2.

Flat cell design (ref. 59).

- |                                   |                             |
|-----------------------------------|-----------------------------|
| A) Sodium anode.                  | E) Stainless steel housing. |
| B) Aluminum housing.              | F) Teflon O-ring.           |
| C) $\text{NaAlCl}_4$ electrolyte. | G) Nasicon disk.            |
| D) Cathode.                       | H) Mounting screw.          |

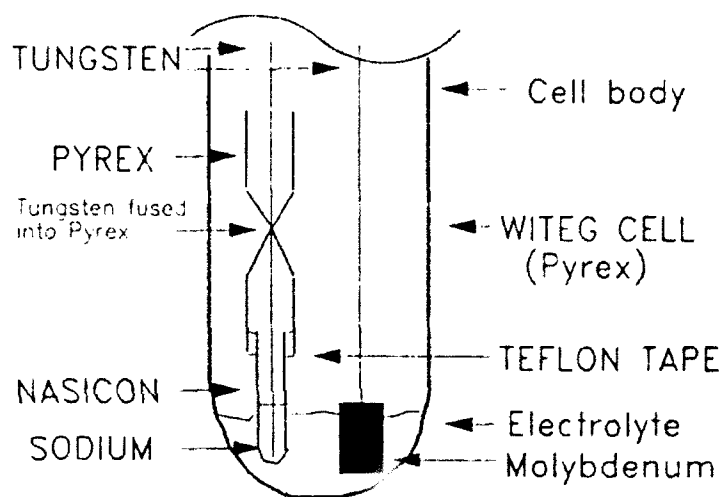
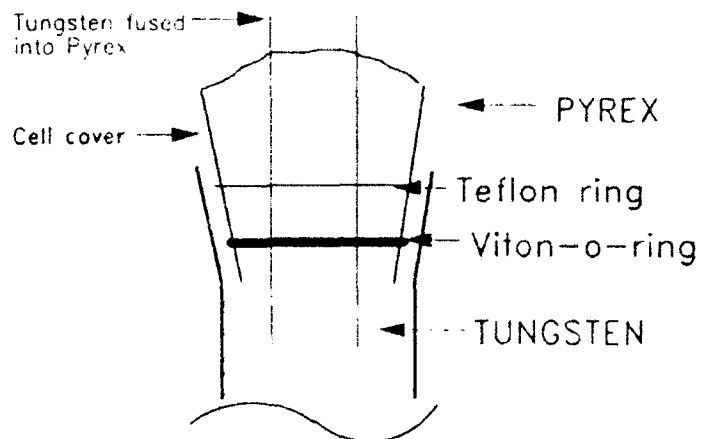


Figure 2.10.3.

Witeq battery cell design for Na/Nasicon tube batteries.

The Teflon tape surrounds the top of the Nasicon tube, to ensure tightness between the Nasicon tube and the Pyrex tube with the sealed tungsten wire. This prevented the electrolyte by capilar effect to react directly with the sodium.

### 3.0

### Results and discussion.

We here present the most important results obtained during the period April 1<sup>st</sup> 1990 to December 31<sup>th</sup> 1991.

### 3.1

### Stability of the organic compounds.

LUMO energies have been used to describe the stability of the organic cations towards reduction (ref. 3). LUMO energies calculated by the MNDO method were the gas phase electron affinity ( $E_A$ ) of the molecule (ref. 3, 60). The electron affinity ( $-LUMO$ ) in cations usually decreases when substituting hydrogen with methyl groups, thus making the reduction potentials ( $E_{1/2}(\text{reduction}) = E_A + \text{constant}$ ) more negative (ref. 3).

Below, in Table 3.1.1, are given the MOPAC results of the calculations on the methyl-methyl and methyl-ethyl systems. Theoretically the  $MEI^+$  cation is the most stable towards reduction. However, some of the triazolium cations are of the same order. Due to the higher heat of formation (HOF), the melting points of some of the triazolium salts might be too high for room temperature applications. Obviously, there are no linear connections between HOF of the gas phase cations and melting points of the corresponding chloride salts.

As can be seen from Table 3.1.1, by substituting a methyl group with an ethyl group, we get a higher LUMO energy (less negative), i.e. a more negative reduction potential. The  $1m3pmb123t^+$  cation has a LUMO value close to that of the  $MEI^+$  ion, but is a heavy compound. Both  $1e4m124t^+$  and  $1m4m124t^+$  have LUMO's in the same order as the  $MEI^+$ , but the dimethyl has a lower molecular weight, favoring battery constructions.

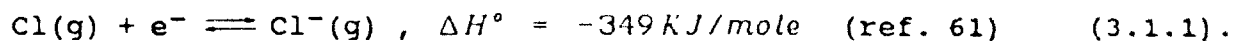
Table 3.1.1.1.  
MOPAC Calculations for some selected organic cations.

Material	HOF Kcal/mol	El. energy eV	Core- core eV	Dipole Debye	Fl	LUMO eV	IP eV	M <sub>w</sub> g/mol	SCF calc.
1-m-3-e-i <sup>+</sup>	192.37	- 6176	4850	1.957	22	- 4.56	14.42	117.17	117
1-m-3-m-i <sup>+</sup>	199.46	- 5024	3854	0.985	19	- 4.68	14.55	97.14	88
1-m-3-pmb-1,2,3-t <sup>+</sup> A	237.99	-14504	11972	9.695	39	- 4.82	12.12	204.25	9
1-m-4-e-1,2,4-t <sup>+</sup>	228.50	- 6276	4886	2.993	22	- 5.05	15.50	112.15	23
1-e-4-m-1,2,4-t <sup>+</sup>	228.20	- 6272	4882	4.177	22	- 5.05	15.28	112.15	94
1-m-2-m-pyr	231.95	- 5093	3925	1.152	19	- 5.09	14.85	97.14	100
1-m-4-m-1,2,4-t <sup>+</sup>	235.86	- 5120	3886	3.168	19	- 5.17	15.61	98.13	45
1-m-3-e-1,2,3-t <sup>+</sup>	246.38	- 6293	4904	1.858	22	- 5.17	15.39	112.15	87
1-m-3-m-1,2,3-t <sup>+</sup>	253.99	- 5133	3900	1.481	19	- 5.31	15.56	98.13	70
1-m-2-e-1,2,4-t <sup>+</sup>	243.62	- 6366	4977	3.181	22	- 5.38	15.50	112.15	94
1-e-2-m-1,2,4-t <sup>+</sup>	244.18	- 6363	4974	3.207	22	- 5.38	15.51	112.15	99
1-butyl-pyridinium <sup>+</sup>	164.13	- 8064	6518	4.623	27	- 5.45	14.58	136.22	444
1-m-2-m-1,2,4-t <sup>+</sup>	251.11	- 5182	3948	3.340	19	- 5.54	15.70	98.13	55
1-m-2-m-1,2,3-t <sup>+</sup>	270.01	- 5192	3960	3.135	19	- 5.62	15.35	98.13	91
3-m-o <sup>+</sup> 1	154.24	- 4047	2929	1.576	16	- 5.76	15.40	84.10	137
1-m-4-m-1,2,3,4-t <sup>+</sup>	283.23	- 5231	3934	4.953	19	- 5.80	16.42	99.12	90
1-m-3-m-1,2,3,4-t <sup>+</sup>	291.22	- 5231	3934	1.552	19	- 5.84	16.31	99.12	84
1-m-2-e-1,2,3-t <sup>+</sup>	311.44	- 6436	5050	3.039	22	- 6.09	14.79	112.15	462
3-m-s <sup>+</sup> 2	195.17	- 3820	2795	2.025	16	- 6.17	15.30	100.16	147
1-m-2-m-1,2,3,4-t <sup>+</sup>	301.42	- 5290	3994	5.337	19	- 6.19	16.35	99.12	74

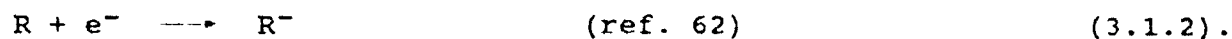
### Comments to Table 3.1.1.

A: Calculations performed by C.J. Dymek, Jr. Lt. Col. European Office of Aerospace Research and Development, London England.

Electron affinity ( $E_A$ ): Usually means  $-\Delta H^\circ$  of processes like:



For organic systems, reactions like 3.1.2 are known to be stable when there is no oxidizing agent in the melt.  $E_A$  can be measured directly if not too small.



$E_A$  (LUMO) are defined to be positive for reactions like 3.1.1, and the energy of the reaction is then  $-E_A$  (ref. 63).

Total energy =  $E_{\text{energy}}$  + Core-Core energy.

El: Electronic.

m = methyl.

e = ethyl.

i = imidazole.

pmb = para-methoxy-benzyl.

pyr = pyrazolium.

t = triazolium / tetraazolium.

IP = Ionization Potential (oxidation potential for the cations).

Lowest Occupied Molecular Orbital (LOMO) energy.

FL = Filled Levels (number of binding electrons/2).

1: 3-methyloxonium cation.

2: 3-methylthiazolium cation.

### 3.2

### Reactivity with aluminum chloride.

The melting points of some of the organic chloride salts are presented in Table 3.2.1 together with their reactivity with aluminum. All compounds were recrystallized before use. The procedure differed slightly from the one mentioned in the experimental section and is summarized here.

#### Recrystallization process:

Materials: Diethyl ether, 100% ethanol dried with molecular sieves (4 Ångström pellets), activated charcoal.

Utensils : Suction filtering flask, Büchner funnel with a #4 porosity fritted disc, oil pump, large beakers, flasks and bottles to collect waste ether, stirring rod, small beaker and flask etc.

Working: All working took place inside a dry oxygen glove box.

#### Procedure:

- 1) Weigh sample to express % recovery.
- 2) Add ethanol slowly - just enough to dissolve sample.  
Around 10-15 ml/g.
- 3) Add a little activated charcoal, stir for a while and then filter until a layer of activated charcoal are formed (use oil pump).
- 4) Rinse beaker, charcoal and filter with small portions of ethanol.  
(Make sure that the vacuum is not too high, i.e. the solution will evaporate.)
- 5) Transfer solution to a large beaker and rinse flask with ethanol.
- 6) Add diethyl ether slowly to beaker and stir continuously.  
(A lot of ether is needed to get a high % recovery).
- 7) If the solution turns white then divide into 2 parts and continue adding ether to the beaker.
- 8) Collect crystals on Büchner funnel and wash with ether.
- 9) Suck crystals dry and place in a brown bottle with screw cap.
- 10) Store crystals in argon glove box until use or place crystals in an ampule for sealing.

Table 3.2.1.1.  
Reactions between organic salt/aluminum chloride.

Organic Compound	mp. °C	XAlCl <sub>3</sub>	Rx at RT.	Par. Rx T (°C).	Com. lq. T (°C).	Color lq phase.	Lq. at RT	RT phase
1,2-Dimethyl- Pyrazolium- Chloride. (Light Sensitive).	110 s	202	No	75	125-150	G, C	No	S, G
	217 d	402	No	50	> 180 d	G, C	No	S, G
		50	No	125	150	Clear	No	S, G
		60	No	40	125	Amber	No	S+lq, B
		70	No	60	80-200 d	Amber	No	L(Am)+S(G)
3-Methyl- Thiazolium- Chloride.	51-52 <sup>3</sup>	70	No	40	40	Amber	No	S+lq (Am)
	57-60 <sup>3</sup>	60	No	40	80	Amber	No	S+lq (Am)
		70	No	40	80	Amber	No	S+lq (Am)
	56-59 <sup>4</sup>	45P	No	RT	> 90			lq, Viscous
1-Methyl- 3-Paramethoxy- Benzyl-1,2,3- Triazolium- Chloride.		63	No	RT	90	Pa Amber	Yes	
		68P	No	RT	40	Pa Amber	No	S+lq
		73	No	RT	70	Pa Amber	No	S
		82	No	RT	125	Pa Amber	No	
1-Ethyl-4-Methyl-1, 2,4-Triazolium- Chloride.		40P	No	RT	> 90			
		55P	No	RT	90	grey		
	135-	60	Yes(sl)	RT	RT	light Am	Yes	lq, Viscous
	165 d	65P	Yes	RT	RT	Pale	No	S, glass
		70	Yes(fs)	RT	RT	red pol		
1,2-Dimethyl- 1,2,3-Triazolium- Chloride.		60	No	RT	> 90	Amber	No	
	170 d	60	No	50	90	Amber	Yes	S
		70	No	50	90	Amber	No	S
		80	No	RT	125	Pale	No	S, Brown
1,4-Dimethyl- 1,2,4-Triazolium- Chloride.	103-	40P	Yes	RT	RT	Pale	Yes	Pale
	106	55P	Yes	RT	RT	Amber	Yes	Amber
		60	No	NO	90	Amber	No	Amber

- 1) Melting point of the pure organic salt without  $\text{AlCl}_3$ . (Gallenkamp melting point apparatus).
- 2) Ampul exploded at  $200^\circ\text{C}$ .
- 3) The lower melting point ( $51-52^\circ\text{C}$ ) was obtained with white crystals while the upper mp. was obtained with light brown crystals (indicating two different compounds).
- 4) Another batch than the one mentioned above.

Abbreviations:

Am : Amber.  
 B : Brownish.  
 Com : Complete.  
 C : Cloudy.  
 d : Decomposes.  
 fs : Fast.  
 G : Grey.  
 lq : Liquid.  
 Rx : Reaction.  
 RT : Room Temperature.  
 P : Powder of  $\text{AlCl}_3$ , otherwise used long particles.  
 Pa : Pale.  
 Par : Partial.  
 Pol : Polymer.  
 Pur : Purification.  
 S : Solid.  
 s : Softens.  
 sl : Slowly.

Comments to Table 3.2.1.

From Table 3.2.1 we see that the only compounds which form liquids at room temperature are the 1m3pmb123tcl and 14dm124tcl. Other compounds are liquid at room temperature after a previous heating, e.g. 3mt2cl and 12dm123tcl.



### 3.3

### Conductivity measurements.

Conductivity is one of the main physical characteristics of electrolytes and we therefore report the conductivity for some of the organic systems: 14dm124tcl, 1e4m124tcl, 1m3pmb123tcl, 3mtzcl, MEICl. Some of the compounds form liquid electrolytes with aluminum chloride as shown in Table 3.2.1. The conductivity of these compounds are reported too.

#### 3.3.1

#### MEICl-AlCl<sub>3</sub>.

The MEICl:AlCl<sub>3</sub> system has been well described by Wilkes et al. (ref. 10, 11), but as a reference some of the features are given in Table 3.3.1.1.

Table 3.3.1.1.  
The MEICl:AlCl<sub>3</sub> system.

Compound	X <sub>AlCl<sub>3</sub></sub>	Melting point °C	$\sigma$ 1 $mS \cdot cm^{-1}$	$\sigma$ 1 $mS \cdot cm^{-1}$	Electrochemical win- dow (Volt), (ref. 64). Anode Cathode Limit Limit
			80°C	125°C	
MEICl		84	14.247	52.881	-----
MEICl:AlCl <sub>3</sub>	0.33	19	21.692	53.165	-----
MEICl:AlCl <sub>3</sub>	0.41	-27	33.871	69.623	0.97 - -1.60 <sup>2</sup>
MEICl:AlCl <sub>3</sub>	0.50	7	59.593	98.546	2.4 - -2.2 <sup>3</sup>
MEICl:AlCl <sub>3</sub>	0.60	-31	45.235	76.504	2.35 - -0.05 <sup>2</sup>

- 1: Conductivity calculated after Wilkes et al. (ref. 11). Note that the temperature (125°C) is just outside the limit ranges for the calculations.
- 2: Sweep rate 50 mV/s, reference electrode Al/MEICl:AlCl<sub>3</sub> (X<sub>AlCl<sub>3</sub></sub>=0.60).  
Counter electrode: W-foil (7.5 cm<sup>2</sup>), working electrode: Glassy carbon (0.196 cm<sup>2</sup>).
- 3: Wilkes et al. (ref. 65). Working electrode Pt.

### 3.3.2 1-methyl-3-paramethoxybenzyl-1,2,3-triazolium chloride-AlCl<sub>3</sub>.

At very high concentrations of AlCl<sub>3</sub> (>60 mole%) 1-m-3-pmb-1,2,3-tCl slowly forms room temperature liquids (over days). Due to the high viscosity and decomposition of the 1-m-3-pmb-1,2,3-tCl it has been very difficult to measure the conductivity of the pure salt. The decomposition of 1-m-3-pmb-1,2,3-tCl starts at about 135°C±10°C, i.e. when the compound melts (under sublimation). Mixtures with aluminum chloride are more easy to handle.

Measurements at  $X_{\text{AlCl}_3} = 0.55$  were done by preheating of the mixture to 125°C. The results are illustrated in Figure 3.3.2.1.

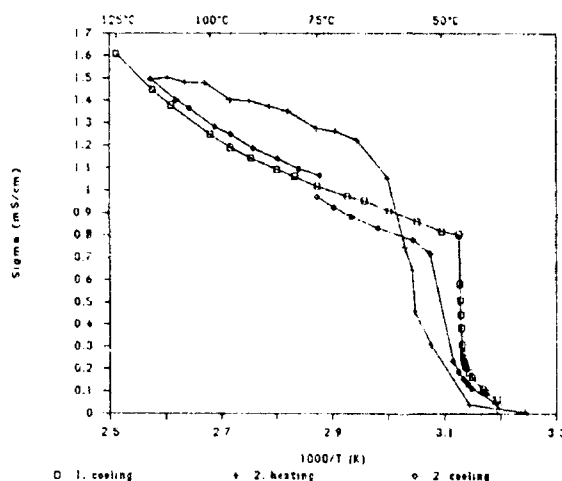


Figure 3.3.2.1.

Conductivity of 1-m-3-pmb-1,2,3-tCl:AlCl<sub>3</sub>, ( $X_{\text{AlCl}_3} = 0.55$ ).

1. Cooling: -0.5°C/minute.
2. Heating: 1.5°C/minute.
2. Cooling: -0.5°C/minute until  $T=74.4^\circ\text{C}$  ( $2.88\text{ K}^{-1} = 10^3/74.4$ ) then waiting for 15 hours and cooling with -0.5°C/minute.

The equilibrium in the melt was reached very slowly and the 2. heating was unintendedly performed too quickly. The 2. cooling can be used to estimate the accuracy of the measurements (±5%).

Least squares fitted parameters to equation 3.3.2.1 are given in Table 3.3.2.1. Only measurements from the 1. cooling curve were used for the regression.

$$\hat{\kappa} = \kappa_0 + A(t-t_0) + B(t-t_0)^2 \quad (3.3.2.1)$$

$\hat{\kappa}$  is the specific conductivity calculated from the regression values,  $t$  is the temperature in °C and  $t_0$  is a fixed reference temperature (80 °C in these calculations).  $\kappa_0$ ,  $A$  and  $B$  are the model parameters.

Table 3.3.2.1.

Least-Squares-Fitted Parameters for specific conductivities of 1-m-3-pmb-1,2,3-tCl:AlCl<sub>3</sub> according to equation (3.3.2.1)<sup>a</sup> with  $t_0 = 80^\circ\text{C}$ .

XAlCl <sub>3</sub>	$\kappa_0$ mS · cm <sup>-1</sup>	A mS · cm <sup>-1</sup> · °C <sup>-1</sup> 10 <sup>3</sup>	B mS · cm <sup>-1</sup> · °C <sup>-2</sup> 10 <sup>6</sup>	t <sub>min</sub> °C	t <sub>max</sub> °C	Number of Points	R <sup>2</sup>
0.55	1.0548 (0.007)	8.3067 (0.17)	85.55 (5.6)	60	125	12	0.99911

a: Standard deviation of parameters  $\kappa_0$ ,  $A$ ,  $B$ , are given in parentheses. The squared correlation coefficient  $R^2$  (correlation index) are given by:

$$R^2 = \frac{\sum_{i=1}^n (\kappa_i - \bar{\kappa})^2 - \frac{(\sum_{i=1}^n (\kappa_i - \bar{\kappa}))^2}{n}}{\sum_{i=1}^n (\kappa_i - \bar{\kappa})^2}, \quad \text{with} \quad \bar{\kappa} = \frac{1}{n} \sum_{i=1}^n \kappa_i \quad (3.3.2.2).$$

### 3.3.3 1,4-dimethyl-1,2,4-triazolium chloride-AlCl<sub>3</sub>.

The possibility of using molten mixtures of 1,4-dimethyl-1,2,4-triazolium chloride and aluminum chloride (AlCl<sub>3</sub>) as secondary battery electrolytes was studied, sometimes extended by a copresence of sodium chloride.

14dm124tcl:AlCl<sub>3</sub> mixtures demonstrated high specific conductivity in a wide temperature range. The equimolar system was most conductive and had  $\kappa$  values between  $4.02 \times 10^{-5}$  and  $7.78 \times 10^{-2}$  S/cm in the range from -31 to 122.7°C, respectively.

The electrochemical window of 14dm124tcl-containing sodium chloroaluminate melts varied in the region of 2.2 to 2.5 V (150-170°C) depending on the melt acidity and anode material. 14dm124tcl, being specifically adsorbed on the tungsten electrode surface, had an inhibiting effect on the aluminum reduction, but this effect was suppressed on the aluminum substrate.

A reversible electrochemical process with high current density (tens of mA cm<sup>-2</sup>) was observed at 0.344 V on the acidic sodium chloroaluminate background. It was explained as involving a free triazolium radical mechanism.

In conclusion, molten 14dm124tCl:AlCl<sub>3</sub> electrolytes are acceptable for battery performance and both the aluminum anode and the triazolium electrolyte can be used as active materials in the acidic 14dm124tcl:AlCl<sub>3</sub> mixtures.

For the voltammetric measurements the idea of Matsunaga et al. (ref. 66) has been used: the electrochemical behavior of 14dm124tCl:AlCl<sub>3</sub> systems in both acidic and basic regions have been studied in a diluted state in sodium chloroaluminate melts. In this way, all the processes due to 14dm124tCl became more pronounced.

Temperatures were stabilized within ±0.1°C. The temperature scanning rate was 0.5 °C/min. Reproducibility of the conductivity values was controlled by performing two cooling and two heating scans in each concentration point.

The specific conductivity of the 14dm124tcl:AlCl<sub>3</sub> system in the temperature range of 29.3-114.0 °C is shown in Figure 3.3.3.1, and the corresponding data are given in Table 3.3.3.1. Like for the 1-alkylpyridinium chloride - AlCl<sub>3</sub> (ref. 67) and 1,3-alkylimidazolium chloride - AlCl<sub>3</sub> (ref. 11) melts, it can be seen that the specific conductivity of 14dm124tcl:AlCl<sub>3</sub> mixtures is strongly dependent on the composition of the melt. For all systems, equimolar mixtures have the highest conductivity values. The 14dm124tcl:AlCl<sub>3</sub> conductivity is a little lower but very close to the corresponding imidazolium melt and the MEICl - AlCl<sub>3</sub> mixture.

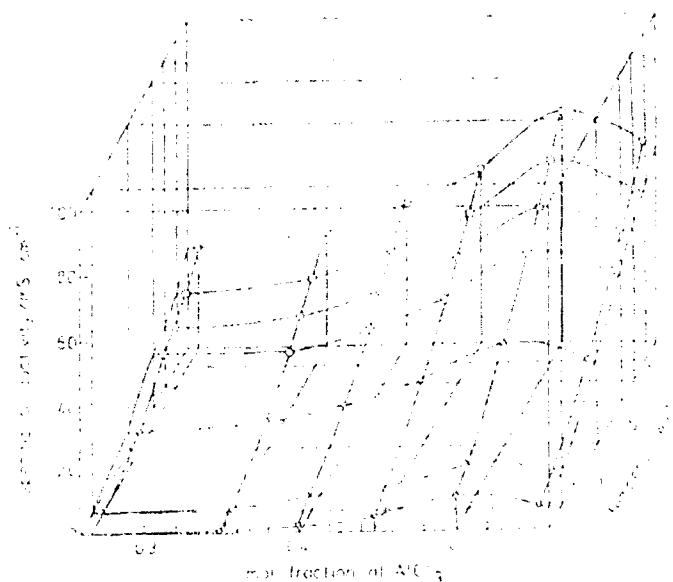


Figure 3.3.3.1.  
Specific conductivity of 1,4-dimethyl-1,2,4-triazoliumchloride:AlCl<sub>3</sub>.  
(See Table 3.3.3.1 for the marked values).

Table 3.3.3.1.

Specific conductivity of 1,4 dimethyl-1,2,4 triazoliumchloride:AlCl<sub>3</sub>.  
Specific Conductivity, mS cm<sup>-1</sup>

X <sub>AlCl<sub>3</sub></sub>	0.268	0.348	0.399	0.448	0.500	0.553
t, °C						
29.3	--	0.798	2.231	4.753	10.644	7.369
39.9	0.95	1.933	4.585	7.533	14.329	10.644
57.7	2.121	5.527	9.676	15.530	26.273	20.825
67.0	5.199	8.475	13.688	20.361	31.742	26.652
76.5	10.644	12.255	18.218	25.929	38.709	32.766
86.0	16.395	16.770	23.377	32.001	46.129	39.463
95.2	19.078	21.725	29.149	38.497	53.682	46.357
104.7	22.708	27.225	35.249	45.607	61.819	53.345
114.0	29.866	33.857	42.148	52.812	70.212	61.137

Experimental values of specific conductivity,  $\kappa$ , was for each composition least-squares fitted to equations of the form previously mentioned (equation 3.3.2.1). The values of the fitted parameters of the equation (3.3.2.1) are given in Table 3.3.3.2.

TABLE 3.3.3.2.

Least-Squares-Fitted Parameters for Specific Conductivities of 1,4-dimethyl-1,2,4-triazolium chloride:AlCl<sub>3</sub> according to Equation 3.3.2.1<sup>a</sup> ( $t_0 = 80^\circ\text{C}$ ).

$X_{\text{AlCl}_3}$	$\kappa_0$ $\text{mS} \cdot \text{cm}^{-1}$	A $\text{mS} \cdot \text{cm}^{-1} \cdot ^\circ\text{C}^{-1}$	B $\text{mS} \cdot \text{cm}^{-1} \cdot ^\circ\text{C}^{-2}$ $10^3$	$t_{\text{min}}$ $^\circ\text{C}$	$t_{\text{max}}$ $^\circ\text{C}$	Number of Points	$R^2$
0.268	11.0001 ( 0.6146)	0.47634 (0.00630)	5.52490 (0.24500)	35	110	32	0.99530
0.348	13.7711 ( 0.3362)	0.45213 (0.00235)	3.85476 (0.09130)	30	120	30	0.99929
0.399	19.8544 ( 0.0955)	0.53710 (0.00077)	3.68924 (0.02770)	30	120	29	0.99995
0.448	28.0325 ( 0.3131)	0.62292 (0.00218)	3.05800 (0.08640)	40	125	29	0.99968
0.500	40.7721 ( 0.6877)	0.75757 (0.00367)	3.47999 (0.04370)	- 30	125	77	0.99922
0.553	35.2458 ( 0.5038)	0.67948 (0.00347)	2.48172 (0.13000)	30	125	30	0.99933

a: Standard deviation of parameters  $\kappa_0$ , A, B, are given in parentheses. The squared correlation coefficient  $R^2$  (correlation index) are given by equation (3.3.2.2).

According to Figure 3.3.3.2, and unlike what was the case for 1,3-dimethyl- and 1-methyl-3-ethyl- imidazolium chloride aluminum chloride melts, the 14dm124tcl:AlCl<sub>3</sub> mixture at  $X_{\text{AlCl}_3} = 0.50$  demonstrates an obvious non-Arrhenius behaviour, having a glass formation temperature,  $T_g$ , below zero. But the most important property for battery application is that the equimolar 14dm124tcl:AlCl<sub>3</sub> melt has a sufficiently high conductivity down to  $-30^\circ\text{C}$ .

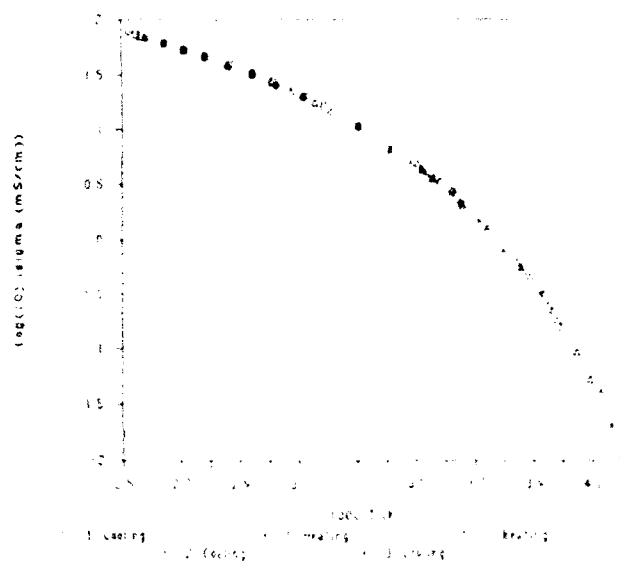


Figure 3.3.3.2.

Specific conductivity of 14dm124tcl:AlCl<sub>3</sub> (X<sub>AlCl<sub>3</sub></sub>=0.50) vs. temperature.

#### 3.3.4 Specific conductivity of the pure salts.

Performing conductivity measurements of the MEICl prepared as described in the experimental section gave the same results as published by Fannin et al. (ref. 11). The results are presented in Figure 3.3.4.1 below.

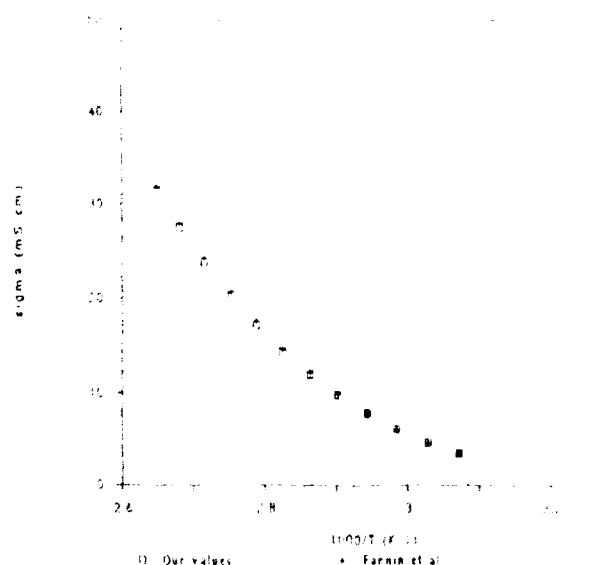


Figure 3.3.4.1.

Specific conductivity of 1-methyl-3-ethyl-imidazolium chloride vs. temperature and compared with Fannin et al. (ref. 11).

Measurements of the 3-methyl-thiazolium chloride showed an improved conductivity for the pure melts compared with the MEICl, as illustrated below in Figure 3.3.4.2.

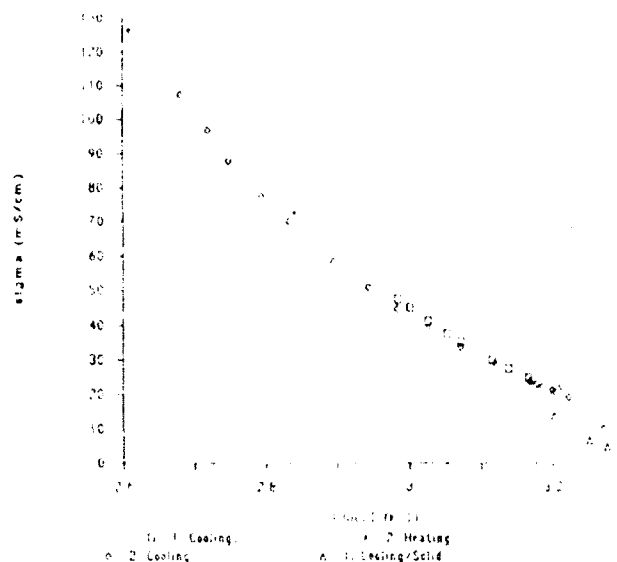


Figure 3.3.4.2.

Specific conductivity of 3-methyl-thiazolium chloride vs. temperature.

Measurements of the 1,4-dimethyl-1,2,4-triazolium chloride showed a specific conductivity for the pure melts almost equal to the MEICl. This is illustrated below in Figure 3.3.4.3.

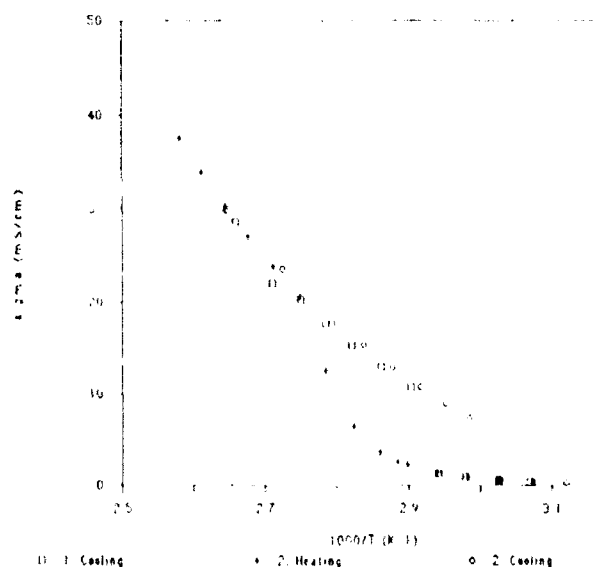


Figure 3.3.4.3.

Specific conductivity of 1,4-dimethyl-1,2,4-triazolium chloride vs. temperature.



Measurements of the 1-ethyl-4-methyl-1,2,4-triazolium chloride also showed a specific conductivity for the pure melts almost equal to the MEICl and the 14dm124tcl. This is illustrated below in Figure 3.3.4.4.

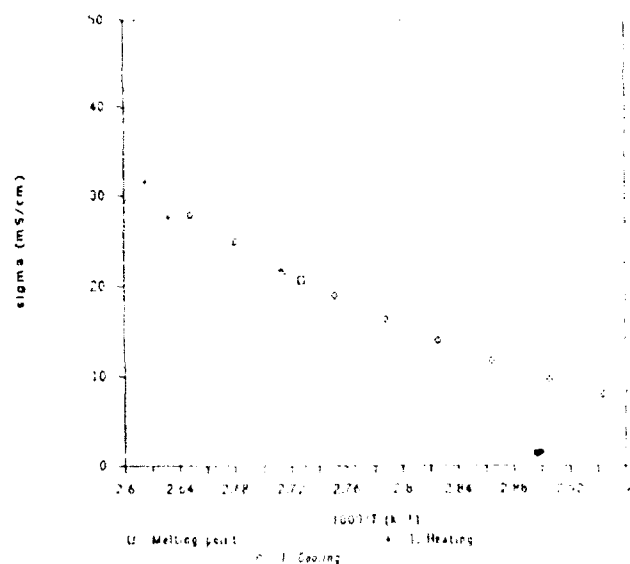


Figure 3.3.4.4.

Specific conductivity of 1-ethyl-4-methyl-1,2,4-triazolium chloride vs. temperature.

The conductivity results clearly show that these new organic salts mentioned above have specific conductivities close to the MEICl or even better. Most promising for room temperature applications is of course the 14dm124tcl because it reacts immediately with  $\text{AlCl}_3$ . To investigate the electrochemical performance of the 14dm124tcl salt, voltammetric measurements were done.

### 3.4 Voltammetric investigations of 14dm124tcl.

Cyclic Voltammetric (CV) curves for the melts of neutral or slightly basic sodium chloroaluminate with 1 and 2 mole % additions of 14dm124tcl are shown in Figure 3.4.1 (obtained with tungsten electrode). It can be seen that, in the presence of 14dm124tcl, the potential of aluminum electroreduction becomes almost 100 mV more negative than for the pure  $\text{NaAlCl}_4$  electrolyte. Moreover four new waves appear on the voltammetric curves: cathodic waves (I and II) with initial potentials of 1.82 and 2.29 V and anodic waves (III and IV) with initial potentials of 2.18 and 1.09 V, the wave parameters depending on the 14dm124tcl concentration.

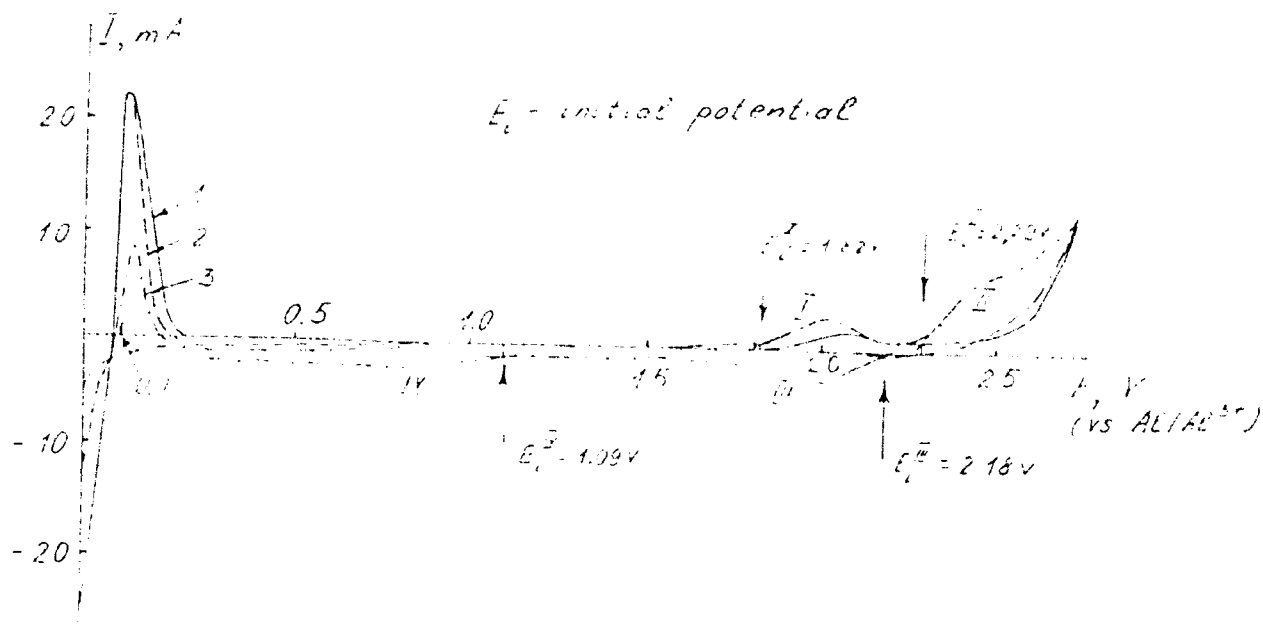


Figure 3.4.1.

CV with working tungsten electrode at 169°C ( $v = 2 \text{ V/min}$ ).  
 14dm124tcl added as the pure salt, not from mixture of  $\text{AlCl}_3$ .  
 1:  $\text{NaCl}:\text{AlCl}_3$  (0.5000:0.5000).  
 2:  $\text{NaCl}:\text{AlCl}_3:14\text{dm124tcl}$  (0.4951:0.4951:0.0098).  
 3:  $\text{NaCl}:\text{AlCl}_3:14\text{dm124tcl}$  (0.4903:0.4903:0.0194).

Wave I disappears during cycling in a potential range more positive than 1.0 V (Figure 3.4.2) and wave III, being obviously an electroreduction of the product of process II, has a strong passivating effect on the aluminum reduction and oxidation: both of them are suppressed when cathodic polarization follows the anodic one (Figure 3.4.3). Peak current ( $I_p$ ) and peak potential ( $E_p$ ) of wave III, depend linearly on the square root of the potential scanning velocity.



Figure 3.4.2.

CV with working tungsten electrode at 169°C ( $v = 2 \text{ V/min}$ ).  
 14dm124tcl added as the pure salt, not from mixture of  $\text{AlCl}_3$ .  
 $\text{NaCl}:\text{AlCl}_3:14\text{dm124tcl}$  (0.4903:0.4903:0.0194). Second potential scan in the anodic part of the electrochemical window.

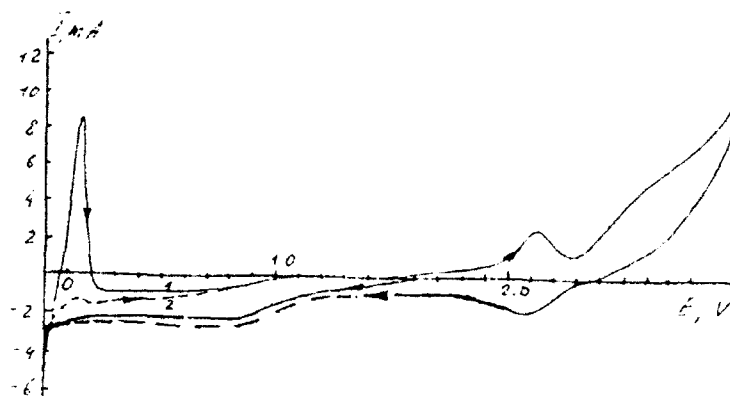


Figure 3.4.3.

CV with working tungsten electrode at  $169^{\circ}\text{C}$  ( $v = 2\text{ V/min}$ ).  
 14dm124tcl added as the pure salt, not from mixture of  $\text{AlCl}_3$ .  
 $\text{NaCl}:\text{AlCl}_3:14\text{dm124tcl}$  (0.4903:0.4903:0.0194). First and second potential scan.

In the case of the slightly acidic melt the electrochemical behavior of 14dm124tcl (added in the form of a 0.447 14dm124tcl:0.553  $\text{AlCl}_3$  melt) differs very much from that in the basic melt (Figure 3.4.4).

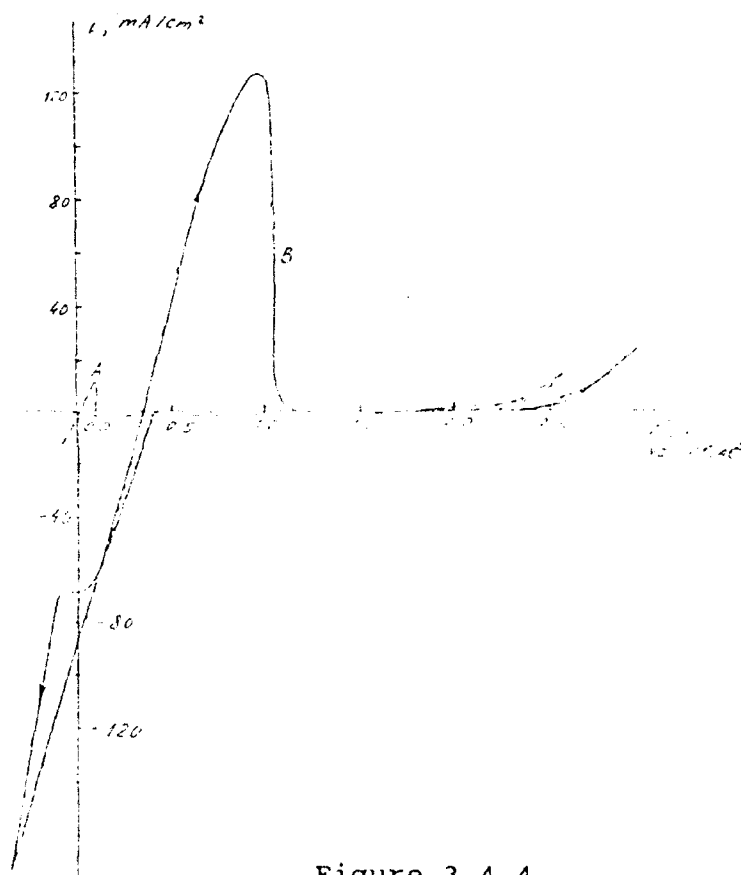


Figure 3.4.4.

CV with working tungsten electrode at  $165^{\circ}\text{C}$  ( $v = 1\text{ V/min}$ ).  
 14dm124tcl added in the form of 0.447 14dm124tcl:0.553  $\text{AlCl}_3$  melt.  
 A:  $\text{NaCl}:\text{AlCl}_3$  (0.5000:0.5000) equimolar.  
 B:  $\text{NaCl}:\text{AlCl}_3:14\text{dm124tcl}$  (0.4763:0.5025:0.0212).

The aluminum electroreduction initial potential, as in the basic melt, becomes 100 mV more negative compared to the pure  $\text{NaAlCl}_4$  melt, but unlike for the triazolium basic melts and for the imidazolium acidic melts, the wave of aluminum electrooxidation disappears, i.e. it is suppressed by 14dm124tcl. Furthermore new high velocity electrochemical processes, involving 14dm124tcl, can be seen in the voltammetric curves (waves V and VI in Figures 3.4.4 and 3.4.5). Both waves have the same initial potential, 0.344V, but the peak potential difference is distinct and exceeds 1 V, decreasing with the temperature (Figure 3.4.6) and scan velocity. For both waves, peak current densities are unusually high (even at 153.3°C and under equilibrium conditions, i.e. 8.3 mV/s, the current density of the cathodic peak is 66 mA/cm<sup>2</sup>),  $i_{pa}/i_{pc}$  decreasing with temperature (Figure 3.4.6) and increasing when lowering scan velocity. Both peak parameters are reproducible (cycling tens of times), even at quasi-equilibrium conditions.

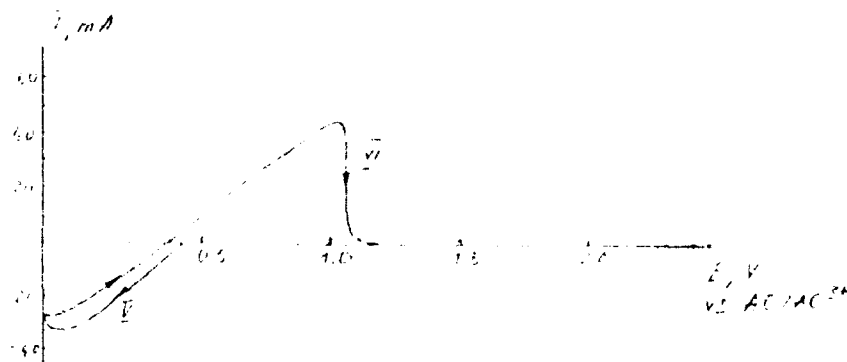


Figure 3.4.5.

CV with working tungsten electrode at 170°C ( $v = 2 \text{ V/min}$ ).  
 $\text{NaCl}:\text{AlCl}_3:14\text{dm}124\text{tcl}$  (0.4763:0.5025:0.0212).  
 Potential scan without aluminum wave.

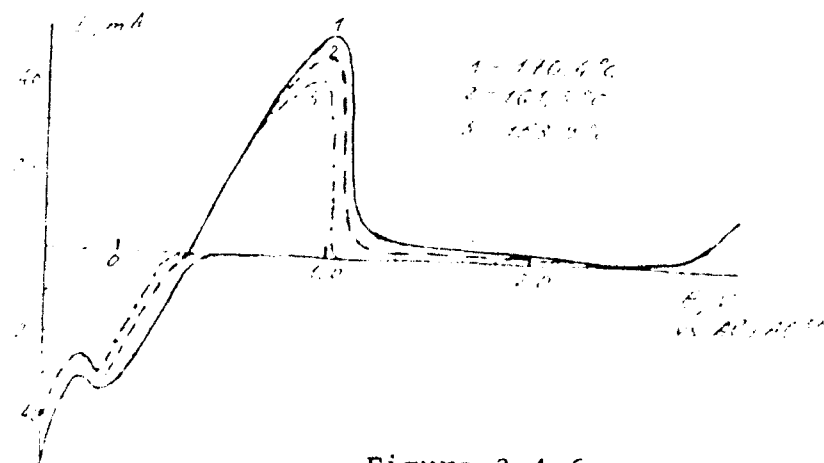


Figure 3.4.6.

Working tungsten electrode at different temperatures ( $v = 2 \text{ V/min}$ ).  
 $\text{NaCl}:\text{AlCl}_3:14\text{dm}124\text{tcl}$  (0.4763:0.5025:0.0212).

The peak currents and potentials depend linearly on the square root of scan velocity. Both triazolium processes depend on the electrode material: triazolium reduction is suppressed at the aluminum electrode and the wave of aluminum electrooxidation appears on the voltammetric curve (Figure 3.4.7).

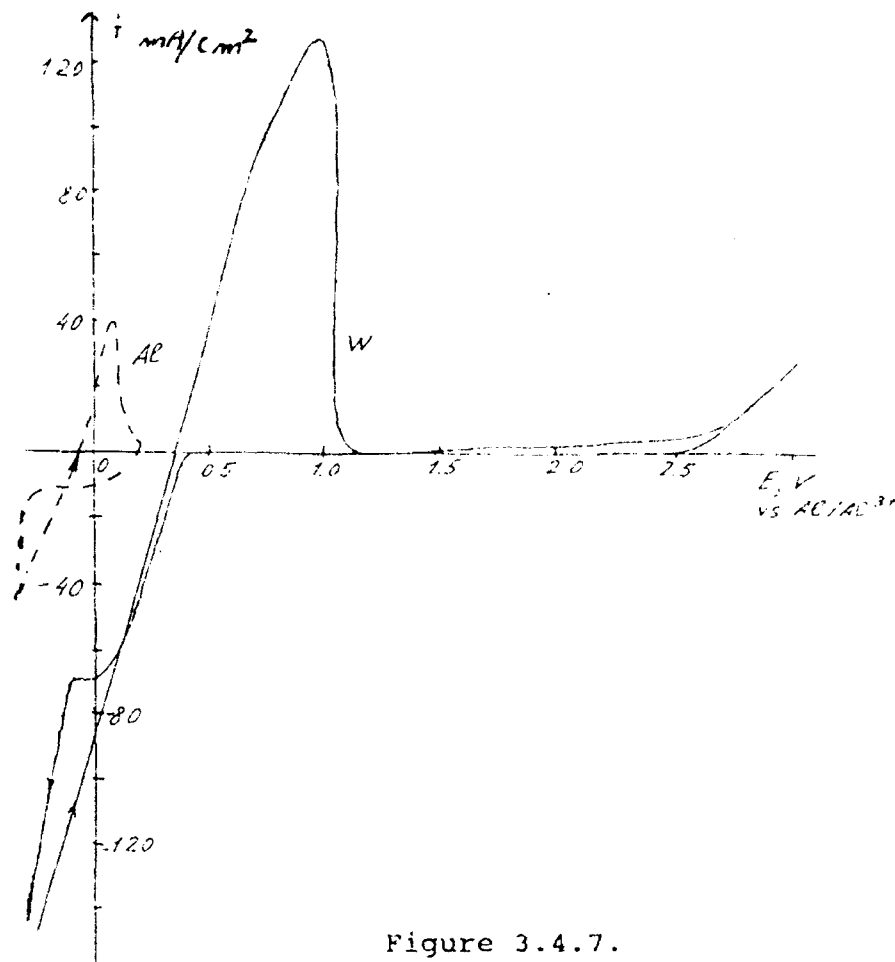


Figure 3.4.7.

CV with working tungsten (W) or aluminum (Al) electrode at 165°C.  
( $v = 10 \text{ mV/min}$ ).

$\text{NaCl}:\text{AlCl}_3:14\text{dm}124\text{tcl}$  (0.4763:0.5025:0.0212).

The Al curve has to be multiplied by 2.186 to get the real current density for the aluminum case!

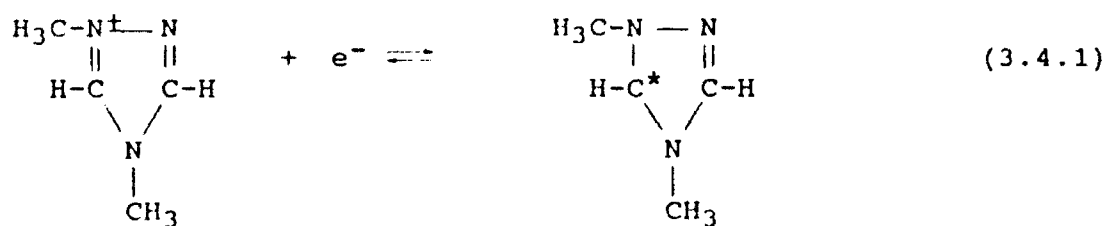
From the results of voltammetric measurements we can conclude that in acidic and basic regions triazolium chloride has a visible effect on the electrochemical behavior of the sodium chloroaluminate melt. Similar to imidazolium chloride (ref. 64, 66), 14dm124tcl has inhibiting effect on the aluminum electroreduction. However, opposite to the behavior of imidazolium melts, the aluminum electrooxidation

on tungsten is suppressed in acidic melts, while being slightly effected in basic melts (mainly because of higher aluminum reduction polarization and fixed potential scanning region (Figure 3.4.1)). Taking into account our new voltammetric data, prior results of electrochemical investigation of diluted MEICl solutions in chloroaluminate melts (ref. 66) and the well-known inhibiting properties of benzotriazole in aqueous solutions (ref. 68), we suppose specific adsorption of the triazolium cation and/or its reduction and oxidation products on the W electrode surface to be the reason for inhibition of aluminum reduction. Dependence of both peak current and potential of wave III on the square root of the potential scan velocity demonstrate ohmic control of this process (ref. 69). It means that an almost nonconductive layer is formed on the electrode surface (obviously polymeric according to (ref. 70) and therefore a strongly passivating effect on aluminum reduction and oxidation is seen in the basic melt.

Wave I can be ascribed to the oxidation of  $\text{Cl}^-$  ions in slightly basic melts (ref. 24) and the disappearance of the wave I when cycling in the anodic part of the potential window can be explained by the passivating effect of the wave III surface layer.

Wave IV can be ascribed to triazolium ion reduction in the basic melt, similar to the imidazolium ion reduction in MEICl molten mixtures (ref. 64).

Despite the obvious ohmic control, waves V and VI cannot be explained by formation of passivating layers because peak current densities are significantly higher than those expected even for pure diffusional control (if, as usually for these melts, the diffusional coefficient is supposed to be ca.  $10^{-7} \text{ cm}^2/\text{s}$  and the diffusion layer is ca.  $10^{-2} \text{ cm}$ ). Perhaps the only explanation of this phenomenon is an electroreduction of specifically adsorbed triazolium-cations with formation of a stable radical and subsequent oxidation of this radical, according to equation 3.4.1:



This explanation is in good agreement with R.A. Osteryoung's observations concerning the remarkable stabilization of aromatic amine radical cations in  $\text{AlCl}_3\text{-NaCl}$  melts, even at  $175^\circ\text{C}$ , and the dependence on the melt acidity (ref. 68). In this case ohmic control can be ascribed to the lower conductivity of the  $12\text{dm}124\text{tcl}$ -rich double layer. The adsorption process has to depend on the kind of electrode material. That is why it's possible to realize a rechargeable aluminum electrode when we use pure aluminum in the acidic melt, hence suppressing triazolium adsorption.

Therefore to conclude,  $14\text{dm}124\text{tcl}:\text{AlCl}_3$  melts can be used as secondary battery electrolytes with aluminum as anode in both basic and acidic mixtures and in the wide temperature range from  $-30$  to  $170^\circ\text{C}$ .

However, the most important property of the studied electrolytes is the electrochemical activity of the triazolium chloride at potentials close to the aluminum reduction-oxidation process in the acidic melts. The utilization of reaction (3.4.1) as an anodic process instead of aluminum electrodes in secondary batteries seems to be promising because of higher reversibility, current density and theoretical capacity. Moreover, the combination of the triazolium process with such cathodic materials as polymers or with chlorine electrodes in secondary battery systems, has the following advantages: 1) absence of the ionic-exchange membrane, subsequent necessity of lower amount of the electrolyte and higher battery specific characteristics; 2) possibility of thin-layer battery design; 3) possible ecological advantage of using organic materials in the battery.

The electrochemical window of  $14\text{dm}124\text{tcl}$ -containing sodium chloroaluminate melts varied in the region of  $2.2$  to  $2.5$  V ( $150\text{-}170^\circ\text{C}$ ) depending on the melt acidity and anode material.  $14\text{dm}124\text{tcl}$ , being specifically adsorbed on the tungsten electrode surface, had an inhibiting effect on the aluminum reduction, but this effect was suppressed on the aluminum substrate.

A reversible electrochemical process with high current density (tens of  $\text{mA cm}^{-2}$ ) was observed at  $0.344$  V on the acidic sodium chloroaluminate background. It was explained as involving a free triazolium radical mechanism.

### 3.5

### Test Batteries.

Several different kinds of test batteries have been examined and they are divided into "special test cells", "unsuccessful batteries" and "partly successful batteries". Most of the successful batteries needed a separator to work.

#### 3.5.1

#### Separators.

Mainly two kinds of separators have been tested, namely Nasicon and Neosepta<sup>R</sup>.

Nasicon is a sodium conducting ceramic separator with the general chemical formula  $\text{Na}_{1+x}\text{Zr}_2\text{Si}_x\text{P}_{3-x}\text{O}_{12}$  ( $0 < x < 3$ ) (ref. 71). The Nasicon utilized to our experiments contained less  $\text{ZrO}_2$  than generally and had the formula  $\text{Na}_{2.94}\text{Zr}_{1.49}\text{Si}_{2.28}\text{P}_{0.80}\text{O}_{10.85}$ . Nasicon normally has to be used at temperatures above  $100^\circ\text{C}$ , because the specific conductivity of the ceramic is too low at room temperature ( $3.75 \cdot 10^{-4}$  S/cm at  $25^\circ\text{C}$ ,  $7.75 \cdot 10^{-3}$  S/cm at  $125^\circ\text{C}$ , (ref. 72)).

Neosepta<sup>R</sup> ion exchange membranes from Tokuyama Soda Corporation LTD., Tokyo, Japan deliver several kinds of anion and cation exchange membranes. The general structure of a cation membranes are illustrated below in Figure 3.5.1.

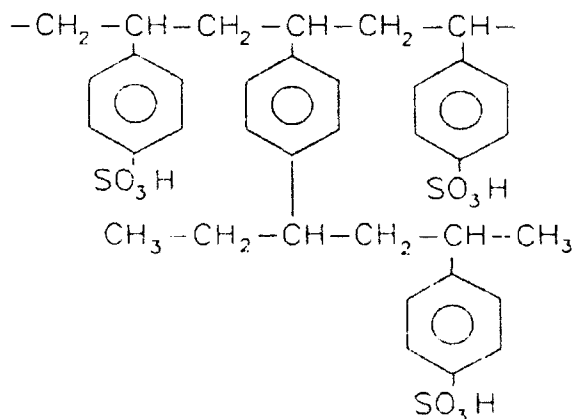


Figure 3.5.1.

General formula of Neosepta<sup>R</sup> cation (hydrogen) exchange membranes. Hydrogen been replaced by sodium in our cases.

In the anion case the  $\text{SO}_3\text{H}$  groups are replaced by a quaternary methyl ammonium chloride (ref. 73).



### 3.5.2

#### Special test cells.

##### Nasicon.

A Na/Nasicon/NaCl:MEICl:AlCl<sub>3</sub>/Nasicon/Na cell was tested at 125°C in a Witeq cell design (Figure 2.10.3) with 2 Nasicon tubes (outer diameter = 9.6 mm, thickness = 1 mm, distance = 10 mm). The cell resistance contribution from the 2 Nasicon tubes at 125°C were theoretically approximately 20  $\Omega$ , and the electrolyte contribution ( $0.40 < X_{\text{AlCl}_3} < 0.60$ ) between 5 - 7  $\Omega$  without NaCl additions, see Table 3.3.1.1. The results with different currents and compositions are given below in Figure 3.5.2.1.

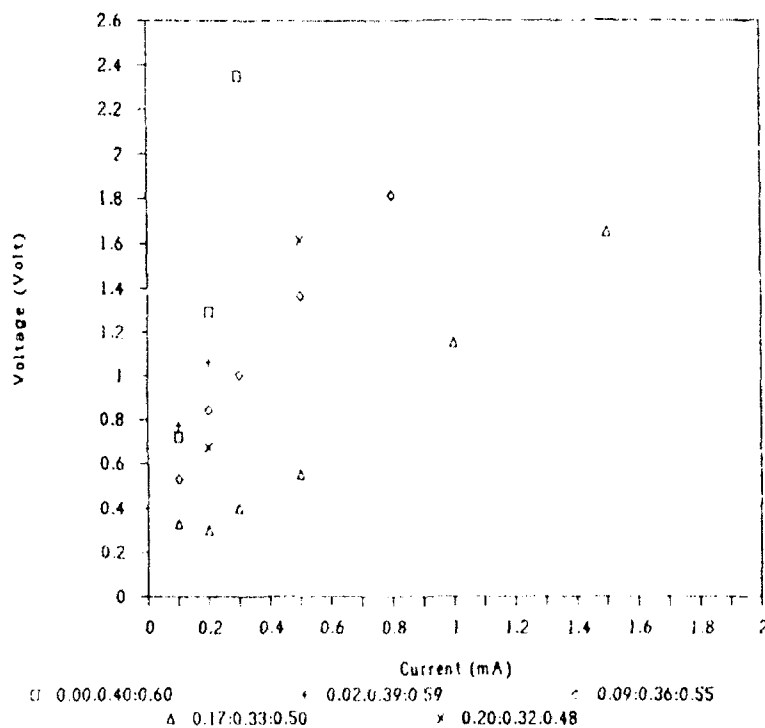


Figure 3.5.2.1.

Charge/discharge voltage (cell resistance) vs. electrolyte composition and current for the Na/Nasicon/NaCl:MEICl:AlCl<sub>3</sub>/Nasicon/Na cell at 125°C. Anodic/cathodic surface area = 5.4 cm<sup>2</sup>. Molar fractions of the electrolyte are given below the Figure, in the order NaCl:MEICl:AlCl<sub>3</sub>.

The results shown are the numeric voltage mean value of the charge/discharge operation. There was some difference between the charge voltage and the discharge voltage, probably due to non homogeneous Nasicon tubes. In the last case for NaCl saturated melts of  $\text{MEICl}:\text{AlCl}_3$  (0.20:0.32:0.48) undissolved sodium chloride crystals were seen at the bottom of the electrolyte. A more suitable molar fraction composition would then be 0.17<sub>sat</sub>:0.33:0.50.

The overall cell resistance was much higher than expected, a feature due to high overvoltages ( $\eta$ ). There is an almost linear relation between the overvoltage and the current, i.e. we have a diffusion controlled process with a 'diffusion resistance'  $R_d$ , see equation 3.5.2.1. below (ref. 74). Also we have:

$$R_d = \frac{RT}{F} \cdot \left( \frac{1}{i_R^d} + \frac{1}{i_X^d} \right) \quad (3.5.2.1.)$$

$i_R^d$ ,  $i_X^d$  are the limiting diffusion reduction and oxidation currents.  $R$ ,  $T$ ,  $F$  have their usual meaning, i.e. we have 8.314 J/mole/K, 398.15 K, 96485 C/mole, respectively.

$$i_R^d = C_R^o \frac{nFD_R}{\nu_R \delta}$$

$$i_X^d = C_X^o \frac{nFD_X}{\nu_X \delta}$$

with  $D_R$  and  $D_X$  as the diffusion coefficients,  $C_R^o$  and  $C_X^o$  as the bulk concentrations,  $n$  as the electrontransfer number,  $\delta$  as the Nernst diffusion layer, and finally  $\nu_R$  and  $\nu_X$  as the coefficients in the reaction equations ( $\nu_R$  and  $\nu_X = 1$  in our case, for  $\text{Na} \rightarrow \text{Na}^+ + \text{e}^-$ ).

The ohmic law equation 3.5.2.2 seems to be obeyed:

$$\eta = i \cdot R_d \quad (3.5.2.2)$$

It is clear that  $R_d$  changed with composition due to the change in the limiting diffusion currents.

Regression calculations of  $R_d$  for the system at the different compositions are given below in Table 3.5.2.1.

Table 3.5.2.1.

Overall cell resistance in the Na/Nasicon/NaCl:MEICl:AlCl<sub>3</sub>/Nasicon/Na cell at 125°C as a function of the compositions of the NaCl:MEICl:AlCl<sub>3</sub> electrolyte. Correlation indexes and the intersection point between the slope and the voltage axis (constant) are given too.

NaCl:MEICl:AlCl <sub>3</sub>	R <sub>d</sub> ( $\Omega$ )	R <sup>2</sup>	Constant Volt.
0.00:0.40:0.60	8150 $\pm$ 1415	0.97	- 0.18
0.02:0.39:0.59	2900 $\pm$ --*	--*	0.48
0.09:0.36:0.55	1765 $\pm$ 122	0.99	0.44
0.17:0.33:0.50	1005 $\pm$ 55	0.99	0.13
0.20:0.32:0.48	3130 $\pm$ --*	--*	0.04

\* Only 2 points !

R<sup>2</sup> defined as in equation 3.3.2.2.

The high cell resistances could perhaps be due to problems with the ceramic tubes, e.g. bad wetting of the sodium/electrolyte etc. (contact resistance). The total resistance of the cell could be expressed as a combination of the tube resistance, the contact resistance and the electrolyte resistance as given in equation 3.5.2.3.

$$R_{\text{total}} = R_d = R_{\text{tube}} + R_{\text{electrolyte}} + R_{\text{contact}} \quad (3.5.2.3)$$

From Table 3.5.2.1 it is seen that the maximal resistance contribution from the Nasicon tubes including contact problems was around 1000  $\Omega$ , i.e. there was certainly an liquid electrolyte effect too. A conductivity measurements (CDM 83) gave 228  $\mu\text{S}$  at the final composition. Calculating the cell resistance with the 228  $\mu\text{S}$  gives around 800  $\Omega$  which is close to the 1000  $\Omega$  mentioned above.

### 3.5.2.1. Neosepta<sup>R</sup> membrane.

A special stainless steel metal cell housing was used to test the cation conductivity of the Neosepta<sup>R</sup> CMX membranes, see Figure 3.5.2.1.1. As both anode and cathode an alloy of NaK (50:50 mole%) was utilized. The surface area of the membrane exposed to the alloy was 0.42 cm<sup>2</sup> and the membrane thickness was 0.017 cm. The resistance was measured by a digital ohm-meter to be around 28 k $\Omega$  before adding of the alloy to the cell. The theoretical exchange capacity (exchanging

$H^+$  with  $Na^+$  or  $K^+$ ) of the membrane was 1.5 - 1.8 times the membrane weight (including skeleton). The estimated weight of the membrane exposed to the alloy was 0.0055 g, thus the membrane exchange capacity was around 9 mAh in the  $Na^+$  case and 3.75 mAh in the  $K^+$  case.

Stainless steel cell

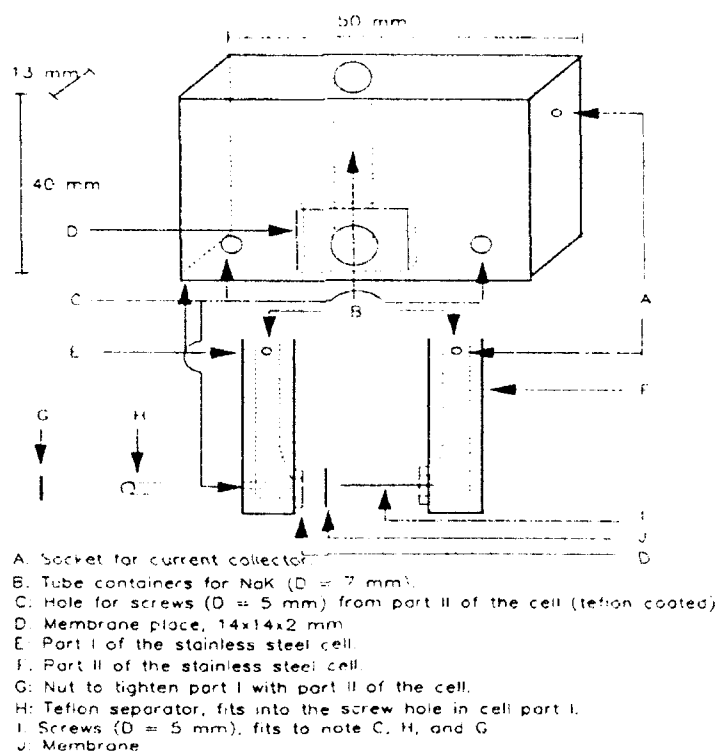


Figure 3.5.2.1.1.

Metal housing used for the NaK cell in the argon glove box.

Anodic and cathodic part of the cell marked with E and F are separated by the membrane. Both the tube containers (D=7mm) are filled with the NaK alloy, which as seen in the Figure are directly in contact with the membrane. Note, that the screws are isolated with teflon coated nuts, meaning that part E and part F are isolated from each other except through the membrane.

The cell was charged/discharged with different increasing currents as shown in Figure 3.5.2.1.2. After 27 hours, the voltage suddenly dropped to about 0 V. This happened after a total numeric load (charge + discharge) of 2.7 mAh, which was well below the theoretical  $Na^+$  exchange capacity, but fairly close to the theoretical  $K^+$  exchange capacity.

Small indications of conduction can be found in Figure 3.5.2.1.2, but by redoing the experiment with teflon rings as isolators (not

seen in Figure 3.5.2.1.1) on both side of the CMX membrane, absolutely no conductivity was seen at all. What we have seen in Figure 3.5.2.1.2 seems to be creeping currents and no real conducting has appeared at all.

We have tried other Neosepta membranes in contact with the reactive NaK alloy. If the membranes contained teflon grid they were destroyed by the alloy, otherwise they were stable.

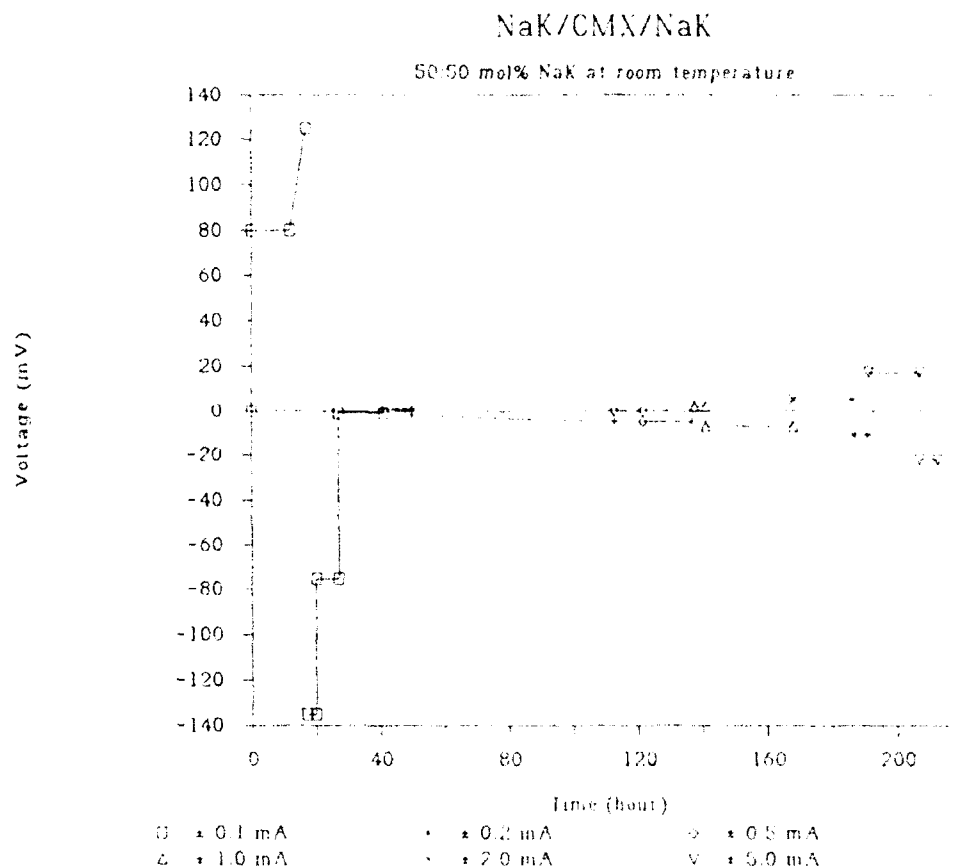


Figure 3.5.2.1.2.  
Charge/discharge of the NaK/CMX/NaK cell (NaK-1).

### 3.5.2.2 AC-impedance measurements.

By AC-impedance measurements it is possible to determine the resistance of the electrolyte and the separator separately, and furthermore to examine the contact resistance between the electrolyte and the separator. Blocking electrodes were used for these experiments. A blocking electrode consists of an inert metal in close contact with

the ionic conductor. The term blocking electrode refers to the fact that ions cannot enter the metal or react with it (ref. 75).

New separators are needed for room temperature battery applications, because the internal resistance of the known substituted NAFION<sup>R</sup> separators are rather high (ref. 17). As AC cell housing we used the brass/stainless-steel cell shown in Figure 3.5.2.2.1.

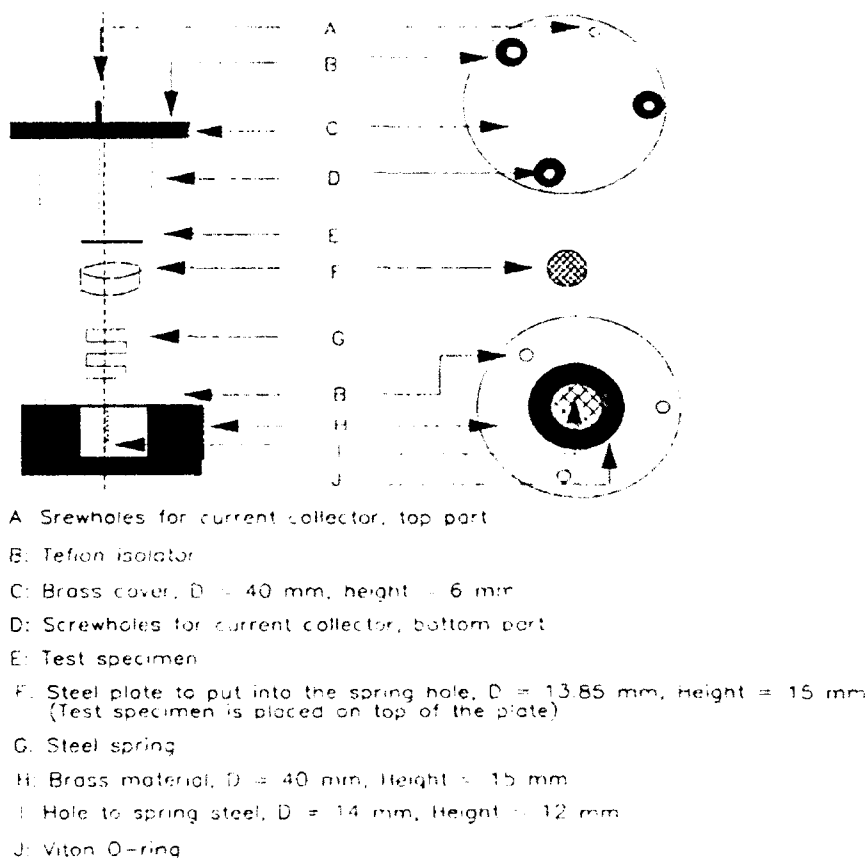


Figure 3.5.2.2.1.  
 The AC-impedance cell design.

We have done AC-impedance measurements of several Neosepta<sup>R</sup> membranes in order to find new room temperature separators, that could be used as anion ( $\text{Cl}^-$ ) or cation ( $\text{Na}^+$ ,  $\text{K}^+$ ) carriers in  $\text{MEICl}:\text{AlCl}_3$  melts:

Cation exchange membranes of the type (l= thickness of the membranes):

CMX (l=0.17mm) and C6610F (l=0.25mm), diameter = 13 mm.

Anion exchange membranes of the type:

ACS (l=0.15mm) and AMH (l=0.26mm), diameter = 13mm.

A typical result with blocking electrodes (Bck) and no liquid electrolyte is shown below in Figure 3.5.2.2.2 for the CMX case.

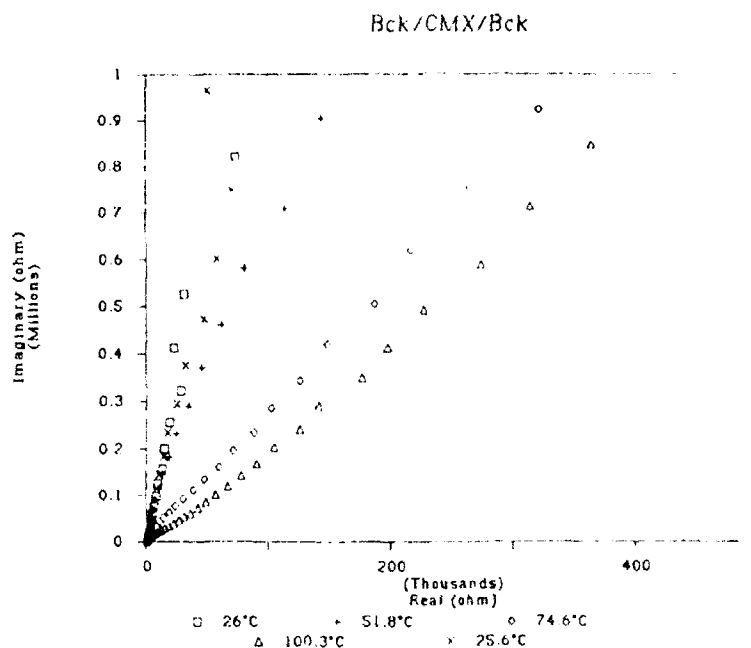


Figure 3.5.2.2.2.

AC-impedance measurements for the dry CMX cation membrane.

Conditions:

25.6°C, 26°C, 51.8°C: 2000 Hz - 1.0 MHz,

74.6°C: 735 Hz - 1.0 MHz, 100.3°C: 200 Hz - 1.0 MHz

At frequencies lower than those given in Figure 3.5.2.2.2, the impedance was not measurable. This indicated that the non wetted membrane almost was an isolator. The bulk resistance was approx. 1100  $\Omega$  for the thin membranes and 2000  $\Omega$ , for the thick types (C6610F and AMH).

Most of the membranes had turned black (except AMH) when the cells were disassembled, i.e. 100°C was too high a temperature for the stability of the membranes under these dry conditions.

To test the conductivity of the ACS and AMH Neosepta<sup>R</sup> anion exchange membranes they were wetted (one drop on each side) with a  $\text{MEICl}_3:\text{AlCl}_3$  ( $X_{\text{AlCl}_3}=0.41$ ) solution in the glove box, and placed in the AC-impedance cell (Figure 3.5.2.2.1). The obtained results are shown below in Figures 3.5.2.2.3 and 3.5.2.2.4 for the ACS case. The temperature was gradually raised to 99.3°C and then returned to room temperature (25.8°C) as shown in the text below Figure 3.5.2.2.3.

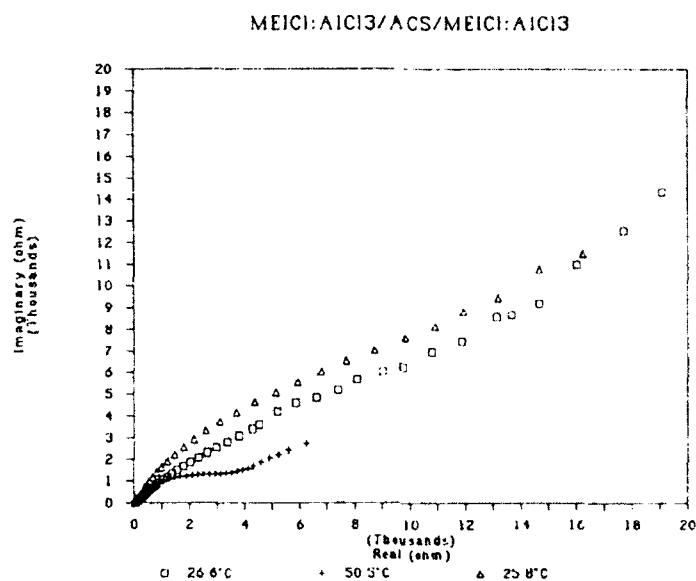


Figure 3.5.2.2.3.

AC-impedance measurements of the ACS anion membrane in a basic MEICl:AlCl<sub>3</sub> ( $X_{\text{AlCl}_3}=0.41$ ) melt, 0.01 Hz - 1.0 MHz.  
 26.6°C: Bulk resistance 65  $\Omega$ .  
 50.5°C: Bulk resistance 13.8  $\Omega$ .  
 74.1°C and 99.3°C shown below in Figure 3.5.1.3.3.  
 25.8°C: Bulk resistance 19.8  $\Omega$ .

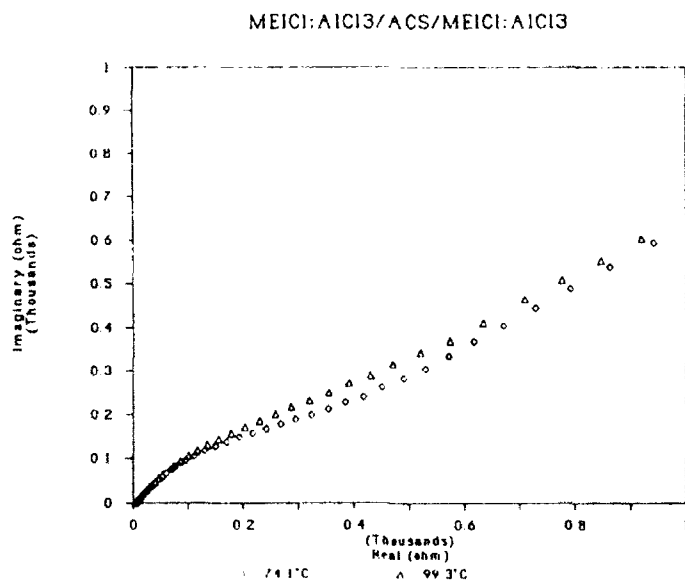


Figure 3.5.2.2.4.

AC-impedance measurements of the ACS anion membrane in a basic MEICl:AlCl<sub>3</sub> ( $X_{\text{AlCl}_3}=0.41$ ) melt, 0.01 Hz - 1.0 MHz.  
 74.1°C: Bulk resistance 5.7  $\Omega$ .  
 99.3°C: Bulk resistance 3.3  $\Omega$ .



The conductivity of the basic electrolyte can be calculated to be 15.5 mS/cm at 50°C (ref. 11), see also Table 3.3.1.1. Assuming the square area of a drop to be 0.07 cm<sup>2</sup> and utilizing the membrane thickness of 0.015 cm, we have a bulk resistance of the MEICl:AlCl<sub>3</sub> electrolyte of 13.7 Ω. Fairly close to the 13.8 Ω obtained by the AC-impedance measurements. However, the size of the drop is not constant when heated, so the above calculation only demonstrated that it is likely, that the bulk resistance is the contribution from the MEICl:AlCl<sub>3</sub> electrolyte. The preliminary high resistance at 26.6°C (65 Ω), could be explained with a bad contact between the membrane and the electrolyte. The slope at 50.5°C (Fig. 3.5.2.2.3) could be due to membrane resistance, which then can be estimated to be around 4-5000 Ω. raising the temperature to 74.1°C and 99.3°C (Fig. 3.5.2.2.4) gave a membrane resistance of approx. 500-700 Ω. When the cell was disassembled, the membrane was black, i.e. the cell has been given a too high operating temperature.

For the AMH membrane we obtained the results shown below in Figure 3.5.2.2.5 and Figure 3.5.2.2.6.

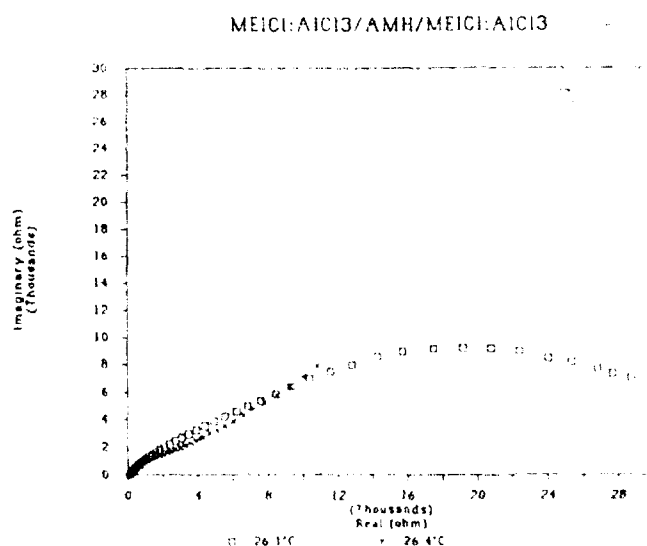


Figure 3.5.2.2.5.

AC-impedance measurements of the AMH anion membrane in a basic MEICl:AlCl<sub>3</sub> (X<sub>AlCl<sub>3</sub></sub>=0.41) melt, 0.01 Hz - 1.0 MHz.

26.4°C: Bulk resistance 113.2 Ω.

51.6°C, 74.6°C, 100.0°C see Figure 3.5.1.3.6

26.1°C: Bulk resistance 74.6 Ω.

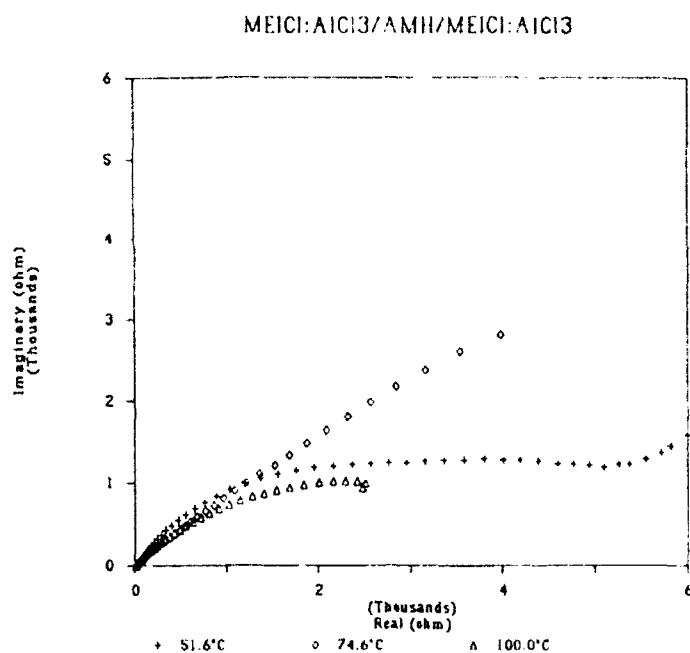


Figure 3.5.2.2.6.

AC-impedance measurements of the AMH anion membrane in a basic MEICl:AlCl<sub>3</sub> ( $X_{\text{AlCl}_3}=0.41$ ) melt, 0.01 Hz - 1.0 MHz.

51.6°C: Bulk resistance 27.3  $\Omega$ .

74.6°C: Bulk resistance 17.9  $\Omega$ .

100.0°C: Bulk resistance 13.0  $\Omega$ .

The resistance of the membranes seemed to be rather high, over 20000  $\Omega$  at the first 25°C, but then they behaved differently. The ACS resistance was 'only' about 500  $\Omega$  at 100°C, while the AMH resistance was about 4000  $\Omega$  at 100°C. The AMH membranes did not turn black even when heated to 100°C (i.e. they were temperature resistant). The conductivity of the membranes was calculated, utilizing  $\sigma = \frac{1}{R} \cdot \frac{l}{A}$  ( $A = 0.07 \text{ cm}^2$ ,  $l = 0.015$  and  $0.026 \text{ cm}$ , respectively) and  $R$  was found as the projected value of the semi circle, when crossing the real axis. The fairly approximate results are given below in Table 3.5.2.2.1.

Table 3.5.2.2.1.  
Estimated conductivities of Neosepta<sup>R</sup> membranes.

Type	ACS		AMH	
Temp. °C	R $\Omega$	$\sigma$ $\Omega^{-1} \cdot cm^{-1}$	R $\Omega$	$\sigma$ $\Omega^{-1} \cdot cm^{-1}$
25.0	24000	0.00013	36000	0.00015
50.0	4000	0.00077	7000	0.00076
75.0	550	0.0056	a	a
100.0	500	0.0061	4000	0.0013
25.0	24000	0.00013	8000	0.00066

a: It was not possible to estimate R at 75°C for the AMH.

#### 3.5.2.2.1 Conclusion.

The AC-impedance measurements have shown, that the idea of using Neosepta<sup>R</sup> membranes as a separator in room temperature batteries could be possible. Figure 3.5.2.2.2 showed that the membranes were good isolators. Figure 3.5.2.2.3 - 3.5.2.2.6 showed that the membranes could conduct anions, probably  $Cl^-$ , but Table 3.5.2.2.1 also showed that the conductivity of the membranes were perhaps too low ( i.e. compared with the 15 mS/cm for the MEICl:AlCl<sub>3</sub> ( $X_{AlCl_3}=0.41$ ) at 50°C). More precise measurements should be done with completely wetted membranes, because incomplete wetting would blur the resistance determination.

The results could be compared with the MEI<sup>+</sup> substituted NAFION<sup>R</sup> results mentioned by Renolds and Dymek (ref. 17): Internal resistances in different room temperature batteries were 150 - 300  $\Omega$ , but over 1700  $\Omega$  when the membrane was not completely wetted.

The AC-impedance measurements without separator were tested in a Na/MEICl:AlCl<sub>3</sub>/Na cell as described below.

### 3.5.2.3

### Na/MEICl:AlCl<sub>3</sub>/Na

The glass beaker cell (Figure 3.5.2.3.1) was constructed with 2 screens of nickel (10·10·0.06 mm) and tungsten current collectors. Freshly cut sodium was pressed onto both nickel screens as firmly as possible. The nickel screens was lowered into a basic MEICl:AlCl<sub>3</sub> melt ( $X_{\text{AlCl}_3} = 0.41$ ). The electrode distance was 3-6 mm. The beaker was placed inside a tight Witeg glass cell with electric feed-throughs and taken out from the argon glove box for AC-impedance measurements.

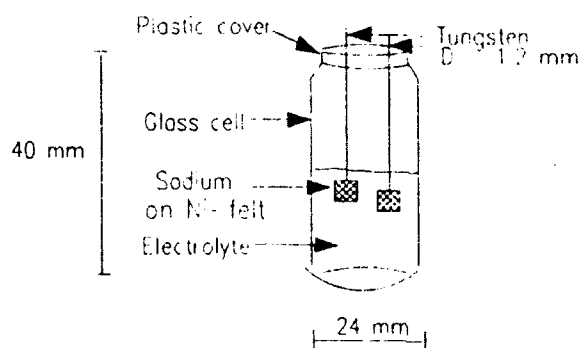


Figure 3.5.2.3.1.  
Glass beaker cell design for AC-impedance measurements.

The results are given below in Figure 3.5.2.3.2.-3.5.2.3.4, the second picture is a closer look at the 0-200  $\Omega$  region.

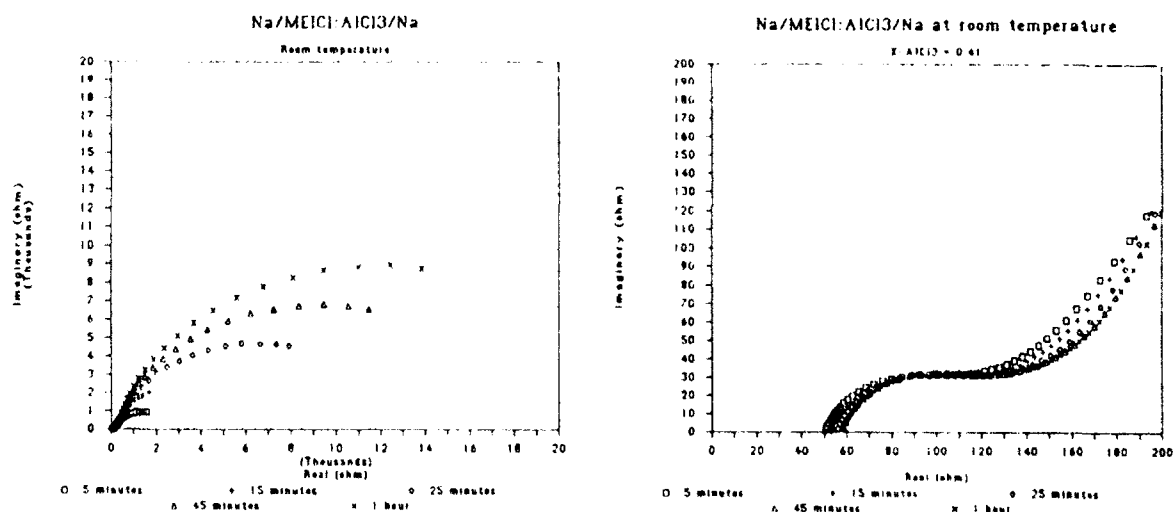


Figure 3.5.2.3.2.  
AC-impedance measurements of Na/MEICl:AlCl<sub>3</sub>/Na in a basic MEICl:AlCl<sub>3</sub> ( $X_{\text{AlCl}_3}=0.41$ ) melt, 0.01 Hz - 1.0 MHz. Cell resistance as a function of time.

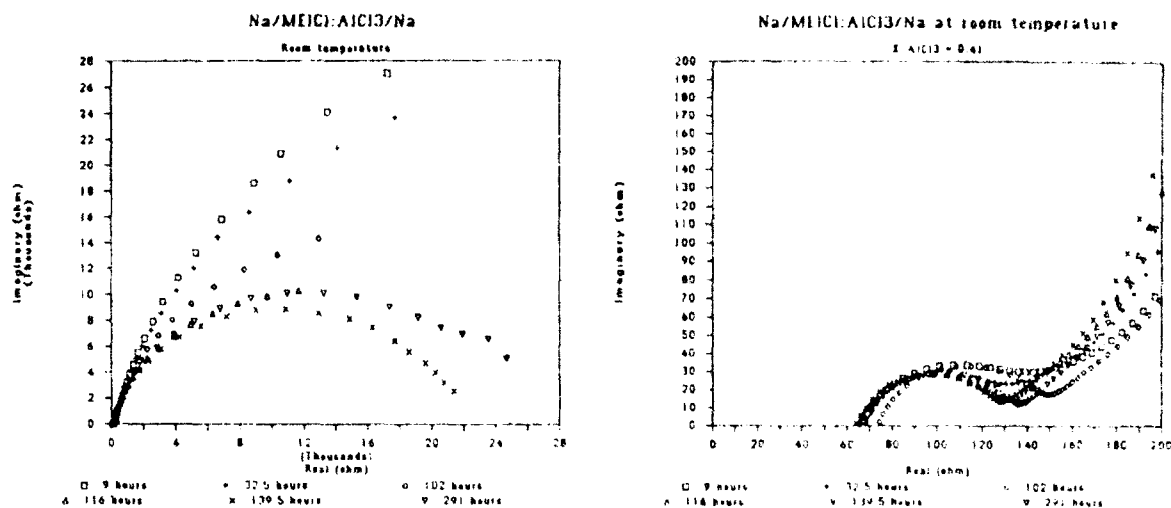


Figure 3.5.2.3.3.  
AC-impedance measurements of Na/MEICl:AlCl<sub>3</sub>/Na in a basic MEICl:AlCl<sub>3</sub> (X<sub>AlCl<sub>3</sub></sub>=0.41) melt, 0.01 Hz - 1.0 MHz. Cell resistance as a function of time.

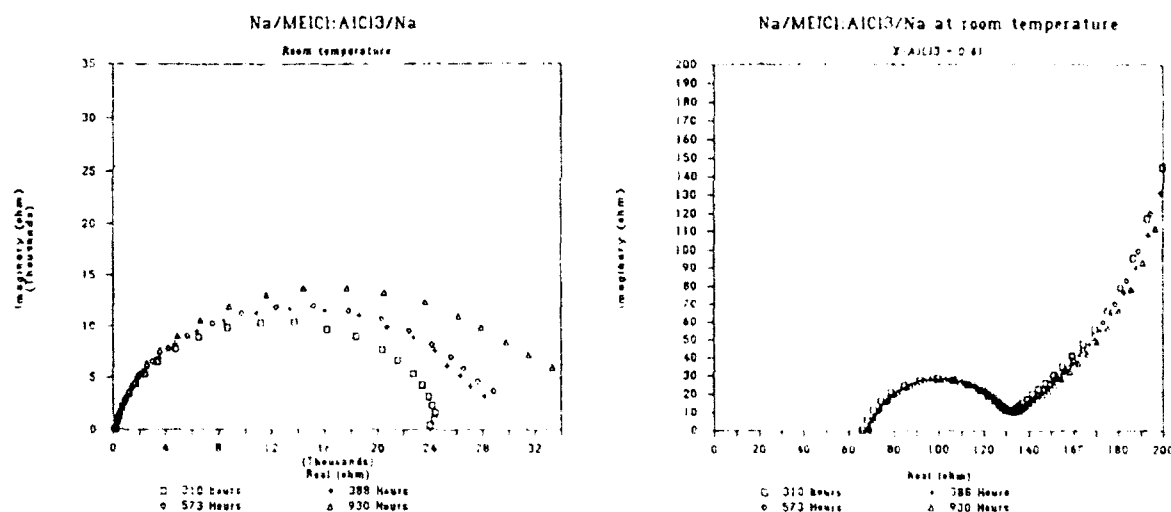


Figure 3.5.2.3.4.  
AC-impedance measurements of Na/MEICl:AlCl<sub>3</sub>/Na in a basic MEICl:AlCl<sub>3</sub> (X<sub>AlCl<sub>3</sub></sub>=0.41) melt, 0.01 Hz - 1.0 MHz. Cell resistance as a function of time.

The results indicated a quick passivation of sodium in the basic MEICl:AlCl<sub>3</sub> melt. After 5 minutes the cell resistance was approx. 3000  $\Omega$  and after 1 hour the resistance was approx. 26000  $\Omega$ , but the sodium surface still looked metallic. From the ninth to the two hundred and ninety first hours (Fig. 3.5.2.3.3) the cell resistance seemed to decrease and this was possibly due to corrosion of the nickel screens or solvation of sodium ions, and after 310 hours the

electrolyte was bluish. This could be due to an organo/nickel complex having a blue/purple color (ref. 76). However, a previous experiment with sodium pressed onto stainless steel screens, also gave a bluish solution.

It is known that reactions of sodium with aromatic hydrocarbons can give blue/green solutions (ref. 77). Dye et al. (ref. 78) found that concentrations of sodium less than  $10^{-6}$  M in ethylamine, would not give any blue color, but higher concentrations gave blue colors and they also found blue cryptate salts containing  $\text{Na}^+$ . Thus, the blue color in  $\text{MEICl}:\text{AlCl}_3$  could be due to the equilibrium mentioned in reaction 3.5.2.3.1.



The last explanation was supported by the fact, that the  $\text{MEICl}:\text{AlCl}_3$  melt contained bluish solid crystals, when we disassembled the cell.

From Figure 3.5.2.3.4 it can be seen that the cell resistance continued to increase with time after the melt probably has been saturated with the  $\text{Na(s)}$ . Figure 3.5.2.3.5 gives 2 measurements (1055, 1056 hours), one immediately after the other, but with 2 different external resistances ( $5527 \Omega$  in the first case and  $332.6 \Omega$  in the last). The voltage amplitude was in both (and all other) cases 50 mV (see Figure 3.5.2.3.6). The difference between the 2 results might be due to different choice of external reference resistances. The low resistance set gives a more accurate measurement at low cell resistance and the high resistance set gives a more accurate measurement at high resistance. This is illustrated very well in Figure 3.5.2.3.5 for the second curve. The little slope between  $65\text{--}120 \Omega$  almost disappeared (1055 hours) when the 'high' resistance set at  $5527 \Omega$  was used, in all other measurements we used the  $332.6 \Omega$  resistance set. The last curve (1098 hours) illustrate the cell resistance 15 minutes AFTER a current has been drawn through the cell (see Fig. 3.5.2.3.7). A further discharge with 1.0 mA (not shown in Figure 3.5.2.3.7) showed oscillations between 2.9 and 3.1 V.

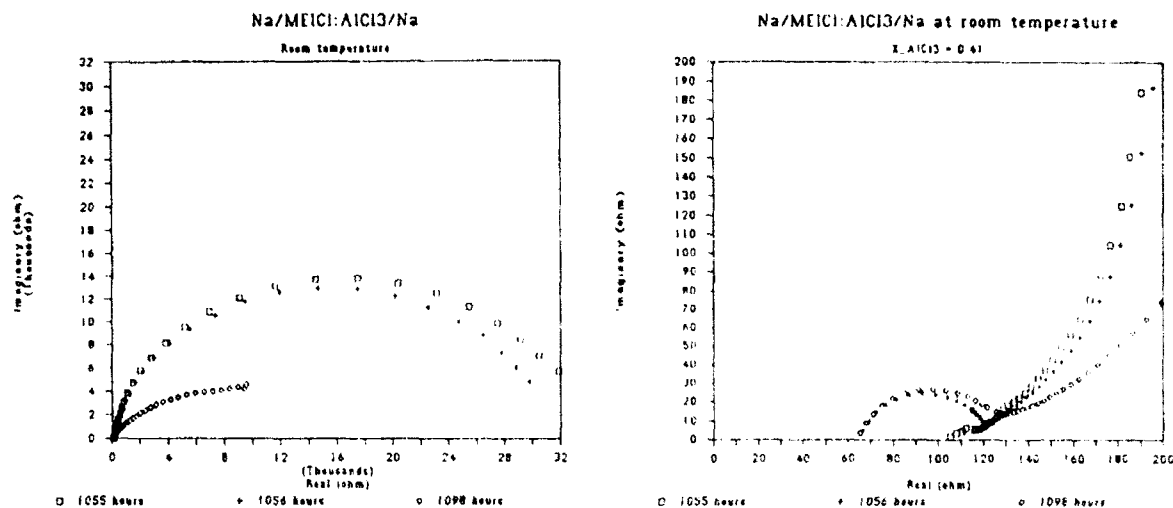


Figure 3.5.2.3.5.

AC-impedance measurements of Na/MeICl:AlCl<sub>3</sub>/Na in a basic MEICl:AlCl<sub>3</sub> (X<sub>AlCl<sub>3</sub></sub>=0.41) melt, 0.01 Hz - 1.0 MHz. Cell resistance as a function of time. 1098 hours (measured 15 minutes after charge has been stopped).

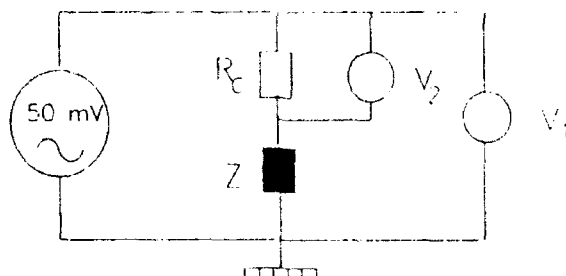


Figure 3.5.2.3.6.

Set-up for impedance measurements.  $R_c = 332.6 \, \Omega$ .  $Z$  = impedance of system measured.  $V_1$  and  $V_2$  are voltages measured by the solartron and utilized to calculate the impedance with the routines shown below:

$$I = \frac{V_2}{R_c}, \quad Z = \frac{(V_1 - V_2)}{I}, \quad \text{and by substitution } Z = R_c \frac{(V_1 - V_2)}{V_2}.$$

Figure 3.5.2.3.7 was repeated with essentially identical results for voltage vs. current and this is illustrated below in Figure 3.5.2.3.8. We have omitted the results for the charge with 5 mA, because the reached level of the closed circuit voltage (CCV) was not at a 'CCV equilibrium' level.

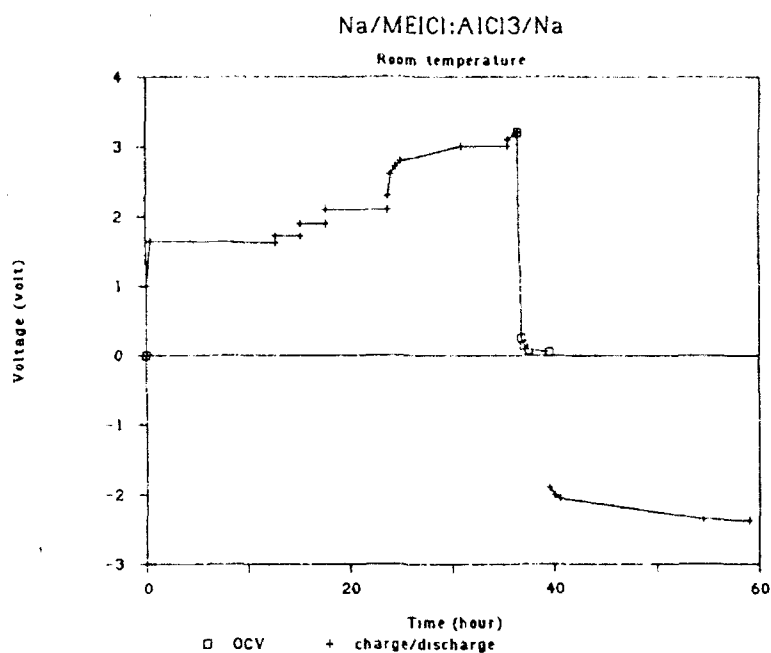


Figure 3.5.2.3.7.

Charge/discharge in the Na/MEICl:AlCl<sub>3</sub>/Na cell with a basic MEICl:AlCl<sub>3</sub> ( $X_{\text{AlCl}_3}=0.41$ ) melt. Charge with 0.1, 0.2, 0.5, 1.0, 2.0, (5.0) mA. Discharge with 1.0 mA. Active surface area approx. 1.0 cm<sup>2</sup>.

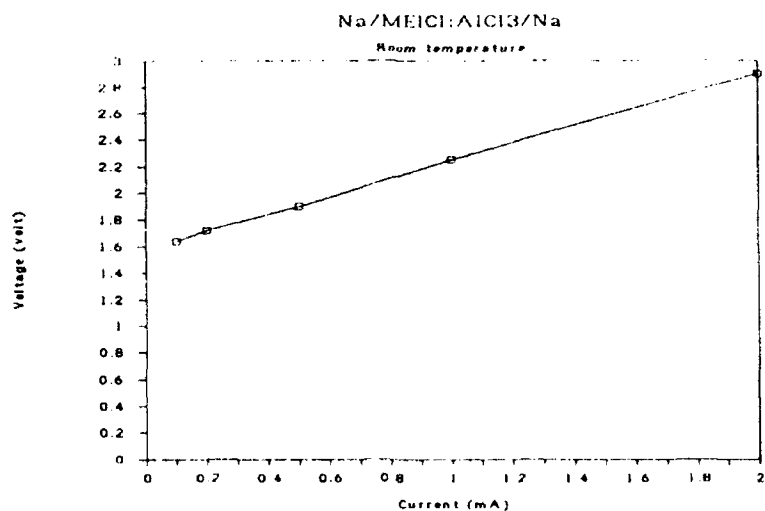


Figure 3.5.2.3.8.

Voltage vs. current in the Na/MEICl:AlCl<sub>3</sub>/Na cell with a basic MEICl:AlCl<sub>3</sub> ( $X_{\text{AlCl}_3}=0.41$ ) melt. Active surface area approx. 1.0 cm<sup>2</sup>.



By using the slope (R) of the line in Figure 3.5.2.3.8 we calculated the results in Table 3.5.2.3.1 below ( $U = \text{constant} + R \cdot I$ ,  $U = \text{close circuit voltage}$ ).

Table 3.5.2.3.1.

Overall cell resistance in the Na/MEICl:AlCl<sub>3</sub>/Na cell at room temperature.

R Ω	R <sup>2</sup>	Const. Volt.
662 ± 6	0.9997	1.58

R<sup>2</sup> defined as in equation 3.3.2.2.

#### 3.5.2.3.1 Reactions between sodium and MEICl:AlCl<sub>3</sub>.

Small ampule tests with small pieces of cleaned sodium in contact with the MEICl:AlCl<sub>3</sub> melt have been performed, and the visible reactions are summarized below in Table 3.5.2.3.1.1.

Table 3.5.2.3.1.1.

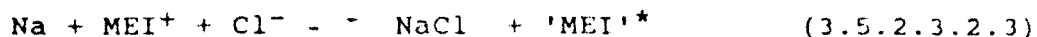
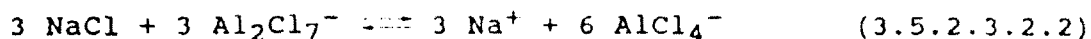
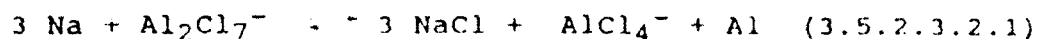
Sodium behavior towards MEICl:AlCl<sub>3</sub> melts.

MEICl:AlCl <sub>3</sub>	°C	Comments
0.40:0.60	25	Violent reaction, sodium looked black. Electrolyte brownish.
0.50:0.50	25	No visible reaction, sodium looked metallic. Electrolyte water clear.
0.60:0.40	25	No visible reaction, sodium looked metallic even after 1 year. Electrolyte water clear.
0.60:0.40	40	No visible reaction, sodium looked metallic even after 1 year. Electrolyte water clear.
0.60:0.40	80-90	Violent reaction, sodium looked black. Electrolyte brownish.

### 3.5.2.3.2 Conclusion.

Sodium will rapidly passivate in basic  $\text{MEICl:AlCl}_3$  melts. When the experiment was done in ampule the sodium looked metallic and the electrolyte were water-clear. When sodium were pressed onto nickel screens or stainless-steel meshes and currents were passed through the cells, the electrolyte turned blue/greenish. In the latter cases the experiments took place outside the glove box, with a beaker glass placed in the Witeq cell. In case that the Witeq cell was not totally tight, small impurities of water could interfere. In the Witeq cells a dark blue solid was formed at the bottom of the electrolyte. This could be due to  $\text{NiCl}_2 \cdot x\text{H}_2\text{O}$  (dark green) or  $[\text{Fe}(\text{H}_2\text{O})_6]^{2+}$  (pale blue-green). Because of the charge/discharge procedure and corrosion, traces of nickel ions or ferro ions could have appeared. In the section 3.5.3 on the 'unsuccessful test cells', we found that when sodium were pressed onto nickel or stainless-steel meshes, and when the cells were tested inside the glove box, the electrolyte turned yellow. Further investigations need to be done to solve this problem.

The resistance contribution from the  $\text{MEICl:AlCl}_3$  melt (6.9 mS/cm at room temperature) could be calculated as approx. 58  $\Omega$ , using an electrode distance of 4 mm. This fits well with the first intersections between the curves and the real axis. The  $\text{MEICl:AlCl}_3$  resistance slowly increased with time, from 50  $\Omega$  after 5 minutes, to 68  $\Omega$  after 930 hours. This could indicate that the melt gets slightly more basic (consumption of  $\text{Al}_2\text{Cl}_7^-$ ) as a function of time, i.e. reaction 3.5.2.3.2.1 and 3.5.2.3.2.2 are perhaps more likely than reaction 3.5.2.3.2.3, even in basic melts where the concentration of the hepta-chloroaluminate ion is expected to be low.



\* It is not clear what the reduction product of  $\text{MEI}^+$  is. The melt did not change color when sodium was wetted (Table 3.5.2.3.1.1), i.e. a very little amount of  $\text{MEI}^+$  must have been reduced if reaction 3.5.2.3.2.3 did take place.

The curves between 60-130  $\Omega$  (Figure 3.5.2.3.2 to 3.5.2.3.5) are not quite understood at present, but they tend to be stable with time, i.e. around 70  $\Omega$ , even after the charge procedure (1098 hours in Figure 3.5.2.3.5).

The charge/discharge curves (Fig. 3.5.2.3.7 and Fig. 3.5.2.3.8) showed that it was possible to break the passivation layer. From Figure 3.5.2.3.8 and Table 3.5.2.3.1 we can estimate an OCV of 1.58 V, indicating a Na/Al plateau or a Na/'MEI' plateau. The reduction of  $\text{MEI}^+$  is supposed to take place at 300-400 mV below the Na/Al plateau, according to cyclic voltammograms (CV's) from Dieter et al. (ref. 16), so it seems to be a Na/Al plateau. If we actually plated aluminum in a basic melt with sodium acting as a catalyst, it is a new and promising invention. A lot of active sodium was still present in the cell when it was disassembled.

By comparing results from the Na/MEICl:AlCl<sub>3</sub>/Na cell (Table 3.5.2.3.1) with the Na/Nasicon/NaCl:MEICl:AlCl<sub>3</sub>/Nasicon/Na cell at 125° (Table 3.5.2.1) it can be seen that a significantly lower working resistance is obtained by omitting the Nasicon separators, even though there is a 100°C temperature disadvantage.

The stability of sodium in the MEICl:AlCl<sub>3</sub> melts is depending both on the temperature and on the composition as shown in Table 3.5.2.3.1.1. Our results demonstrate that the claimed stability of sodium in basic MEICl:AlCl<sub>3</sub> melts saturated with NaAlCl<sub>4</sub> (C.-L. Yu et al., ref. 7), seems not to be obeyed when omitting the NaAlCl<sub>4</sub> salt.

### 3.5.3

### Unsuccessful test cells.

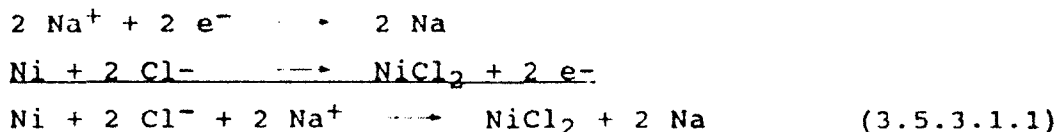
Two moderate temperature sodium cells with nickel or nickel sulphide as a cathode and with Nasicon or beta"-alumina as a separator have been tested, as presented below. Nine room temperature sodium anode batteries have been examined too, together with two aluminum anode cells.

#### 3.5.3.1

Na/Nasicon/MEICl:AlCl<sub>3</sub>/Ni<sub>3</sub>S<sub>2</sub> and  
Na/Beta"-alumina/MEICl:AlCl<sub>3</sub>/Ni.

The Na/Nasicon/MEICl:AlCl<sub>3</sub>/Ni<sub>3</sub>S<sub>2</sub> cell (NaNi-71) with a basic electrolyte ( $X_{\text{AlCl}_3} = 0.38$ ) and a stable OCV of 2.46 V at 125°C was discharged at 1 mA (0.2 mA/cm<sup>2</sup>). However, after 36 minutes the closed circuit voltage dropped below 0 V, due to the opposing overpotential. From Table 3.5.2.1 we can estimate the overpotential to be around -3 V, i.e. the cell failed to work because of the behavior of the Nasicon ceramic. The electrolyte became immediately bluish in contact with the nickel sulphide.

A similar experiment with a Na/Beta"-alumina/MEICl:AlCl<sub>3</sub> + NaCl<sub>sat</sub>/Ni cell (NaNi-72) with the binary MEICl:AlCl<sub>3</sub> mole fraction of aluminum chloride ( $X_{\text{AlCl}_3}$ ) equal to 0.40, gave an OCV of 2.23 V (T = 122°C). Again the electrolyte was bluish. A second nickel electrode was introduced into the melt to help understanding the reactions during charge. The assumed occurring reactions are given below, equation 3.5.3.1.1.



In Figure 1.3.2 we displayed the observed Na/NiCl<sub>2</sub> plateau's. By charging with 1 mA (0.1 mA/cm<sup>2</sup>) the voltage immediately increased

from the 2.23 V to 3.0 V, indicating an initial charge resistance of 770  $\Omega$ . During the next 5 hours the voltage increased linearly to the limit of the test equipment (4.095 V). The stable OCV after charging was measured to be : Na/nickel(1) = 2.74 V, nickel(2)/nickel(1) = - 0.042 V with nickel(1) being the charged electrode. Obviously, no stable  $\text{NiCl}_2$  was formed during the charging procedure.

It was possible to discharge the cell with 1 mA for 24 hours before 0 V (closed circuit voltage) was reached. Initially the CCV reached 0 volt, before it slowly (during 1 hour) increased to 0.9 V. The discharge plateau was around 0.9 V for the first 10 hours and then slowly dropping to 0 V during the next 14 hours. The discharge resistance then seems to be more than twice the value of the initial charge resistance, i.e. approx. 1800  $\Omega$ . The final charge resistance was however also around 1800  $\Omega$ . As for the Sodium/Nasicon special cell in Table 3.5.2.1, the cell resistance was too big for battery application.

### 3.5.3.2 Na/Nasicon/ $\text{FeCl}_3$ :1m3pmb123tcl: $\text{AlCl}_3$ /Mo.

From Table 3.2.1 and Table 3.3.2.1 it can be seen that 1m3pmb123tcl was a possible candidate as an electrolyte component for batteries. Furthermore the MOPAC calculations presented in Table 3.1.1 predicted the 1m3pmb123t<sup>+</sup> cation to be very stable towards reduction. A Witeq cell (Figure 2.10.3) with Na/Nasicon/ $\text{FeCl}_3$ :1m3pmb123tcl: $\text{AlCl}_3$ /Mo (NaFe-21) was examined at 125°C, the molar fraction of the electrolyte ( $\text{FeCl}_3$ :1m3pmb123tcl: $\text{AlCl}_3$ ) being 0.09:0.36:0.55, respectively. The electrolyte was heated to 70°C to accomplish a complete liquid solution and the OCV was measured to be 2.72 V. Unfortunately there was some red gas evolution at 70°C and the electrolyte turned black. Probably the paramethoxy-benzyl group was decomposing. After that, the electrolyte was very viscous and no discharge current ( 1 mA, 0.33 mA/cm<sup>2</sup>) could be drawn, without the CCV dropping below 0 V.

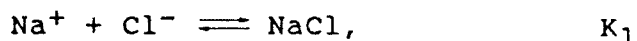
Other test batteries without separators have been examined.

### 3.5.3.3

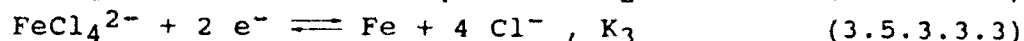
### Na/FeCl<sub>3</sub>:MEICl:AlCl<sub>3</sub>/C-felt/W.

The expected charge/discharge reactions for the Na/FeCl<sub>3</sub>:MEICl:AlCl<sub>3</sub>/C-felt/W (NaFeC-2) are illustrated below in equation 3.5.3.3.1, 3.5.3.3.2 and 3.5.3.3.3.

Anodic:



Cathodic:



By assuming that the activity coefficients of the ions are unity, the Nernst half cell equations can be written as shown below. The electrode potential is solvent dependent, so one should write the electrode half cell potential as  $\epsilon = (\pi_{\text{electrode}} - \phi_{\text{solvent}})$ .

The  $\theta$  superscript denotes a normal oxidation potential (1 atm., 25°C) and the square brackets denote concentrations in mole/L (ref. 79).

Anode:

$$(\pi - \phi) = (\pi - \phi)_{\text{Na}^+/\text{Na}}^\theta + \frac{RT}{F} \cdot \ln[\text{Na}^+] \quad (3.5.3.3.4)$$

Cathode:

$$(\pi - \phi) = (\pi - \phi)_{\text{FeCl}_4^-/\text{FeCl}_4^{2-}}^\theta + \frac{RT}{F} \cdot \ln\left(\frac{[\text{FeCl}_4^-]}{[\text{FeCl}_4^{2-}]}\right) \quad (3.5.3.3.5)$$

$$(\pi - \phi) = (\pi - \phi)_{\text{FeCl}_4^{2-}/\text{Fe}}^\theta + \frac{RT}{2F} \cdot \ln\left(\frac{[\text{FeCl}_4^{2-}]}{[\text{Cl}^-]^4}\right) \quad (3.5.3.3.6)$$

All of the equilibria above are chloride dependent ( $\text{pCl}^-$ ), i.e. by measuring the OCV as a function of the  $\text{pCl}^-$  one should probably obtain a curve with several plateaus (at least two from the cathode). It is a little difficult to measure the OCV as function of  $\text{pCl}^-$ , because the potential of sodium is not stable in the melt. It would therefore be better to do a potentiometric study, e.g. with a fixed anodic potential (Pt) and a fixed cathodic current collector (RVC or perhaps molybdenum), and then dissolve some FeCl<sub>3</sub> in the melt.

This basic glass beaker cell was made as shown in Figure 3.5.2.3.1 (using carbon felt and dissolved  $\text{FeCl}_3$  as cathode), and was tested in an argon glove box with an oxygen content of less than 10 ppm, and a dew point below  $-50^\circ\text{C}$ . The basic melt was not saturated with  $\text{FeCl}_3$  and the molar ratio of the electrolyte ( $\text{FeCl}_3:\text{MEICl}:\text{AlCl}_3$ ) was 0.02:0.59:0.39, respectively. The anodic capacity was 118 mAh and the cathodic capacity was 95 mAh. The surface area was approx.  $2\text{ cm}^2$  for the anode and  $2.5\text{ cm}^2$  for the cathode (without considering the porosity of the carbon felt).

By connecting a recorder to the anode/cathode couple before they were lowered into the melt, the OCV was measured as a function of time from the true beginning. The self discharge curve is shown in Figure 3.5.3.3.1, and as expected, the rate was exponential decreasing. According to equation 3.5.3.3.1 to 3.5.3.3.3 and the theory, it should be possible to see at least two plateaus in the curve due to the equilibrium constants ( $K_2$ , and  $K_3$ ), and actually this was the case.

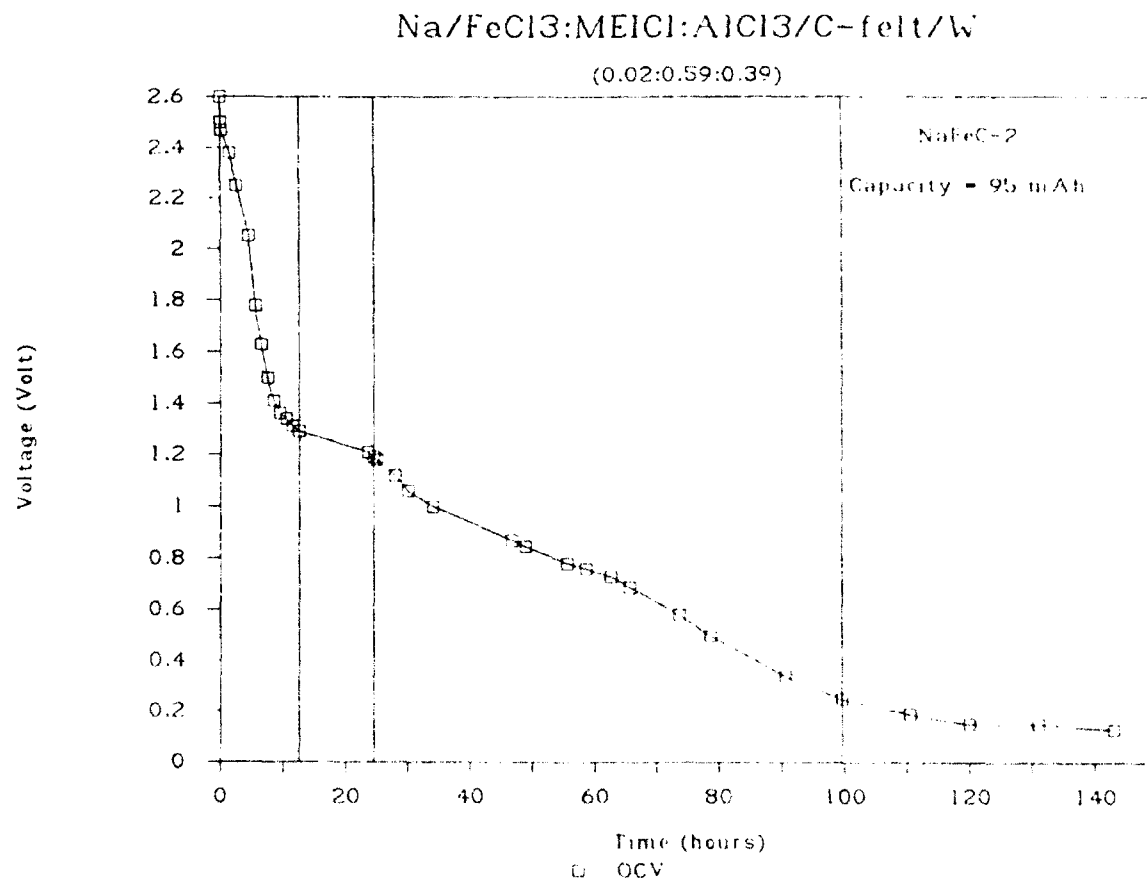


Figure 3.5.3.3.1.  
Self discharge of the NaFeC-2 cell, showing that at least two equilibrium constants are involved in the discharge mechanism.

We tried to charge the cell during an accelerated test, with anodic current densities of approx.  $0.0005 \text{ mA/cm}^2$ ,  $0.005 \text{ mA/cm}^2$  and  $0.05 \text{ mA/cm}^2$  as shown in Figure 3.5.3.3.2. When charging with  $0.1 \text{ mA}$  ( $0.05 \text{ mA/cm}^2$ ) the electrolyte became red, which indicated a reduction of the organic cation (ref. 17). After 1 hour of charge with the  $0.1 \text{ mA}$ , the voltage increased sharply from  $2.85 \text{ V}$  to  $3.25 \text{ V}$ . It was possibly here that the melt started to decompose ( $\text{MEI}^+ + \text{e}^- \rightarrow \text{'MEI'}$ ).

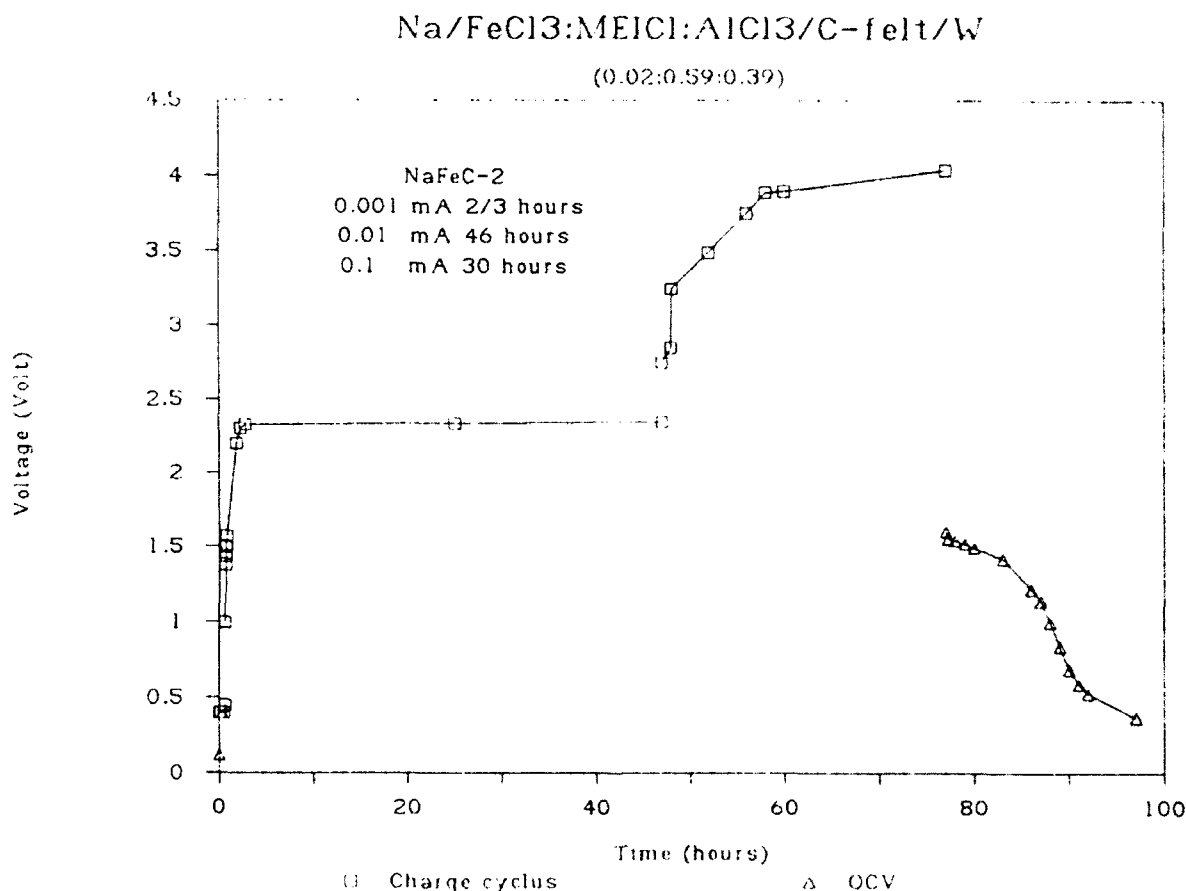


Figure 3.5.3.3.2.  
Accelerated charge curve for the NaFeC-2 cell. Probably, the organic cation was reduced after 1 hour of charge with  $0.1 \text{ mA}$ .

### 3.5.3.3.1 Conclusion.

A room temperature molten salt sodium battery of the type concerned was not stable in the basic  $\text{FeCl}_3\text{:MEICl:AlCl}_3$  electrolyte as estimated by the impedance measurements in chapter 3.5.2.3. Furthermore there



was not enough  $\text{FeCl}_3$  in the cell to saturate it. When omitting the separator, the solvent contribution will be 0 V ( $\phi_{\text{anode}} - \phi_{\text{cathode}} = 0$  V), therefore it is important to operate with saturated cathodic melts. There has to be some undissolved  $\text{FeCl}_3$  (inside the carbon felt) to give a high potential difference, or else we would just measure the potential of  $\pi_{\text{Na}^+/\text{Na}} - \pi_{\text{C}^{4+}/\text{C}}$ .

Another chloride cathode was tried as described below.

3.5.3.4 Na/CuCl<sub>2</sub>:MEICl:AlCl<sub>3</sub>/Stainless steel mesh (NaCu-1)  
and Na/MEICl:AlCl<sub>3</sub>/CuS (NaCuS-1).

Hussey et al. (ref. 80), who introduced  $\text{CuCl}_2$  into an acidic aluminum chloride-N-methyl-pyridinium chloride (0.67:0.33 mole%) melt observed a bright yellow solution in contrast to the green colour of  $\text{Cu(II)}$  in the ternary  $\text{AlCl}_3$ - $\text{NaCl}$ - $\text{KCl}$  melt (0.66:0.20:0.14 mole%) at 135°C (see ref. 80). They claimed that the yellow color was due to solvation of  $\text{Cu(II)}$  by the  $\text{Al}_2\text{Cl}_7^-$  ion instead of a solvation by chloride. Because Raman examinations of an aluminum chloride-N-(n-butyl) pyridinium chloride (0.67:0.33 mole%) melt showed that in the acidic case it almost entirely consists of the  $\text{Al}_2\text{Cl}_7^-$  ion (see ref. 80).

By polarizing a copper foil, copper(I) acidic solutions were found to be colorless, and the reduction of  $\text{Cu}^{2+}$  to  $\text{Cu}$  were found by voltammetry to take place in 2 single steps (ref. 80). In that work, Hussey et al. also mentioned that  $\text{Cu(I)}$  solutions became faintly yellow when exposed to a dry atmosphere containing oxygen, and they suggested the reforming of  $\text{Cu(II)}$  to explain the color. Finally, they decided the copper(II)/copper(I) and the copper(I)/copper redox pairs to have standard potentials of 1.851 V and 0.777 V, respectively, at 30°C in the previous mentioned acidic melt vs. Al in a pure  $\text{AlCl}_3$ -N-methyl-pyridinium chloride (67-33 mole %) melt.

It is known from the literature (ref. 76) that  $\text{Cu(I)}$  easily makes Cu-C bondings and that alkyl groups react in copper solutions with copper(I) to give alkyl copper. Methyl copper is a slightly yellow polymer, which is insoluble in many organic solvents. Normally the formed  $\text{Cu}_2\text{O}$  is red but a yellow modification can also be obtained

(ref. 76). Cu(II) chloride complexes are mainly  $\text{CuCl}_4^{2-}$ , except in water where  $[\text{Cu}_2\text{Cl}_6]^{2-}$  is formed.

Osteryoung and Nanjundiah (ref. 81) investigated the Cu-Cu(I)-Cu(II) couples in the butyl-pyridinium chloride (BuPyCl) - aluminum chloride ionic liquid at 40°C. They reported values for the standard potentials both in basic and acidic cases, vs. aluminum in a 2:1  $\text{AlCl}_3$ :BuPyCl mixture. Their results are shown below in Table 3.5.3.4.1.

Table 3.5.3.4.1.

Standard potential of copper couples in  $\text{AlCl}_3$ :BuPyCl melts versus aluminum in acidic 2:1 (molar)  $\text{AlCl}_3$ :BuPyCl melt (ref. 81).

Molar melt composition. $\text{AlCl}_3$ :BuPyCl	Redox couple.	Standard potential. $E^\theta$
0.67:0.33	$\text{Cu(I)} + e^- \rightleftharpoons \text{Cu(0)}$	0.784 V
0.67:0.33	$\text{Cu(II)} + e^- \rightleftharpoons \text{Cu(I)}$	1.825 V
0.67:0.33	$\text{Cu(II)} + 2e^- \rightleftharpoons \text{Cu(0)}$	1.305 V*
0.43:0.57	$\text{Cu(I)} + e^- \rightleftharpoons \text{Cu(0)}$	-0.647 V
0.43:0.57	$\text{Cu(II)} + e^- \rightleftharpoons \text{Cu(I)}$	0.046 V
0.43:0.57	$\text{Cu(II)} + 2e^- \rightleftharpoons \text{Cu(0)}$	-0.301 V*

\* Calculated value.

The cells were made in a glass beaker as shown in Figure 3.5.2.3.1, and they were all tested in an argon glove box. In the case of NaCu-1, it turned out that sodium (pressed onto a stainless steel mesh) kept its metallic surface in the basic  $\text{CuCl}_2$ :MEICl: $\text{AlCl}_3$  electrolyte (0.08:0.55:0.37, respectively).  $\text{CuCl}_2$  dissolved readily in the melt which became yellow, even though it was a basic melt, i.e. it is not likely that Cu(II) is solvated by  $\text{Al}_2\text{Cl}_7^-$ , as mentioned by Hussey et al. (ref. 80). Furthermore, when both Na and  $\text{CuCl}_2$  were in the melt together, an unknown yellow layer was formed on the sodium surface. The sodium metal probably reduced Cu(II) to Cu(I). The  $\text{Cu}^+$  might then react with impurities such as oxygen (if any) forming a yellow layer of  $\text{Cu}_2\text{O}$ , or perhaps  $\text{Cu}^+$  might react with the MEICl, removing the alkyl groups and forming methyl copper as a yellow layer. The alkyl

groups then interacts with the sodium surface, giving the impression that the formation was directly on the sodium surface.

An experiment with a copper(II) chloride solution in a basic  $\text{MEICl}:\text{AlCl}_3$  melt which further contained a stainless steel mesh and nothing else, showed discoloring as time passed by. The Fe from the stainless steel could be oxidized by the  $\text{Cu}^{2+}$  ion and thereby reducing the copper(II) concentration in the melt and thus lowering the color. The  $\text{Na}/\text{MEICl}:\text{AlCl}_3:\text{CuCl}_2/\text{stainless steel mesh}$  showed no measurable potential after 1 hour.

In the  $\text{NaCuS-1}$  case, the basic molar melt composition of the  $\text{MEICl}:\text{AlCl}_3$  electrolyte was 0.58:0.42, and with a theoretical CuS amount of 169 C (47 mAh). If CuS was included into the electrolyte the composition was 0.576:0.414:0.010, respectively. The sodium anode consisted of Na (400 mAh), pressed onto a steel mesh with a tungsten current collector welded onto the mesh. The cathode was made in the same way, with the CuS pressed onto the mesh but with 5 w/w % active carbon and 5 w/w % teflon binder added to the CuS. Active surface area of anode or cathode was approximately  $0.5 \text{ cm}^2$ .

An OCV of 0.98 V was measured about 10-15 min. after assembling the cell. It had a fast decreasing rate. Unfortunately there was no recorder connected to the cell. After 3 days the OCV was 0 Volt.

The anode (sodium) kept its metallic surface. The CuS was soluble in the melt, which turned yellow immediately after the copper sulfide was put into the melt. The color is not quite in agreement with the observations of Hussey et al. (ref. 80), because they claimed the yellow color to be due to solvation of  $\text{Cu}^{2+}$  by  $\text{Al}_2\text{Cl}_7^-$ . Our melt is basic i.e. the dominant ions are  $\text{Cl}^-$  and  $\text{AlCl}_4^-$  and not  $\text{Al}_2\text{Cl}_7^-$ . During self discharge/passivation the solution lost much of its color.

We tried to charge the cell with 0.1 mA (Figure 3.5.3.4.1), and reached a stable plateau at 1.65 V for the first 5 hours, then a tendency to oscillate started. After 16 hours the oscillations were intensive, with peak voltages over 5 V (unfortunately out of the recorder range, and not given in Figure 3.5.3.4.1). The charge was terminated after 28h (voltage polarization over 20 V was reached, not shown in Figure 3.5.3.4.1). The OCV quickly dropped to 1.4 V, and then more slowly down to 0.28 V as shown in Figure 3.5.3.4.1. During the OCV/self discharge measurement, the voltage continued to oscillate. Whether there were 2 plateaus or not during the self discharge could not be detected due to the oscillations.

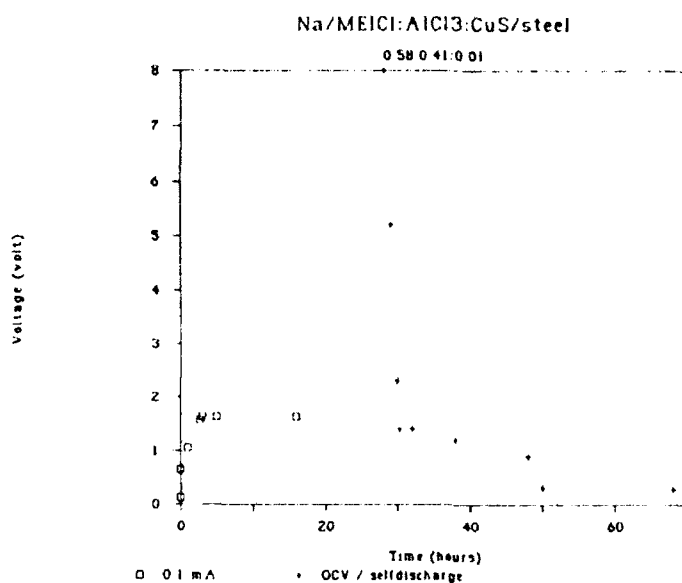
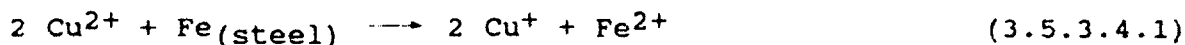


Figure 3.5.3.4.1.  
Charge/self discharge curve for NaCuS-1 at room temperature.

#### 3.5.3.4.1 Conclusion.

The experiments showed that it was possible to put current through the system. The expected voltages are given below, calculated by assuming equation 3.5.3.4.1 to be dominating:



Assuming that the Cu(II)/Cu(I) standard potential of the basic BuPyCl melt (0.046 V) is still valid for the basic aluminum chloride imidazolium-chloride melt, the 'loaded' Fe<sup>2+</sup>/Fe couple potential can be calculated. This is given in equation 3.5.3.4.2, below, again assuming activity coefficients of unity.

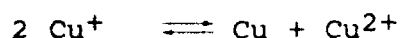
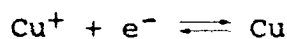
$$E = E_{\frac{\text{Cu}^{2+}}{\text{Cu}^+}}^{\theta} - E_{\frac{\text{Fe}^{2+}}{\text{Fe}}}^{\theta} + \frac{RT}{F} \cdot \ln \frac{[\text{Cu}^{2+}]}{[\text{Cu}^+][\text{Fe}^{2+}]^{0.5}} \quad (3.5.3.4.2)$$

Half the way during oxidation of Cu<sup>+</sup> to Cu<sup>2+</sup>, we should theoretically have [Cu<sup>2+</sup>] = [Cu<sup>+</sup>] = 0.0428 M and [Fe<sup>2+</sup>] = 0.0214 M. For obtaining this result we have used the density equation a + b(T-60) from ref. 11 to calculate the molar concentrations.

Inserting a voltage value of 1.1 V (taken from the self discharge curve in Figure 3.5.3.4.1), gives  $E_{\frac{1}{2}}^0 = -1.0$  V. The value expected,

from reference 25 in basic aluminum chloride butyl-pyridinium chloride melt, is around -1.0 V to -1.15 V at cell equilibrium, depending on the degree of basicity.

It fits well to assume reversibility of the reaction mentioned in equation 3.5.3.4.1, but we also have to consider the reactions shown below:



This gives the Nernst equation (3.5.3.4.4) below, assuming equilibrium and activity coefficients of unity.

$$E = E_{\frac{\text{Cu}^{2+}}{\text{Cu}^+}}^0 - E_{\frac{\text{Cu}^+}{\text{Cu}}}^0 + \frac{RT}{F} \cdot \ln \frac{[\text{Cu}^{2+}]}{[\text{Cu}^+][\text{Cu}]} \quad (3.5.3.4.4)$$

Half the way during oxidation of  $\text{Cu}^+$  to  $\text{Cu}^{2+}$  and Cu, we should theoretically have  $[\text{Cu}^{2+}] = [\text{Cu}^0] = 0.5 [\text{Cu}^+] = 0.0214$  M.

Again inserting the voltage of 1.1 V into equation 3.5.3.4.4 gives a Cu(I)/Cu(0) standard potential of -0.99 V, which is far from the value of -0.647 V observed by Osteryoung et al. (ref. 81) in basic aluminum chloride-n-butylpyridinium chloride.

Finally, it seems that  $\text{Cu}^{2+}$  was reduced to  $\text{Cu}^+$  by iron from the steel, so steel meshes can not be used together with copper solutions in basic  $\text{MEICl}:\text{AlCl}_3$  melts. Impurities of  $\text{Fe}^{2+}$  will give pale yellow and bright yellow solutions in basic and acidic  $\text{MEICl}:\text{AlCl}_3$  melts, respectively (ref. 64). Sodium was passivated, and was perhaps not involved at all in the charge/discharge reactions. The cell gave an OCV of 0 V, because of the sodium passivation (we just had two steel meshes dipped into the same solution). The copper(II)/copper(I) couple presumably was a reversible pair in the basic melt.

### 3.5.3.5

### Na/MEICl:AlCl<sub>3</sub>/FeS (NaFeS-22).

The Na/MEICl:AlCl<sub>3</sub>/FeS cell was made in a glass beaker as shown in Figure 3.5.2.3.1, and was tested in an argon glove box. The molar composition of the basic electrolyte MEICl:AlCl<sub>3</sub> was 0.582:0.418 with an anodic capacity of 245 mAh and a cathodic capacity of 23 mAh. The surface area of anode or cathode was estimated to be 0.50 cm<sup>2</sup>. Including the FeS into the electrolyte gives the molar composition 0.576:0.413:0.011, respectively.

5-10 minutes after the cell was made, the OCV was measured as 1.1 V, decreasing fast, and after 12 hours the OCV was 0.42 V. An almost stable plateau at 0.16 V was reached after 48 hours. By charging the cell with 0.1 mA (approx. 0.2 mA/cm<sup>2</sup>) for 22 hours we slowly reached 2.0 V, but immediately after stopping the charge, the voltage dropped as shown in Figure 3.5.3.5.1.

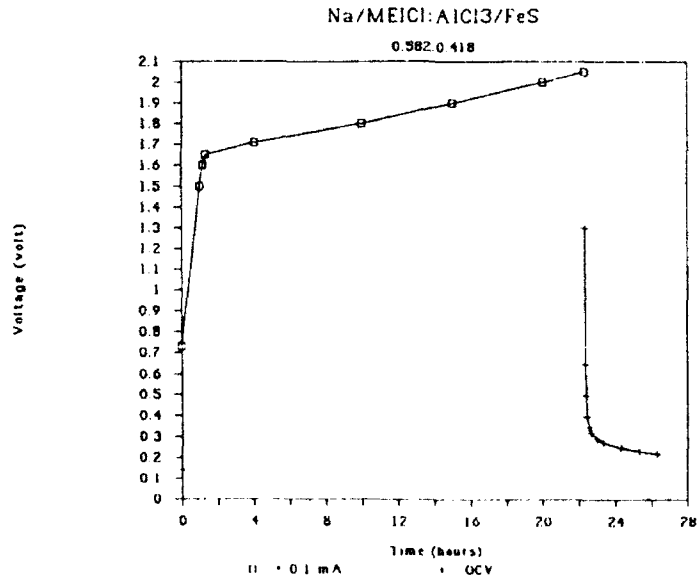


Figure 3.5.3.5.1.  
Charge/self discharge curve for NaFeS-22 at room temperature.

Again, the reason for the decreasing OCV was a passivation (or self discharge) of the sodium anode, because as mentioned in a previous

chapter (3.5.3.1), the potential of a Na/separ-  
tor/MEICl:AlCl<sub>3</sub>/Ni<sub>3</sub>S<sub>2</sub>(or Ni) (separator = Nasicon or Beta"-alumina)  
was stable at 2.46 V (or 2.23 for the pure Ni mesh) at 120°C. I.e.  
the sulfide cathode was stable in the MEICl:AlCl<sub>3</sub> basic melt.

#### 3.5.3.5.1 Conclusion.

Obviously, there was a difference between the sodium/iron trichloride  
battery (NaFeC-2) mentioned earlier (Fig. 3.5.3.3.1, 3.5.3.3.2), and  
this sodium/iron sulfide battery, because the voltage was lower in  
the sulfide case. This is in agreement with theoretical calculations  
using JANAF's thermodynamic tables. Furthermore the CCV charge plateau  
is not stable in the sulfide case, but it increases with time. The  
reason for this continuous increase could be sodium ion diffusion  
caused by too high current densities, but it could also be a cathodic  
potential change with time, due to intercalation of ions like Cl<sup>-</sup>,  
Na<sup>+</sup> or Al<sup>3+</sup>, thereby forming new compounds like Na<sub>p</sub>Fe<sub>q</sub>SrCl<sub>s</sub>.

In conclusion sulfur must thus be an active part of the elec-  
trochemical reaction, even during charge.

#### 3.5.3.6 Na/MEICl:AlCl<sub>3</sub>/V<sub>2</sub>O<sub>5</sub>- NaVo-1.

We made a basic (X<sub>AlCl<sub>3</sub></sub>=0.42) battery in the same way as for the  
other glass beaker cell (sodium pressed onto a steel mesh with a  
welded tungsten current collector). The cathode was V<sub>2</sub>O<sub>5</sub> pressed  
directly onto the steel mesh without adding teflon suspension or  
carbon powder (this turned out to be a bad idea because some of the  
cathode was falling off the mesh). The cathodic capacity was theo-  
retically 6.84 C (assuming x = 3 in Na<sub>x</sub>V<sub>2</sub>O<sub>5</sub>), and the anodic capacity  
was 254 mAh. As for the other sodium cells, the measured voltage

(0.60 V) was much lower than the expected, and it obviously depends on the time the sodium has been exposed to the melt. The cell was destroyed by a mistake.

3.5.3.7                      Na/MEICl:AlCl<sub>3</sub>/Al.  
                                 NaAl-3.

We tried to make a 'primary' room temperature molten salt Na/Al battery (NaAl-3) in a basic MEICl:AlCl<sub>3</sub> ( $X_{\text{AlCl}_3} = 0.42$ ) melt. Theoretically, we should neither be able to discharge the cell (plating of Al) nor charge the cell (formation of sodium).

The cell was made in the same way as for the other glass beaker cells (NaCuS-1 and NaFeS-22) with sodium pressed onto a steel mesh with a welded tungsten current collector. The cathode was an aluminum cylinder (diameter = 0.7 cm and height = 0.5 cm) pressed onto a tungsten current collector. The cell (NaAl-3) quickly reached a constant potential of -0.80 V (Na/Al) !. Another battery made with sodium directly pressed onto a tungsten current collector instead of steel mesh gave an initial OCV of 1.26 V, but dropped quickly to a stable plateau of -0.40V.

The second cell was charged with 0.1 mA (approx. 0.07 mA/cm<sup>2</sup> anodic and cathodic) for 47h at a plateau of approx. 1.05 V. After the first 2 hours, the closed circuit voltage suddenly dropped as can be seen in Figure 3.5.3.7.1. By increasing the current to 1 mA (0.7 mA/cm<sup>2</sup>) for the next 51 hours the CCV raised to more than 3 V. Further increase to 2 mA (1.4 mA/cm<sup>2</sup>) only raised the CCV slightly to 3.5 V (Figure 3.5.3.7.1), but with some oscillations in the first period of charge. The electrolyte was colorless in the beginning, but this slowly changed to yellow during the charging procedure, and by the high voltages to red/brown. By stopping of charging the OCV rapidly dropped through a smooth voltage/time curve, ending on a value of 0.07 V, after a week.



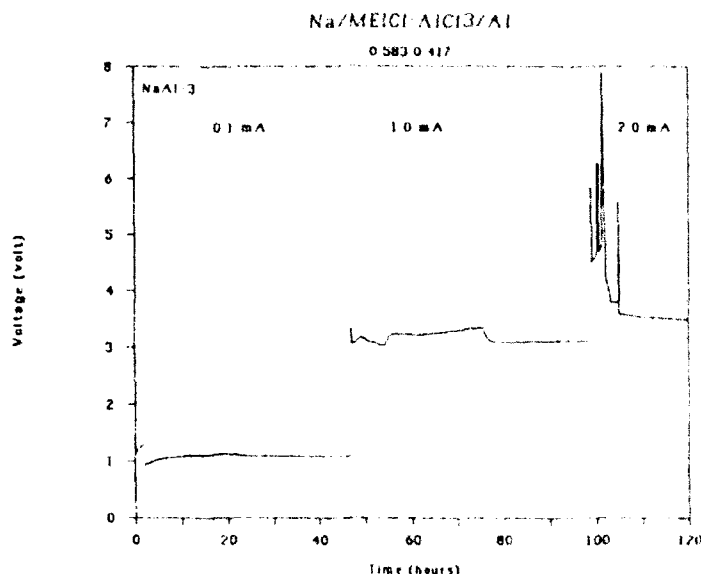


Figure 3.5.3.7.1.  
Charge curve for NaAl-3 at room temperature.

#### 3.5.3.7.1 Conclusion.

The negative OCV values obtained could be explained by a complete passivation of the sodium, such that we actually were measuring the potential difference between steel/Al or in the second case W/Al. Expected calculated voltages for a Fe/(0.4)/Al, C/0.4/Al and a W/0.4/Al cell would be -0.91 V, -1.60 V and -1.65 V, respectively (ref. 64) (0.4 means  $X_{\text{AlCl}_3} = 0.40$  in a MEICl:AlCl<sub>3</sub> melt). Our measurements are then probably a mixed potential between Na/Fe, carbon or wolfram and Al.

The voltage drop after 2 hours in the charging procedure is probably due to a passivation of the Al cathode, because the other cells (NaCuS-1 and NaFeC-2) did not show this behavior. Furthermore, many other scientists have found passivation of aluminum in acidic melts. Donahue (ref. 18) found that the passivating film probably consisted of reaction intermediates that were generated during oxidation of aluminum in the acidic MEICl:AlCl<sub>3</sub>. This was probably also the case here, even though our melt was basic.

During charge it seemed possible to strip aluminum from the cathode, but what happened at the anode?

It is a fact that sodium is unstable in acidic melts with a fast reaction turning the surface black, but is relatively stable in basic melts. Does this indicate that the  $\text{Al}_2\text{Cl}_7^-$  ion is involved in the process? A possible dissolution process of sodium has been given in equation 3.5.2.3.2.1 and 3.5.2.3.2.2.

In acidic melts with a high concentration of  $\text{Al}_2\text{Cl}_7^-$  ions and a

fairly high solubility of sodium chloride (1.82 M at  $X_{\text{AlCl}_3}=0.60$  (ref. 82)), reactions 3.5.2.3.2.1 and 3.5.2.3.2.2 are supposed to be rather fast. Reactions 3.5.2.3.2.1 and 3.5.2.3.2.2 are of course much slower in basic melts, because the concentration of  $\text{Al}_2\text{Cl}_7^-$  ion is low and the solubility of the sodium chloride is less than  $7.5 \cdot 10^{-3}$  M in these melts (ref. 82). Furthermore reaction 3.5.2.3.2.1 is suppressed in basic melts, because it is difficult/not possible to plate aluminum in those melts. That is perhaps why sodium looks stable in basic melts (Table 3.5.2.3.1.1). The blackness of sodium in acidic melts could be caused by Al being plated directly onto the sodium or a passivated surface of sodium. But usually it is not possible to form alloys between sodium and aluminum, so probably it has to be an intermediate in between. Many investigators have reported a black aluminum surface after plating (see ref. 18).

Equation 3.5.2.3.2.3 is probably dominating when the cell was charged with 1-2 mA (Fig. 3.5.3.7.1), because the electrolyte changed in color to brown/red due to a decomposition of the organic compound. We estimated the ordinate value of a straight line between the 2 voltage plateau values corresponding to 1 mA and 2 mA in charging current (see Figure 3.5.3.7.2) to give an approximate voltage of 2.7 V for the overall cell reaction. This probably corresponds to the oxidation of the organic ring, which can be calculated to take place at approximately 2.35 V (ref. 64) for a basic  $\text{MEICl}:\text{AlCl}_3$  melt ( $X_{\text{AlCl}_3} = 0.40$ ). 2.35 V is close to the estimated 2.7 V, when the oscillations during the charging process is considered.

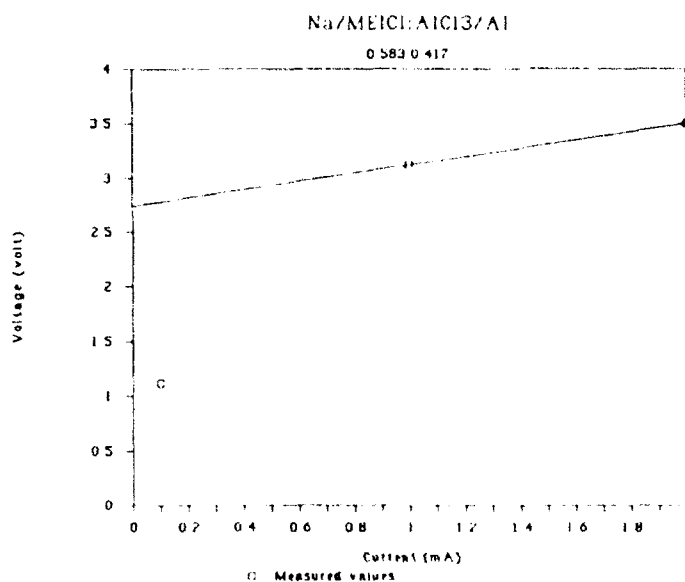


Figure 3.5.3.7.2.  
Voltage/charge current for the NaAl-3 battery at room temperature.

Lastly we tried some batteries with aluminum anodes instead of the passivated sodium.

3.5.3.8                      Al/MEICl:AlCl<sub>3</sub>/FeS.  
FeS-38.

The expected OCV for this system is around 0.8 V. Investigations at our laboratory have shown that a sodium/Nasicon/NaAlCl<sub>4</sub>/FeS battery has an OCV of 2.4 V at 175°C. Substituting Na with aluminum decreases the voltage with approx. 1.6 V. Furthermore the Gibbs free energy of FeS is almost constant between room temperature and 175°C (actually it is decreasing slightly according to JANAF's thermodynamical tables), i.e. the OCV only changes a little with the temperature. The system was made basic to compare with the newly tested sodium batteries, then being a primary cell. Previous investigations by Wilkes and Piersma (ref. 83) have shown high irreversibility of cells containing sulfur compounds.

The cell was assembled as the previously mentioned beaker glass cells (Figure 3.5.2.3-1). The theoretical amount of FeS was 43 mAh (a 2 electron process), with a cathodic surface area of 2.0 cm<sup>2</sup>. The anodic surface area was 1.5 cm<sup>2</sup> and the capacity around 1700 mAh. The composition of the basic MEICl:AlCl<sub>3</sub> electrolyte was 0.58:0.42. The OCV was recorded to be 1.35 V immediately after assembling the cell, but OCV quickly dropped to a value of 0.80 V, stable for several days. We tried to discharge the cell with different current densities, but at 0.040 mA (0.020 mA/cm<sup>2</sup> cathodic) the voltage dropped below 0 V within 1 hour. Changing the discharge rate to 0.030 mA (0.015 mA/cm<sup>2</sup>) immediately raised the closed circuit voltage to 0.40 V. During the next 13 hours the CCV dropped linearly from the 0.40 V to 0 V. After terminating the discharge, the OCV slowly increased to 0.78 V during the next 35 hours, see Figure 3.5.3.8.1.

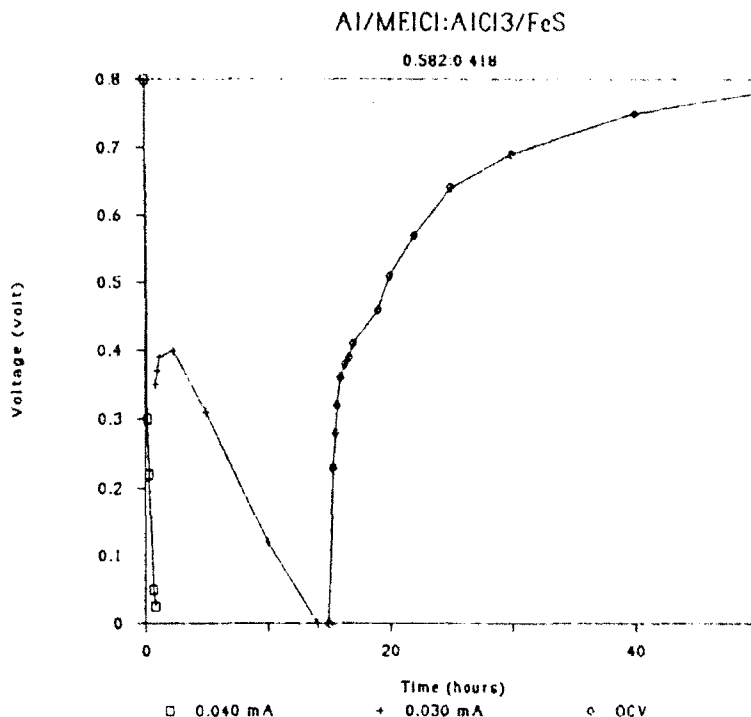


Figure 3.5.3.8.1.

OCV of the Al/MEICl:AlCl<sub>3</sub>/FeS cell discharged with 0.020 and 0.015 mA/cm<sup>2</sup> cathodic current densities.

#### 3.5.3.8.1 Conclusion.

The internal cell resistance was very high (voltage drop of 0.40 V when discharging with 0.030 mA, i.e. a resistance larger than 10000 Ω). The resistance is probably caused by the sulfur containing cathode, because it is well known that aluminum can be stripped of at high current densities in MEICl:AlCl<sub>3</sub> melts. The previously mentioned Al/MEICl:AlCl<sub>3</sub>:FeCl<sub>3</sub>/RVC cell (Fig. 1.3.1) was easily discharged with 1.25 mA/cm<sup>2</sup> (ref. 18). The resistance problem was also mentioned by Takami and Koura (ref. 23), who claimed that a high polarization of the FeS<sub>2</sub> cathode occurred below 100°C in butylpyridinium:AlCl<sub>3</sub> melts.

Therefore, as mentioned by Wilkes and Piersma (ref. 83), it is desirable to avoid sulfides as electrochemical active species in the room temperature melts. Introduction of NaCl to the melt could perhaps

help the cathodic discharge reaction by making some kind of 'NaAlSCl<sub>2</sub>' compound. This might indicate an acidic electrolyte with small additions of NaCl could be worth trying as a last attempt.

3.5.3.9                      Al/NaCl:MEICl:AlCl<sub>3</sub>/TiS<sub>2</sub>.  
TiS-1.

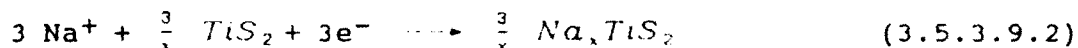
The cell was assembled as previously (beaker glass cell, Figure 3.5.2.3.1).

The cathode mixture contained 90 w/w % TiS<sub>2</sub>, 5 w/w % C and 5 w/w % dry teflon suspension. The TiS<sub>2</sub> mixture was pressed onto squared Pt meshes giving a total area of 0.5 cm<sup>2</sup>. An aluminum rod with tungsten current collector was used as anode. The theoretical capacity was 5.8 mAh based on Na<sub>x</sub>TiS<sub>2</sub> (x=1). An acidic electrolyte of MEICl:AlCl<sub>3</sub> (X<sub>AlCl<sub>3</sub></sub> = 0.525) was saturated with NaCl. The electrolyte composition could then be specified as NaCl:MEICl:AlCl<sub>3</sub> (0.2298:0.3661:0.4041) or more accurately due to the saturation by NaCl (0.025:0.475:0.500, respectively). The OCV was measured to be 1.0 V, as shown in Figure 3.5.3.9.1. Expected reactions are given below in equation 3.5.3.9.1 and 3.5.3.9.2.

Anode:



Cathode:



The discharging took place with very low current densities due to the problems illustrated in Figure 3.5.3.9.1. After ending of discharge, the cell slowly gained some voltage (OCV = 0.15 V after 10 hours).

The electrode kinetics seem to be too slow for battery applications.

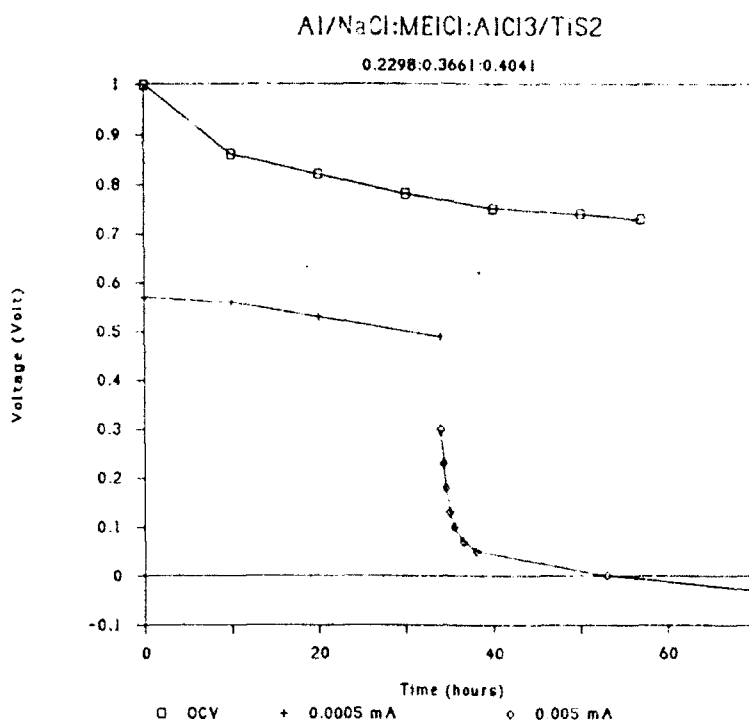


Figure 3.5.3.9.1.  
OCV of the Al/NaCl:MEICl:AlCl<sub>3</sub>/TiS<sub>2</sub> cell discharged  
with 0.001 and 0.01 mA/cm<sup>2</sup> cathodic current densities.

#### 3.5.4                      Partly successful test cells.

As mentioned in section 3.5, all the successful cells needed a separator.

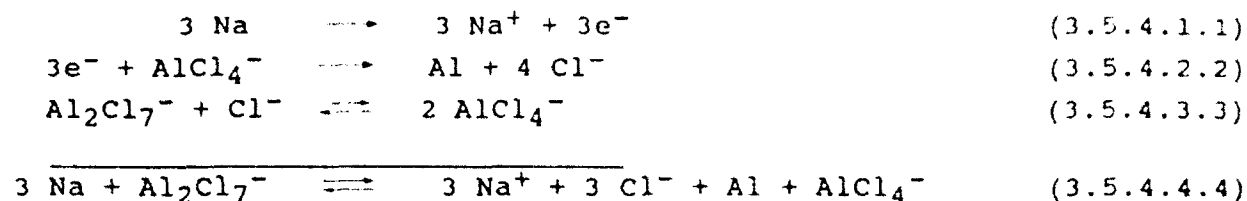
Below we present the 8 cells we have tested.

##### 3.5.4.1                      Na/Nasicon/MEICl:AlCl<sub>3</sub>/Al.

Using the Witeg cell design of Figure 2.10.3 and replacing the molybdenum current collector with an aluminum rod (height = 6 mm, diameter = 7 mm) pressed on a tungsten wire, we tested two Na/Nasicon/MEICl:AlCl<sub>3</sub>/Al cells (NaAl-1 and NaAl-2) at 125°C (for NaAl-1 an extra Na/Nasicon electrode was introduced into the melt. We denote the two Na/Nasicon electrodes Na(1) and Na(2), respectively). For the NaAl-1 cell we omitted the Pyrex/Teflon tape/Nasicon seal

shown in Figure 2.10.3. The electrolyte was acidic, having a molar fraction  $X_{\text{AlCl}_3} = 0.60$ . The aluminum anodes were chosen, in order to have electrodes known to work in acidic  $\text{MEtCl}:\text{AlCl}_3$  melts.

The reactions expected during charge and discharge are :



When discharging the cells ( $\rightarrow$ ) the electrolyte becomes more basic. When charging the cells ( $\leftarrow$ ) we should be able to reach the starting point again ( $X_{\text{AlCl}_3}=0.60$ ).

The coulombic limitation of the discharge was calculated from the amount of sodium (885 mAh for the NaAl-1 cell and 815 mAh for the NaAl-2 cell), the amount of Al (1700 mAh for both cells), and the amount of electrolyte available (2000 mAh\* for both cells). The coulombic limitation for the maximum charge was the amount of sodium ions formed in the electrolyte during discharge.

For the NaAl-1 cell we measured the OCV to be 2.29 V at room temperature and 2.22 V at 125°C. The conductivities between the two Na/Nasicon electrodes and the Al electrode were measured at room temperature. The conductivities were expressed as resistances by estimating electrode distances and surface areas. These estimates gave room temperature resistances of 4650  $\Omega$ , and 39900  $\Omega$ , respectively, between the Na/Nasicon electrodes and the Al electrode (see Table 3.5.4.1.1). These values indicated a bad contact between the sodium and the Nasicon, when sodium has not been melted. After heating to 125°C, the same resistances were estimated to be 12  $\Omega$  and 77  $\Omega$ , respectively.

The NaAl-1 cell was then discharged with 0.5 mA between Na(1)/Al using a galvanostat (a high precision instrument). The closed circuit voltage dropped immediately to 1.87 V, and then slowly increased, during the discharge, to 1.97 V. After 51 h the discharge was stopped and the OCV was measured. The discharge process were repeated as shown in Table 3.5.4.1.1 and Figure 3.5.4.1.1.

\* The capacity of the electrolyte with respect to Al plating (during discharge) depends on the excess of  $\text{AlCl}_3$  (i.e. the amount of  $\text{AlCl}_3$  that changes  $X_{\text{AlCl}_3}$  from 0.50 to 0.60). As it is known, one cannot plate Al from a basic melt.

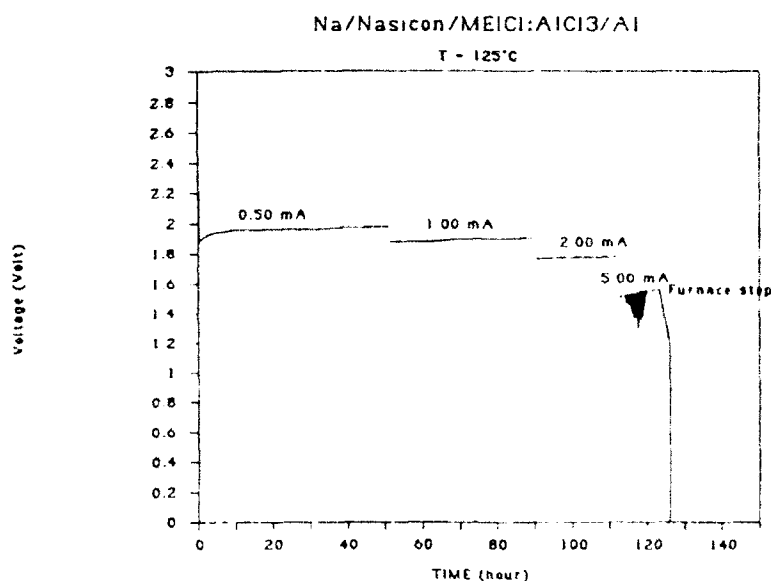


Figure 3.5.4.1.1  
Discharge of the Na/Nasicon/MEICl:AlCl<sub>3</sub>/Al (NaAl-1) cell.  
(See also Table 3.5.4.1.1, note 2).

Table 3.5.4.1.1.  
Na/Nasicon/MEICl:AlCl<sub>3</sub>/Al (NaAl-1).  
Voltage and resistance after different discharge currents.  
TIME denotes the total time the cell has been discharged.

	Current mA	Na(1)/Al	Na(2)/Al	Na(1)/Na(2)	TIME(h) Total	mAh Total
OCV 20°C ohm 20°C	0	2.30 V 39900	2.28 V 4650	0.021 V 8825	0	0
OCV 125°C ohm 125°C	0	2.21 V 77.0	2.22 V 12.4	- 0.012 V 57.3	0	0
OCV 125°C ohm 125°C	0.50	2.17 V 48.8	2.19 V 14.2	- 0.013 V 39.0	51	25.5
OCV 125°C ohm 125°C	1.00	2.14 V 50.0	2.14 V 14.2	- 0.006 V 36.3	90	64.5
OCV 125°C ohm 125°C	2.00	2.11 V 41.2	2.12 V 12.7	- 0.005 V 35.3	112 <sup>1</sup>	108.5
OCV 30°C ohm 30°C	5.00	- 0.05 V 46800	2.07 V 885	- 1.94 V 363375	124 <sup>2</sup>	168.5

- 1: After discharge, the Al cathode turned black, furthermore there was black sodium in the top of the Nasicon tubes.
- 2: The cell was discharged with 5.0 mA for approximately 12 h, and during this period there was an oven malfunction, causing the sodium to solidify. The Nasicon tube (no. 1) cracked, and the electrolyte looked reddish.

The electrode distances and surface areas used to calculate the ohmic resistances in Table 3.5.1.1.1 were:  
Na(1)/Al = 2.75 cm, Na(2)/Al = 0.70 cm, Na(1)/Na(2) = 1.25 cm.  
Surface areas Na/Al = 1.3 cm<sup>2</sup>, Na/Na = 2 cm<sup>2</sup>.



The result of the unintended furnace stop showed, that it was not possible to discharge the cell (NaAl-1) with 5 mA (approximately 3.8 mA/cm<sup>2</sup>) at room temperature. Then we tried to charge the cell (NaAl-1) with 0.5 mA between the electrodes Na(2) and Al at room temperature. However, the closed circuit voltage exceeded the voltage limit of the test equipment (4 V), probably due to a bad contact (room temperature) between the sodium and the ceramic separator. By visual inspection, we found that also Nasicon tube 2 had a minor crack. The low ohmic resistance measurements between the Na(2)/Al couple had indicated this from the very beginning. From the slope of the line in Figure 3.5.4.1.2, we calculated ohmic resistances (R) as shown in Table 3.5.4.1.2 below.

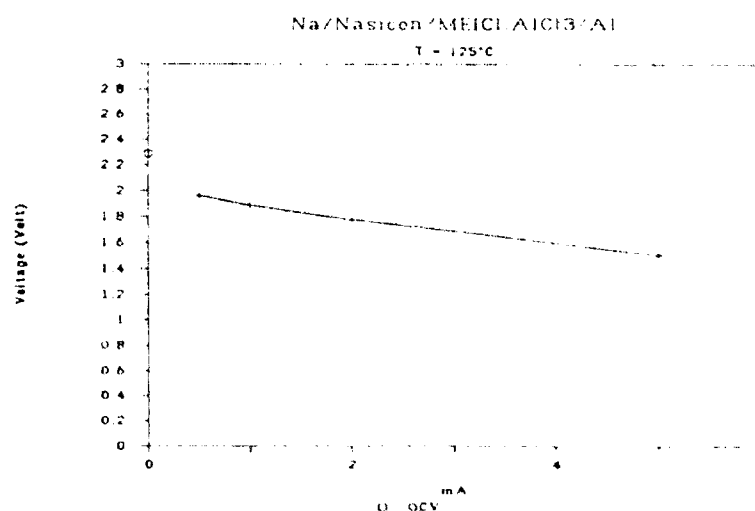


Figure 3.5.4.1.2.

Voltage vs. current in the Na/Nasicon/MEICl:AlCl<sub>3</sub>/Al (NaAl-1) cell with an acidic MEICl:AlCl<sub>3</sub> (X<sub>AlCl<sub>3</sub></sub>=0.60) melt. Active surface area approx. 1.3 cm<sup>2</sup>.

Table 3.5.4.1.2.

Overall cell resistance in the NaAl-1 cell at 125°C.

R Ω	R <sup>2</sup>	Const. Volt.
98 ± 5	0.9947	1.99

R<sup>2</sup> is defined in equation 3.3.2.2. Const. is the intercept value at the voltage axis.

For the NaAl-2 cell the Open Circuit Voltage (OCV) was measured to be 2.25 V (126°C). To begin with, the cell was discharged with 2

mA for 5 h, before the cycling test ( pause, charge, pause, discharge) was started. The charge/discharge conditions during cycling were 2 mA for 5h, with pauses of 0.5h (see comments below Table 3.5.4.1.3).

Table 3.5.4.1.3.

Charge/discharge performance of the  
Na/Nasicon/MEICl:AlCl<sub>3</sub>/Al (NaAl-2) cell at 125°C.

Cycle no.	Pause mV <sup>1</sup>	Total charge mAh <sup>2</sup>	Charge Voltage mV <sup>3</sup>	Pause mV <sup>4</sup>	Total discharge mAh <sup>5</sup>	Discharge Voltage mV <sup>6</sup>	[Na <sup>+</sup> ] mM <sup>7</sup>
0	-	-	-		12.0	1515	31.1
1	1950	-	> 4095	2020	23.9	1466	61.9
5	1910	10.8	4018	1950	71.7	1282	157.8
8	1820	32.1	3974	1910	107.6	1139	195.6
10	1780	48.2	3937	1910	131.5	1099	215.8
15	-	88.5	3808	-	191.2	782	266.1
20	-	128.7	3697	-	251.0	279	316.9
43	-	234.4	> 4095	-	254.5	0	52.1

The reel current values was measured by a Keithley<sup>R</sup> 175 autoranging multimeter with an accuracy of  $\pm 1\%$ .

- 1 : Leak current during pause measured to be - 0.2 mA (discharge).
- 2 : Current during charge measured to be 1.61 mA.
- 3,6: Maximum charge/discharge voltage (given in the Table) was almost identical with the average voltage.
- 4 : Leak current during pause measured to be - 0.1 mA (discharge).
- 5 : Current during discharge measured to be 2.36 mA.
- 7 : The volume of the electrolyte was approximately 14.4 mL, and assumed to be constant during the test.  
(mM =  $10^{-3}$  Mole/L).

Direction for reading Table 3.5.4.1.3 (digits are given in the Table):

After cycle no. 4 e.g. the OCV was measured to be 1910 mV. After charging in cycle no. 5 with 1.61 mA for 5 hours, the total charge from cycle no. 0 to cycle no. 5, has been 10.8 mAh. The OCV, before discharging in cycle 5, was measured to be 1950 mV. After discharging with 2.36 mA for 5 hours, the total discharge including the preliminary discharge was 71.7 mAh. The maximum CCV during charge was 4018 mV and the minimum CCV during discharge was 1282 mV. The [Na<sup>+</sup>] concentration was calculated to be 157.8 mM after cycle no. 5.

OCV was measured to be 2.12 V after ending cycling (cycle no. 43).

During the first 5 cycles, it was a problem to charge the cell, because the voltage exceeded the upper limit (4.095 V) of the testing system. This was probably due to the extremely low sodium concentration in the electrolyte, which increased the internal resistance during

charge considerably. From cycle 10-20 it was possible to charge/discharge the cell, within the testing system voltage limits (0-4.095 V), for full 5 hours. However, the CCV during discharge became closer and closer to 0 V after each cycle. The results are shown schematic in Table 3.5.4.1.3, using the actual measured values of the currents. A typical charge/discharge curve is shown in Figure 3.5.4.1.3.

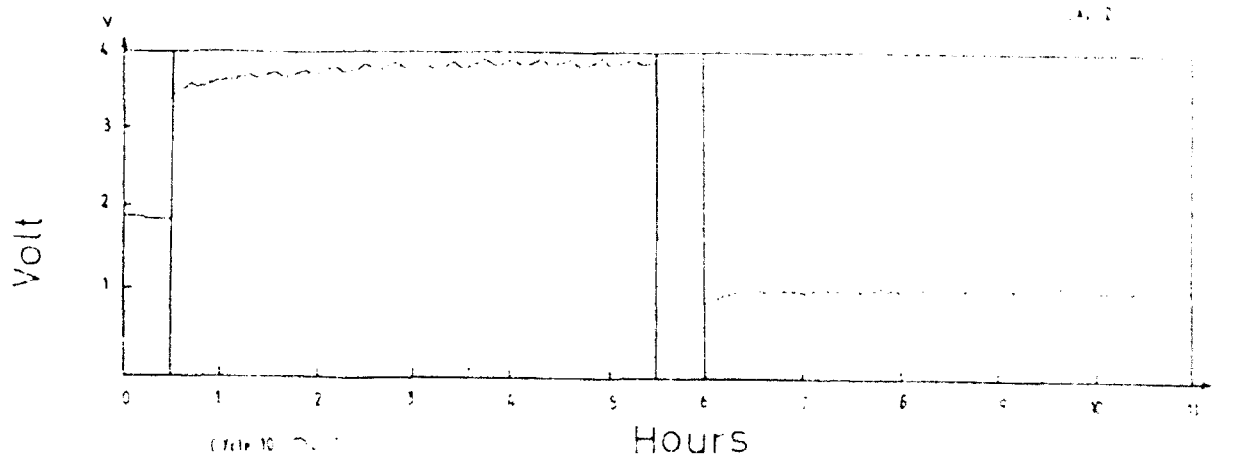


Figure 3.5.4.1.3.  
Charge/discharge (2 mA) performance of cycle 10 for  
the Na/Nasicon/MEICl:AlCl<sub>3</sub>/Al (NaAl-2) cell at 125°C.

#### 3.5.4.1.1 Conclusion.

It turned out to be possible to dissolve sodium ions in an acidic electrolyte of MEICl:AlCl<sub>3</sub>, so that the Na/Al battery could be discharged at 125°C. Current densities of 3.8 mA/cm<sup>2</sup> (5 mA) was achieved (NaAl-1). As mentioned before, the top of the Nasicon tubes (NaAl-1) were not tightened with the Pyrex/teflon tape such as shown in Figure 2.10.3, and therefore the sodium were exposed to the electrolyte by capillary effects. Furthermore, by tighten the cell with Pyrex/teflon tape, it was possible to avoid the gas phase of the electrolyte to condense on/react with the sodium metal. However, it was not possible to cycle the NaAl-1 cell at room temperature, due to a bad contact between solid sodium and the ceramic separator. The resistivity measurements at equilibrium can be interpreted in the same way (Table 3.5.4.1.1). There was more than a factor 500 in difference between the (Na/Al) resistivity at 20°C and at 125°C, even though the specific resistance of Nasicon in theory, only should

change by a factor of 20. (The specific resistance of our Nasicon was 2668 ohm·cm at 25°C and 129 ohm·cm at 125°C, respectively (ref. 72).

It was possible to charge/discharge the NaAl-2 cell, with approximately 2 mA (4.0 mA/cm<sup>2</sup> cathodic, and 1.0 mA/cm<sup>2</sup> anodic), but the internal resistance in the cell was very high. The difference between the closed circuit voltages during charge and discharge, and the pause voltages in Table 3.5.4.1.3, are an expression of the internal cell resistance (1000 Ω). During charge, the internal resistance probably will depend on the sodium ion melt concentration, because the maximum CCV during charge was decreasing at the same time as the [Na<sup>+</sup>] in the electrolyte increases.

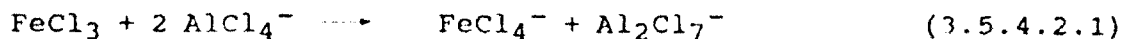
After cycle 20 it was not possible to discharge the cell any more, but it could still be charged until cycle 43, and this of course decreased [Na<sup>+</sup>] in the electrolyte, and increased CCV during charge.

The CCV during discharge decreased continuously, and was not depending on [Na<sup>+</sup>]. The reason for this behavior is not clear at the moment.

A comparison between the cells NaAl-1 and NaAl-2 gave identical OCV values, but the CCV during discharge was greater (including the first discharge cycle) for the NaAl-2 cell, than for the NaAl-1 cell. The most likely explanation for this difference would be that the voltage drop over the ceramic separator differed in the two cases. This however, does not explain why the CCV during discharge decreased with the cycle number, and why the capacity utilization was so extremely low for both cells.

#### 3.5.4.2 Na/Nasicon/FeCl<sub>3</sub>:MEICl:AlCl<sub>3</sub>/Mo or stainless steel.

Dissolution of the Lewis acid FeCl<sub>3</sub> in the MEICl:AlCl<sub>3</sub> (in the acidic case) might take place in the following way :



The reactions expected during charge and discharge, have been given in the equations 3.5.3.3.1 to 3.5.3.3.3.

### 3.5.4.2.1

### Na/Nasicon/FeCl<sub>3</sub>:MEICl:AlCl<sub>3</sub>/Mo (NaFe-13 & NaFe-14).

By use of the Witeg cell design from Figure 2.10.3, we preliminary tested two Na/Nasicon/FeCl<sub>3</sub>:MEICl:AlCl<sub>3</sub>/Mo cells (NaFe-13 and NaFe-14) at 125°C. The Mo foils were 20·20·0.06 mm. For both NaFe-13 and NaFe-14 a second Mo electrode were introduced into the melt as a reference, and for NaFe-14 sodium chloride was added to the electrolyte, too. The electrolyte compositions (FeCl<sub>3</sub>:MEICl:AlCl<sub>3</sub>) were 0.09:0.36:0.55 (NaFe-13) and 0.12:0.53:0.35 (NaFe-14), respectively, with NaFe-14 being saturated by NaCl. We thus had an acidic (NaFe-13) and a basic (NaFe-14) electrolyte. The limiting cathodic capacity, based on a complete reduction of iron(III) to iron(0) were 485 and 743 mAh for NaFe-13 and NaFe-14, respectively.

The OCV was measured to be 4.31 V immediately after assembling of the NaFe-13 cell at 25°C. Subsequently, a stable value of 4.10 V was reached during the following 24 hours when heating the cell to 125°C. The NaFe-13 cell was discharged for 71 hours with 1 mA (0.67 mA/cm<sup>2</sup>) using Na/Mo(1) as working electrodes. A malfunction of the furnace after 51 hours turned the heat off for a period of 7 hours, resulting in sodium solidification. The discharge curve is given in Figure 3.5.4.2.1.1 and the OCV, together with internal calculated cell resistances, are given in Table 3.5.4.2.1.1.

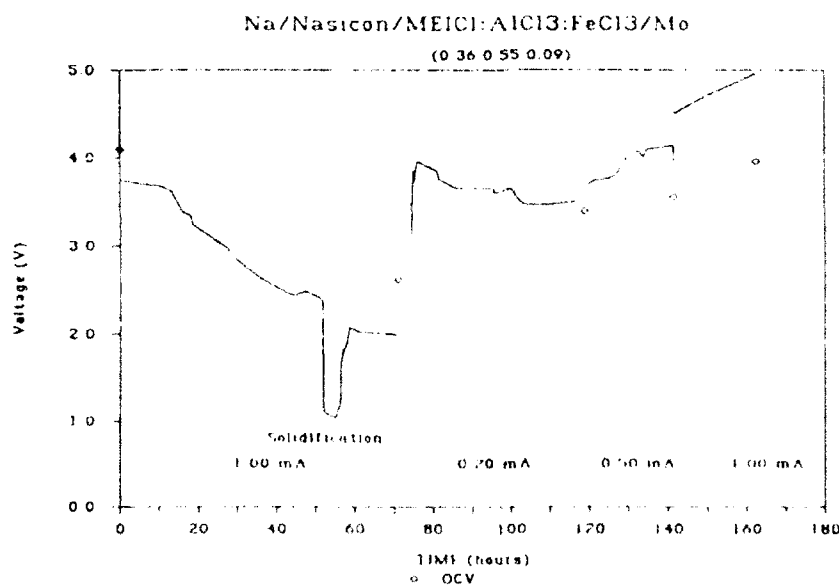


Figure 3.5.4.2.1.1

Discharge/charge of the Na/Nasicon/MEICl:AlCl<sub>3</sub>:FeCl<sub>3</sub>/Mo (NaFe-13) at 125°C. Currents -1 mA, 0.20 mA, 0.50 mA, 1.00 mA.

Table 3.5.4.2.1.1.

Na/Nasicon/ $\text{FeCl}_3$ : $\text{MEICl}$ : $\text{AlCl}_3$ /Mo (NaFe-13). Voltage and resistance vs. discharge (1 mA) and different charge currents. TIME denotes total time since the cell was assembled.

	Current mA	Na/Mo(1)	Na/Mo(2)	Mo(1)/Mo(2)	TIME(h) Total	mAh Total
OCV 20°C ohm 20°C	0	4.31 V 6060	4.31 V 6165	0.01 V 3.8	0	0
OCV 125°C ohm 125°C	0	4.10 V 26.0	4.10 V 27.7	0.01 V 0.6	24	0
OCV 125°C ohm 125°C	- 1	2.62 V 46.0	2.66 V 40.9	0.10 V 20.8	95	- 71
OCV 125°C ohm 125°C	0.2	3.40 V 59.0	3.40 V 60.6	0.01 V 1.3	142	- 62
OCV 125°C ohm 125°C	0.5	3.49 V 52.2	3.49 V 55.1	0.01 V 0.9	166	- 50
OCV 125°C ohm 125°C	1.0	3.97 V 50.9	3.97 V 43.0	0.01 V 1.0	187	- 29

Electrode distances and surface areas used to calculate the ohmic resistances in Table 3.5.4.2.1.1:

All electrode distances are set to be 1.00 cm. Surface areas  
 $\text{Na/Mo} = 1.5 \text{ cm}^2$ ,  $\text{Mo(1)/Mo(2)} = 4 \text{ cm}^2$ .

We tried to charge the cell (NaFe-13) again. By charging with 0.2 mA ( $0.13 \text{ mA/cm}^2$ ) for 47 hours the OCV raised to 3.40 V. Further charging, with 0.5 mA ( $0.33 \text{ mA/cm}^2$ ) for 24 hours increased the OCV to 3.49 V. Finally, charging with 1 mA for another 21 hours raised the OCV to 3.83 V. However, by leaving the cell for a week with open circuit, we measured the OCV to be 3.97 V. After another week, OCV was stable at 3.96 V, so there was no significant self discharge in the system. The Mo plates seemed not to be attacked by the acidic melts, and they were shiny (metallic) when disassembling the cell.

In the basic case (NaFe-14), the OCV was measured to be stable at 3.22 V over a period of 80 hours. On trying to discharge the cell NaFe-14, with 1 mA ( $0.67 \text{ mA/cm}^2$ ), the voltage dropped down to about 1.38 V and started to oscillate. By changing the discharge rate (after 3 hours) to 0.2 mA ( $0.13 \text{ mA/cm}^2$ ), the CCV increased to 2.15 V for a short period, but after 1 hour further, it dropped down to approximately 1.2 V and oscillated around this point, until the discharge was

stopped. The total discharge was 6.88 mAh, and the final OCV was measured to be 2.97 V. It seemed to be easier to charge the NaFe-14 cell than discharging, and charging with 0.1 mA ( $0.07 \text{ mA/cm}^2$ ) for 90 hours showed, (after some oscillations during the first 15 hours) a constant CCV value of 4.38 V. Immediately after charging, the OCV was measured to be 3.34 V, slowly dropping down to a constant value of 3.25 V.

#### 3.5.4.2.2

#### Na/Nasicon/ $\text{FeCl}_3$ :MEICl: $\text{AlCl}_3$ /W

(NaFe-17).

After these initial experiments (NaFe-13 & NaFe-14), an acidic cell of the same kind (NaFe-17) was made with an electrolyte molar composition ( $\text{FeCl}_3$ :MEICl: $\text{AlCl}_3$ ) of 0.09:0.55:0.36, respectively. The coulombic discharge limitations for the cell (NaFe-17) were : Na (875 mAh) and  $\text{FeCl}_3$  (309 mAh - for an one electron transfer reaction). The cathodic current collector was a tungsten wire ( $D = 0.8 \text{ mm}$ , surface area =  $0.50 \text{ cm}^2$ ). The OCV of the NaFe-17 cell was measured to be 2.57 V. By discharging with 1 mA ( $0.5 \text{ mA/cm}^2$  anodic and  $2 \text{ mA/cm}^2$  cathodic), we saw hardly any indication of the  $\text{FeCl}_3$  plateau after 15h. A considerable voltage drop (0.7-0.8 V) was expected to occur, going from Fe(III) to Fe(II), as mentioned by Wilkes et al. (ref. 84). Even though, we discharged longer (517 mAh) than the 309 mAh limitation, the voltage did not drop in a drastic way, and we were not able to detect the Fe(III), • Fe(II) plateau. In Figure 3.5.4.2.2.1, the accelerated test of NaFe-17 is reproduced. The results in Figure 3.5.4.2.2.1 probably show, that  $\text{FeCl}_4^-$  is not involved in the reduction process (only one plateau). Most likely, what happens is, that the  $\text{Al}_2\text{Cl}_7^-$  ion (reaction 3.5.2.3.2.1) is reduced to Al. As can be seen from Figure 3.5.4.2.2.1, the discharge plateaus looked almost identical to the plateaus from the Na/Nasicon/MEICl: $\text{AlCl}_3$ /Al battery in section 3.5.4.1. Thus, Al was probably plated on the tungsten current collector, instead of the expected iron(III) reduction.

Na/Nasicon/MEICl:AlCl<sub>3</sub>:FeCl<sub>3</sub>/Mo  
(0.36:0.55:0.09)

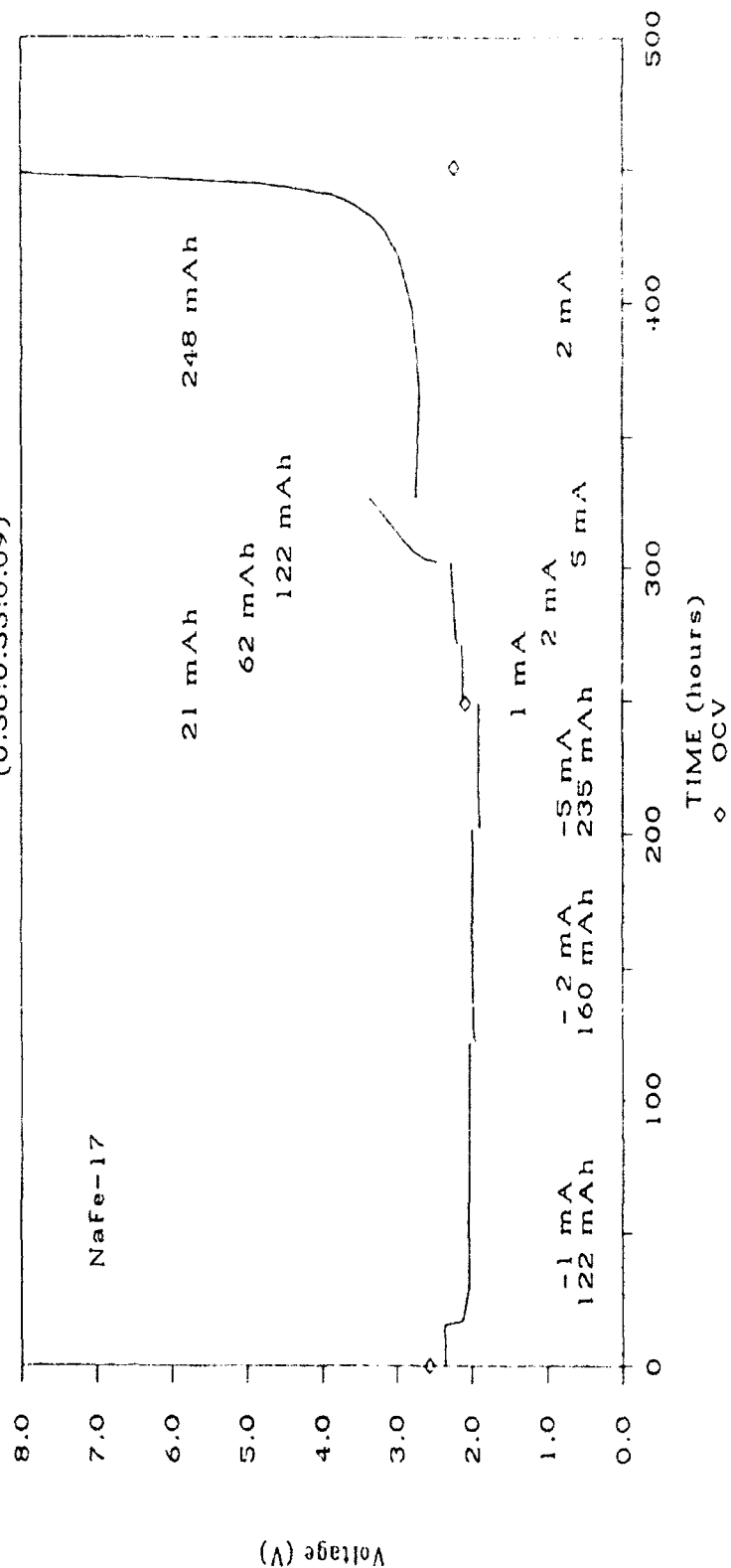


Figure 3.5.4.2.2.1

The cell NaFe-17 was discharged with different currents (the minus sign denotes discharge) 1, 2 and 5 mA with a total discharge of 517 mAh (122+160+235). The cell was then charged with different currents 1, 2, 5 and 2 mA with a total charge of 453 mAh. The charging current of 5 mA was too high, the internal resistance increased, and after a total charge of 453 mAh, the sodium concentration was so low in the melt, that even a 2 mA current could not be passed through the cell (surface areas Anodic = 2 cm<sup>2</sup>, cathodic = 0.50 cm<sup>2</sup>).



3.5.4.2.3 Na/Nasicon/FeCl<sub>3</sub>:MEICl<sub>3</sub>:AlCl<sub>3</sub>/Mo or Stainless steel.  
(NaFe-19, NaFe-20).

To obtain a faster equilibrium, the Witeq cells (Figure 2.10.3) were first placed for 24h in an oil bath at  $175^{\circ}\text{C} \pm 5^{\circ}\text{C}$ . Then they were quickly moved to another oil bath ( $125^{\circ}\text{C} \pm 5^{\circ}\text{C}$ ). Only the lower half of the Witeq glass cell was submerged into the oil, and this unfortunately gave some temperature gradients in the cells. Actually, at the internal wall of the cell top a bright yellow layer was formed, probably due to sublimation of some dissolved iron(III) chloride. The molybdenum plate and the steel mesh was  $20 \cdot 20 \cdot 0.06$  and  $20 \cdot 30 \cdot 0.15$  mm, respectively. The mask dimension in the mesh was  $0.8 \cdot 1.0$  mm. That gave, in both cases an efficient cathodic area of approximately  $4 \text{ cm}^2$ .

The Nasicon tubes had an inner diameter of 7 mm, and an outer diameter of 10 mm. The sodium depth inside the tubes were 39 mm (NaFe-19) and 46 mm (NaFe-20), respectively. The Nasicon was wetted by the electrolyte approximately up to height of 20mm, and that gave a mean surface area of the tubes of  $5.5 \text{ cm}^2$  ( $D_{\text{mean}} = (D_{\text{outer}} + D_{\text{inner}})/2$ ). The cells were cathodic limited to 1150 mAh and the molar composition of the FeCl<sub>3</sub>:MEICl<sub>3</sub>:AlCl<sub>3</sub> electrolytes were 0.10:0.35:0.55, respectively.

The cells were charged/discharged with two KEITHLEY<sup>R</sup> 224 programmable current sources of high precision (deviation less than 1% of the current set value). The measured voltages were registered on a SERVOGOR<sup>R</sup> 120 double channel recorder and transferred into a "spread sheet" PC-program for graphical treatment.

The OCV value for both cells was 4.0 V at  $125^{\circ}\text{C}$  before cycling started. The initial cycle for both cells was a 20h discharge and a 20h charge period with 1 mA ( $0.25 \text{ mA/cm}^2$  cathodic). The second discharge was an accelerated process as can be seen in Figure 3.5.4.2.3.1, which also gave the actual current values (a minus sign denotes discharge). The cells were discharged with varying current densities (0.25, 0.5, 1.25, 2.5 and finally again  $0.5 \text{ mA/cm}^2$  cathodic) until the presumable Na/Al plateau at 1.6 V (ref. 28, 29, 30) was reached, using 62% of the theoretical amount of FeCl<sub>3</sub>. During the discharge, at least 2 plateaus were seen, indicating the FeCl<sub>3</sub>  $\rightleftharpoons$  FeCl<sub>2</sub> and the FeCl<sub>2</sub>  $\rightleftharpoons$  Fe conversions (ref. 28, 85).

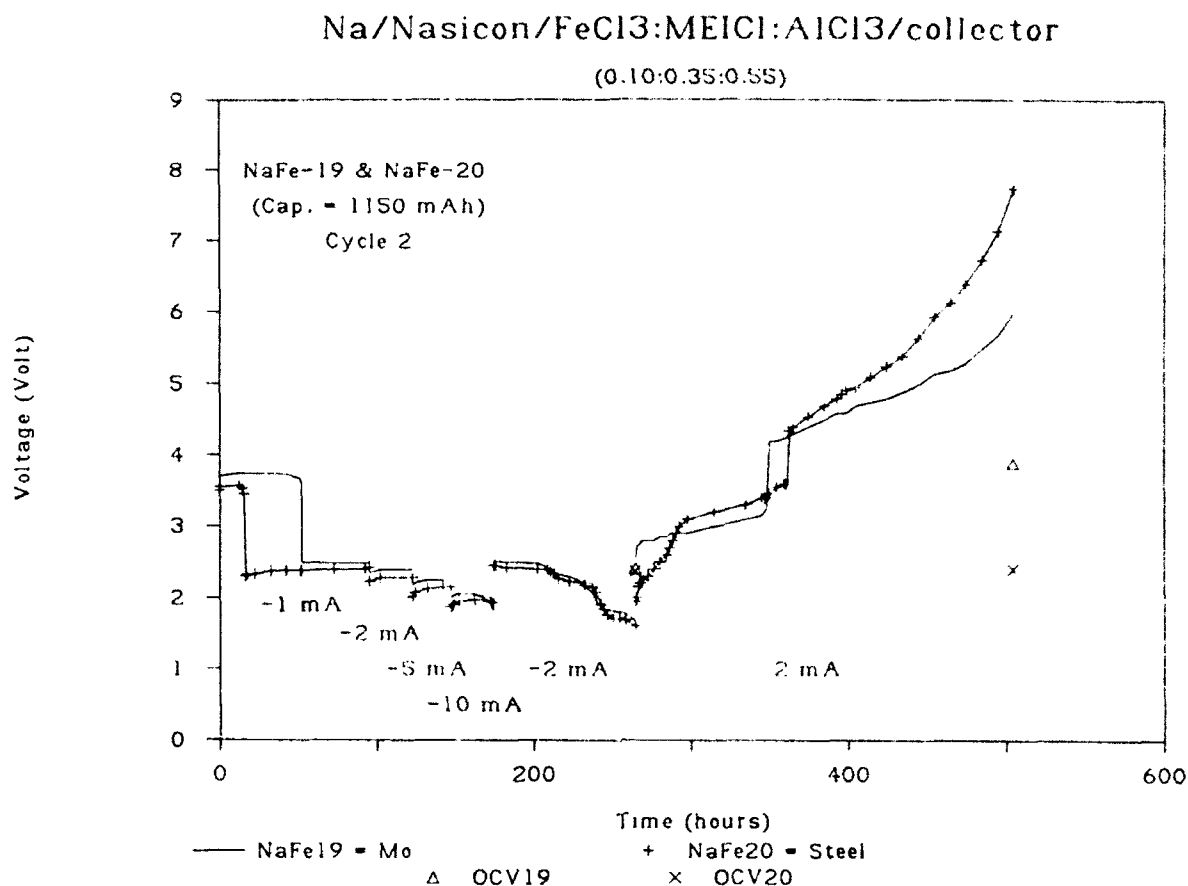


Figure 3.5.4.2.3.1.  
Second discharge/charge cycle for NaFe-19 & NaFe-20 cells at 125°C. Anodic surface area = 5.5 cm<sup>2</sup> and cathodic area = 4.0 cm<sup>2</sup>.

After the second discharge the OCV was around 2.4 V for both cells, indicating that Al has not been plated, and that the discharge unintended was stopped at the Na/FeCl<sub>2</sub> plateau. We observed a big voltage drop when going from the FeCl<sub>3</sub> to the FeCl<sub>2</sub> plateau as expected (Wilkes et al. in reference 84). Charging the cells again with 0.5 mA/cm<sup>2</sup> for 240h also gave a big voltage increase, due to the reverse reaction. The total discharge in the second cycle was 713.3 mAh. The total charge was only 480 mAh, after which the overvoltage increased to more than 3V. After charge and pause for 67h, the OCV was measured to be 3.90 V for the NaFe-19 (Mo) cell. Immediately after disconnection of the circuit, the OCV of the NaFe-20 (steel) was 3.5 V, but after another 4 hours it dropped sharply down to 2.8 V and during the next 63 hours it continued decreasing slowly down to 2.41 V.

Both cells performed in a very similar way as shown in Figure 3.5.4.2.3.1. Perhaps the Mo-current collector was slightly better than the stainless steel mesh, because the overvoltage was slightly lower for the cell with the Mo-plate. Furthermore, in the solution, Mo was more stable than stainless steel. As mentioned above, stainless steel (AISI 1316) corrodes in the  $\text{MEICl:AlCl}_3$  melts. Extra iron from the steel mesh could react with  $\text{FeCl}_3$  to give  $\text{FeCl}_2$ . (The way of making  $\text{FeCl}_2$  from  $\text{FeCl}_3$  is :  $\text{Fe} + 2 \text{FeCl}_3 \rightarrow 3 \text{FeCl}_2$ , with THF as solvent (ref. 75)). This is a possible explanation for the lower OCV value for the stainless steel cell (NaFe-20) after the charging procedure, i.e. we have measured the Na/ $\text{FeCl}_2$  plateau instead of the Na/ $\text{FeCl}_3$  equilibrium voltage.

In cycle 3, the cells were discharged at a constant current rate of 2 mA ( $0.5 \text{ mA/cm}^2$ ) for 215h (NaFe-19). As can be seen in Figure 3.5.4.2.3.2, the limit of 1.6 V was reached immediately for the NaFe-20 cell. The discharge was stopped after 76 hours. After discharge the OCV was 2.62 V for NaFe-19 and 2.18 V for NaFe-20, respectively. NaFe-19 was charged again for 213h, but NaFe-20 was only charged for 95h, and the finally OCV, after 26 hours pause, was 3.90 V (NaFe-19). The OCV for (NaFe-20) was measured, after a pause of 168h, to be 2.31 V.

The 3.90 V indicates a very reversible process, and in Figure 3.5.4.2.3.2 two plateaus can clearly be seen. In cycle 3, the total 'Depth of Discharge' (DOD) (including the overdischarge from cycle 2) was kept around 60% of the theoretical amount for NaFe-19 (657.5 mAh, see appendix A, section 3.5.4.2.6). The NaFe-19 cell could only be charged again up to 430 mAh leaving the last 20% (227.5 mAh) in the solution. A potentiostatic examination of cycles 2 and 3 has shown good rechargeability for NaFe-19. In both of the cycles 2 and 3, the cells NaFe-19 and NaFe-20 were discharged to a cut-off voltage of 1.7 V. Thus, by calculating the amount of charge needed to reach 5.0 V in cycles 2 and 3, we would obtain a picture of the rechargeability. NaFe-19 needed 180h (360 mAh) to reach a CCV of 5.0 V during charging in cycle 2, and 175h (350 mAh) to reach a CCV of 5.0 V in cycle 3. Table 3.5.4.2.3.1 lists the charge needed to reach a CCV of 5.0 V for both cells and both cycles.

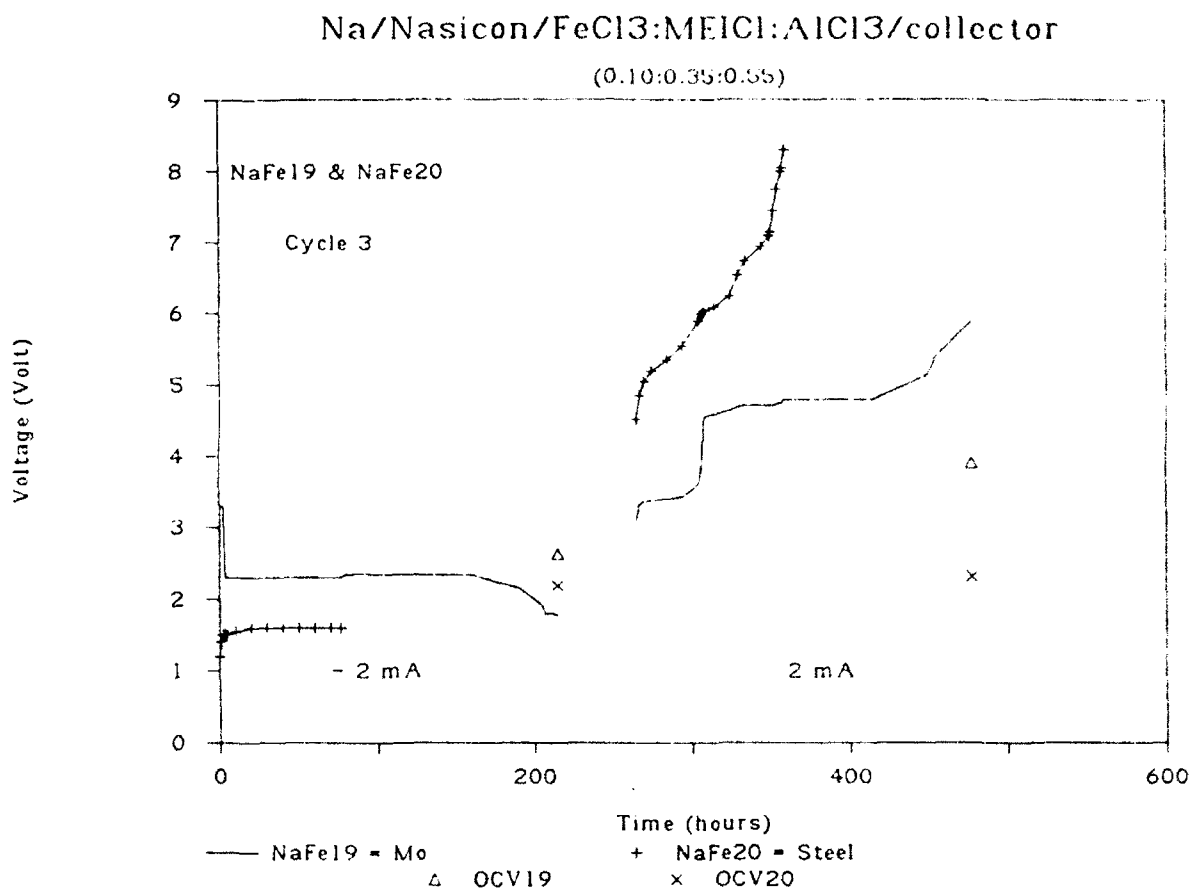


Figure 3.5.4.2.3.2.  
 Third discharge/charge cycle for NaFe-19 & NaFe-20 at 125°C.  
 Anodic surface area = 5.5 cm<sup>2</sup> and cathodic area = 4.0 cm<sup>2</sup>.

Table 3.5.4.2.3.1.  
 Charge needed to reach 5.0 V during a  
 0.5 mA/cm<sup>2</sup> charging process after discharge  
 to a constant level of 1.7 V.

	Cycles 2	Cycles 3
NaFe-19, Mo	360 mAh	350 mAh
NaFe-20, Steel	290 mAh	10 mAh

The Mo system was reversible while the steel system  
 probably was degrading.

After a pause of 1 month, the OCV of the NaFe-19 (Mo) cell was almost constant at 2.91 V, and the OCV of the NaFe-20 (steel) cell increased to 2.85 V (compare to the values given in Figure 3.5.4.2.3.2 3.90 V and 2.31 V, respectively). Obviously, there had been a self discharge in the NaFe-19 cell, and perhaps the acidic melt was slightly unstable toward Fe(III), as mentioned by Hussey (ref. 26) for the AlCl<sub>3</sub>:BPC (1-butylpyridinium chloride) case ?

In order to reach the Na/Al plateau, the two cells were then discharged with 2 mA ( $0.5 \text{ mA/cm}^2$ ) for 360h, until a constant plateau of approx. 1.45 V was reached (see Figure 3.5.4.2.3.3). Then accelerated testing process was performed. During charge/discharge small pauses (0.5-1.0 h) were introduced in order to investigate the overvoltage. For exceptions, see note to Figure 3.5.4.2.3.3.

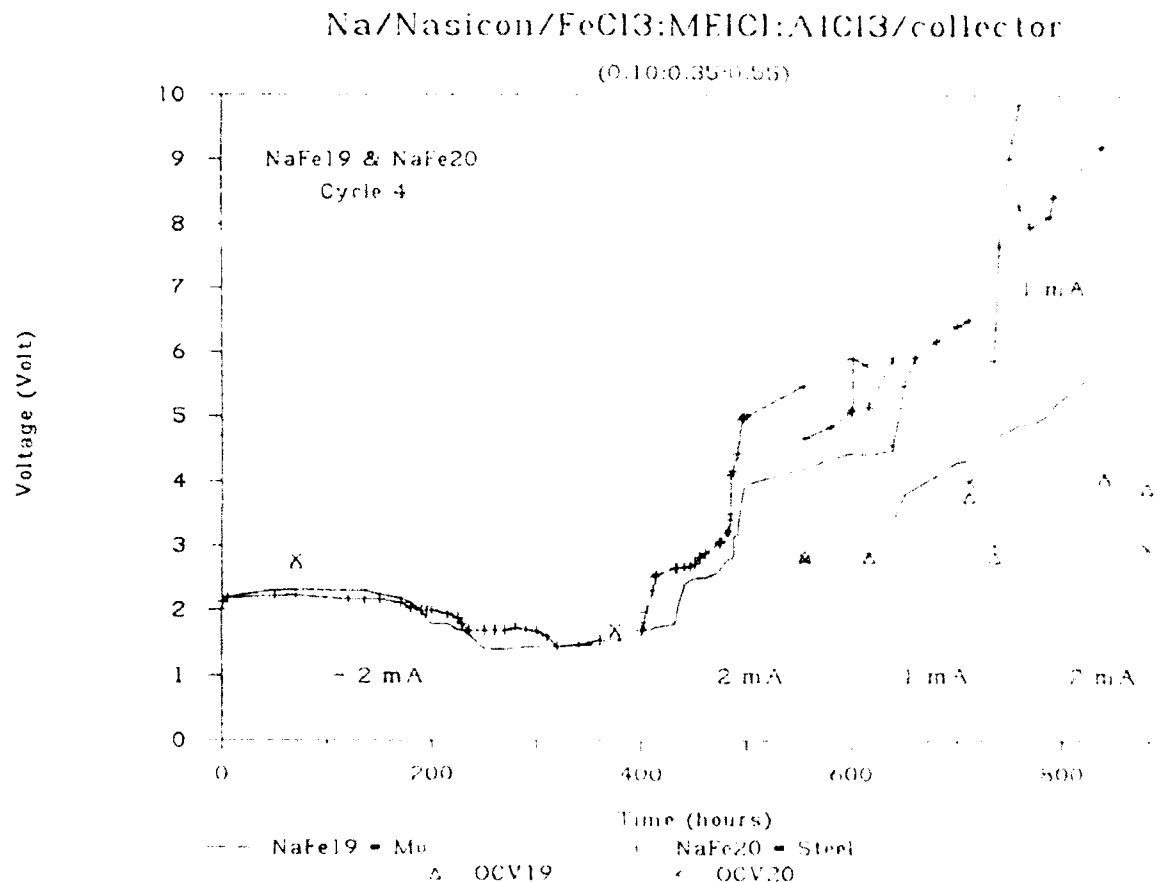


Figure 3.5.4.2.3.3.

Fourth discharge/charge cycle for NaFe-19 & NaFe-20 at  $125^\circ\text{C}$ . Anodic surface area =  $5.5 \text{ cm}^2$  and cathodic area =  $4.0 \text{ cm}^2$ .

Note:

Exception 1: After 711 hours (311 h of charge) the OCV was determined 2 times, the first one after 1 h of pause, and the second one after 24 h of pause.

Exception 2: After 840 hours (440 h of charge) the OCV was determined 2 times, the first one after 1 h of pause, and the second one after 40 h of pause.

Before starting the Al plating, it was possible to estimate the theoretical amount of  $\text{FeCl}_3$  used. The results were:

NaFe-19 used  $702 \text{ mAh}/1150 \text{ mAh} = 63\%$  of the  $\text{FeCl}_3$ , and NaFe-20 used  $804 \text{ mAh}/1150 \text{ mAh} = 70\%$  of the  $\text{FeCl}_3$ .

By charging the cells (cycles 4, Figure 3.5.4.2.3.3) with 2.0, 1.0 or 2.0 mA, respectively (see appendix A, section 3.5.4.2.6, for

a detailed description of the testing procedure), we ended up with approximately the same OCV plateaus as before. The value was 4.04 V for the NaFe-19 cell, slowly decreasing to 3.9 V after 41h of rest ( $\text{FeCl}_3$ ). The value was 4.10 V for the NaFe-20 cell, slowly decreasing to 2.95 V after 41h ( $\text{FeCl}_2$ ).

A typical OCV curve is shown in Figure 3.5.4.2.3.4 (continuation of Figure 3.5.4.2.3.3). The self discharge for the NaFe-20 (steel) cell was probably due to a reduction of  $\text{Fe(III)}$  by the steel.

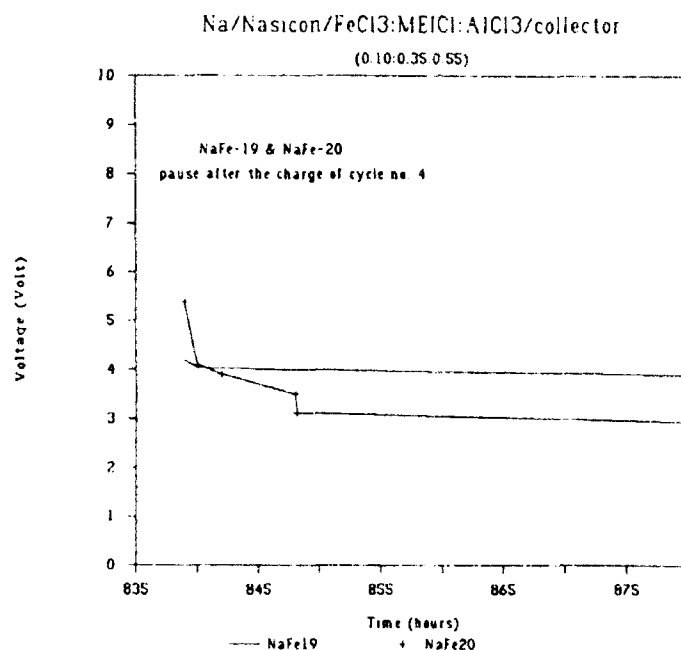


Figure 3.5.4.2.3.4  
OCV curves for NaFe-19 and NaFe-20 (steel) after cycles 4.

During charging, the cell voltage tends to oscillate at around 4.1-5.0 V, as shown in Figure 3.5.4.2.3.5 for the NaFe-19 system (see also note a, in appendix A, section 3.5.4.2.6).

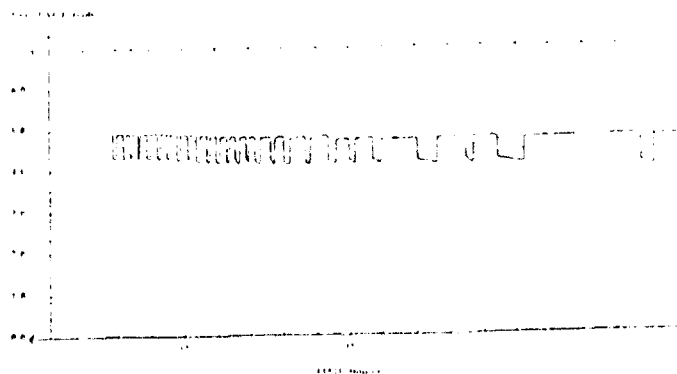


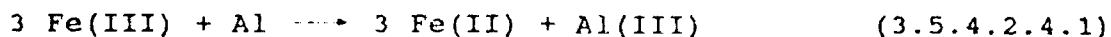
Figure 3.5.4.2.3.5.  
Voltage oscillation of the NaFe-19 cell during charge in cycle 3.

The cells were disconnected after 7 months of operation. An examination of the Nasicon tubes and the electrodes clearly showed, that the stainless steel was very much corroded: The mesh was separated from the tungsten wire, but the molybdenum plate was stable. The Nasicon tubes looked slightly corroded, but they were free of visible holes.

3.5.4.2.4 Na/Nasicon/FeCl<sub>3</sub>:MEICl:AlCl<sub>3</sub>/Stainless steel.  
(Flat cell design, NaFe-23).

This flat cell (see Figure 2.10.2) was made as earlier described (ref. 58). The newly developed polishing technique (ref. 58) was included to obtain a smooth metal surface and to improve the tightness of the cell. After assembly, the cell was placed in a hot air furnace at  $125^{\circ}\text{C} \pm 5^{\circ}\text{C}$  and had an OCV of 3.5 V (10h after melting of sodium). The OCV stabilized at 3.05 V after 3 days.

The theoretical amount of discharge was 45 mAh, based on a 3 electron  $\text{Fe}^{3+}/\text{Fe}$  transfer process. The discharge/charge current was controlled by the previously mentioned KEITHLEY<sup>R</sup> 224 instrument. In cycle 1 (Figure 3.5.4.2.4.1) the cell was discharged with 1 mA ( $0.67 \text{ mA/cm}^2$ ) for 45h, and in this case the stable Na/Al-plateau appeared after 29h. The utilization of capacity was 67% of the theoretical amount and the OCV became stable at 1.63V. The voltage curve obtained by charging again with 1 mA for 45h seems to indicate complete reversibility, however the  $\text{Al}/\text{Al}^{3+}$  process seemed only to take place for 2h. Hence, it is basically a recharging based on the iron, i.e. the oxidation of the iron/iron complexes took place before the oxidation of the aluminum started (Al could have been passivated). After 21h of charge there was a little decrease in the closed circuit voltage (!). This could be a reduction of the formed  $\text{FeCl}_3$  due to a reaction with the steel cup or due to a reaction with the (passivated) aluminium (equation 3.5.4.2.4.1):



The final OCV was 2.85 V, most likely the Na/ $\text{FeCl}_2$  plateau.

By repeating cycle 1 in cycle 2, it was shown that the Na/Al plateau was reached after 42h of discharge, i.e. an almost complete utilization of the  $\text{FeCl}_3$  ( $\text{FeCl}_2$  + the newly formed  $\text{FeCl}_2$  from the cup). The last part of the discharge (28h) involved a plating of Al, and the OCV was again 1.63V. Charging the cell, probably resulted in a utilization of only 9 mAh of the plated Al and then 42 mAh of the

iron (Fig.3.5.4.2.4.1). After charging, the final OCV was 2.80 V, and the utilization of the iron was almost complete.

By discharging with 2 mA (1.33 mA/cm<sup>2</sup>) in cycle 3, a utilization of approx. 35 mAh was reached before the Na/Al plateau appeared. The total discharge in cycle 3 was 51 mAh. After a new total charge of 51 mAh, the cell ended with an OCV of 2.80 V. However, as can be seen in Figure 3.5.4.2.4.1, a self discharge process occurred from the 2.80 V plateau down to the 2.20 V plateau. Due to the self discharge, the capacity associated with the discharge curve was only 24 mAh in cycle 4. Finally, the cell was stopped and examined, and a major crack of the Nasicon disk was found.

In Table 3.5.4.2.4.1 a summary is given of the voltages during discharge/charge.

Table 3.5.4.2.4.1.  
Voltages during discharge/charge for NaFe-23.

cycle No.	Discharge			Charge		
	Time h	Plateau V	Comment	Time h	Plateau V	Comment
1	19	2.00		2	1.75	Na/Al ?
	3	1.75		2	2.55	Na/FeCl <sub>2</sub>
	3	1.20		5	2.80	
	15	0.99	Na/Al	22	3.17	Na/FeCl <sub>3</sub>
	5	-----	No plateau	11	---	No plateau
2	14	2.15		9	1.77	Na/Al ?
	6	1.88		9	2.05	
	15	1.50		15	2.65	
	29	1.18	Na/Al	8	2.90	
	6	-----	No plateau	11	---	No plateau
3	2.5	1.55		10	2.10-4.20	Linear
	2.5	1.40		7	4.40	
	12.5	1.10		8	> 5.0V	No Plateau
	7	0.70	Na/Al			
	1	-----	No plateau			

Example of reading Table 3.5.4.2.4.1:

Cycle no. 1: During discharge we obtained 4 plateaus (2.00 V, 1.75 V, 1.20 V, and 0.99 V). The length of the plateaus was 19h, 3h, 3h, and 15h, respectively. The total time of discharge was 45h. This gives 5 hours (45 - 40) with no plateaus. During charge we also obtained 4 plateaus as shown in the Table.



# Na/Nasicon/FeCl<sub>3</sub>:MEICl:AlCl<sub>3</sub>/Steel

(0.09:0.36:0.55)

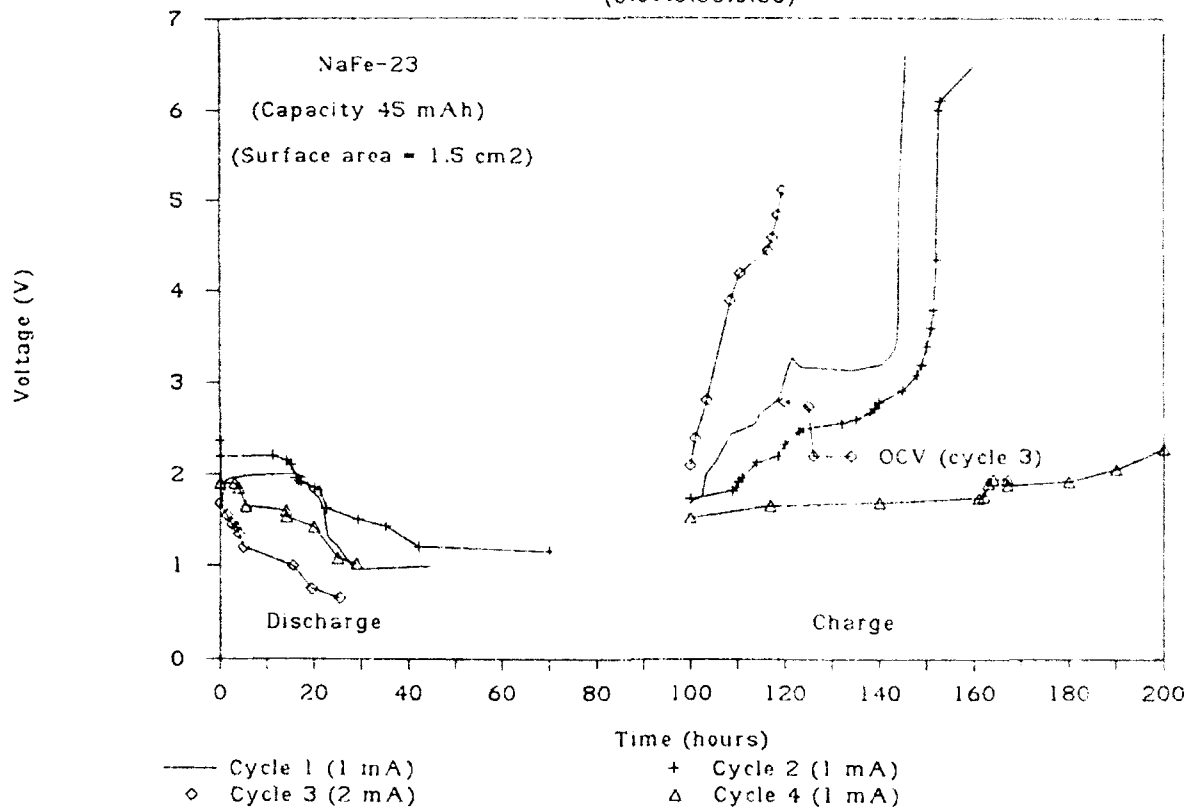


Figure 3.5.4.2.4.1.  
Discharge/charge cycles for NaFe-23 at 125°C.  
Anodic/cathodic surface area = 1.5 cm<sup>2</sup>.

## 3.5.4.2.5 Conclusion.

It was possible to charge and discharge the Na/Nasicon/FeCl<sub>3</sub>:MEICl:AlCl<sub>3</sub>/current-collector system at 125°C, almost reversibly with molybdenum as the cathodic current collector and an acidic electrolyte composition. Stainless steel could not be used in connection with FeCl<sub>3</sub> at that temperature. Results of the NaFe-14 cell showed, that basic electrolytes could not be used in combination with Nasicon separators. Cells NaFe-19 and NaFe-20 showed, without any optimization at all, that it was possible to use 60-70% of the theoretical amount of FeCl<sub>3</sub> by discharging/charging with 2 mA (0.5 mA/cm<sup>2</sup>). However, especially during charging there were some problems with overvoltage (Figure 3.5.4.2.3.3). This was probably due to the cathode design, which was not optimal for the cathode reaction. It might be better to use graphite (RVC) in the bottom of the cell, such

that a direct contact between the free iron and the current collector always exists. Furthermore, in this way the risk is limited of capacity loss due to free iron falling off the cathode current collector.

In the flat cell NaFe-23, a 64% utilization of the  $\text{FeCl}_3$  was obtained (cycle 1) in good agreement with the 63% of the NaFe-19 cell. In cycle 2 (no  $\text{FeCl}_3$ ) there was an almost 100 % utilization of the  $\text{FeCl}_2$  (formed during charging in cycle 1). This supports the theory by Hussey et al. (ref. 26), that Fe(III) was reduced in the melt. Actually, the  $\text{FeCl}_3 \rightleftharpoons \text{FeCl}_2$  plateau disappeared (Figures 3.5.4.2.3. 1 to 3) as a function of time. Furthermore, the  $\text{FeCl}_3 \rightleftharpoons \text{FeCl}_2$  plateaus (cells NaFe-19 and NaFe-20) in Figure 3.5.4.2.3.1 were much shorter than the expected 380 mAh. A total reduction of Fe(III) to Fe(II) by the melt would result in a capacity loss of 33 %, i.e. the theoretical utilization ( $\text{FeCl}_3$ ) should be around 67% of the 1150 mAh. This was the utilization we actually observed, such that all Fe(III) was probably reduced by the melt.

We have found no evidence for a poisoning of the Nasicon ceramic by  $\text{Fe}^{3+}$  ions at this 'low' temperature ( in contrast to the beta-alumina mentioned in section 1.3). Table 3.5.4.2.5.1 below, gives the estimated total cell resistance for NaFe-19 and NaFe-23. The resistance was calculated as the difference between the OCV and the CCV immediately after the discharge was started ( $\Delta V$ ) divided by the current change ( $\Delta I$ ).

Table 3.5.4.2.5.1.  
Overview of the total resistance in NaFe-19 and NaFe-23 immediately after discharge.

NaFe-19 (Mo)				NaFe-23 (steel)			
Nr.	Time h	mA/cm <sup>2</sup>	$\Omega$	Nr.	Time h	mA/cm <sup>2</sup>	$\Omega$
1	262	-0.25	470	1	96	- 0.67	1100
2	406	-0.25	370	2	198	- 0.67	500
3	1102	-0.50	250	3	524	- 1.33	575
4	2352	-0.50	375	4	619	- 0.67	320

The accelerated test of the NaFe-19 cell in Figure 3.5.4.2.3.1 (cycle 2), was used to estimate the resistance of a working cell. In Figure 3.5.4.2.5.1 below, the connection between voltage and current is shown for NaFe-19 (cycle 2), at the Na/FeCl<sub>2</sub> plateau.

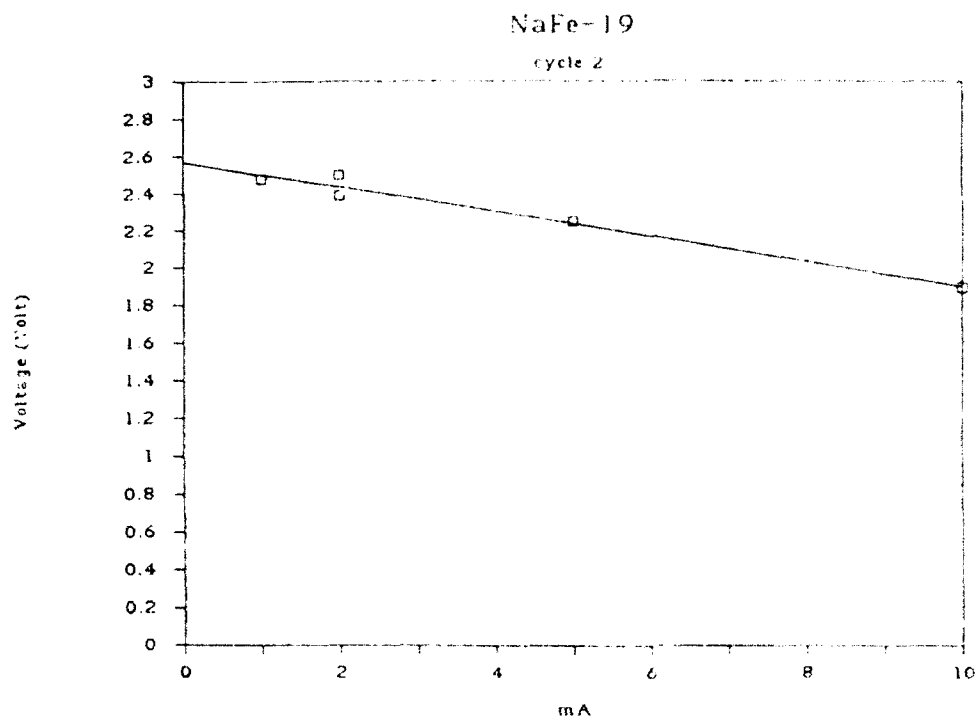


Figure 3.5.4.2.5.1.

Voltage vs. current of the Na/Nasicon/ $\text{FeCl}_3\text{:MEICl:AlCl}_3\text{/Mo}$  (NaFe-19) cell. Cycle no. 2 at the Na/ $\text{FeCl}_2$  discharge plateau.

The slope of the line in Figure 3.5.4.2.5.1 is related to the working resistance of the cell. The intersection of the line at zero gives the Na/ $\text{FeCl}_2$  plateau at equilibrium. The results are summarized in Table 3.5.4.2.5.2 below.

Table 3.5.4.2.5.2.

Cell resistance and Na/ $\text{FeCl}_2$  plateau in the NaFe-19 cell.

R $\Omega$	R <sup>2</sup>	Na/ $\text{FeCl}_2$ plateau Volt
66 $\pm$ 6	0.9716	2.57 $\pm$ 0.05

From the two Tables 3.5.4.2.5.1 and 3.5.4.2.5.2 we see, that the total cell resistance was a combination of at least 2 contributions, an intrinsic value and a current rate dependent value.

Furthermore, the resistance of the ceramic separator (theoretical around 1  $\Omega$ ), does not contribute much to the overall cell resistance. The flat cell (NaFe-23) had a thinner ceramic separator than the tube cell (NaFe-19), but the cell resistance was not lower in the flat cell case.

3.5.4.2.6 Appendix A. (NaFe-19 & NaFe-20).  
Charge/discharge performances of the Na/Nasicon/FeCl<sub>3</sub>:MEICl:AlCl<sub>3</sub>/Mo or Steel cell system at 125°C.

		Na/Nasicon/FeCl <sub>3</sub> :MEICl:AlCl <sub>3</sub> /Mo 0.10 : 0.34: 0.56 NaFe-19					Na/Nasicon/FeCl <sub>3</sub> :MEICl:AlCl <sub>3</sub> /Stainless Steel 0.10 : 0.35: 0.55 NaFe-20				
Cycle no.	mA	Time h	Total Charge mAh	CCV V	Eq. Voltage V		mA	Time h	Total Charge mAh	CCV V	Eq. Voltage V
1	--	---	---	---	4.03		--	---	---	---	4.05
	1	19.0	- 18.8	3.606h 2.5013h	2.76 3.57P1		- 1	19.0	- 18.8	3.516h 2.4613h	2.78 3.60P1
	1	21.5	2.9	4.5 - 8.2	5.04 4.03P2		1	21.5	2.9	4.6 - 8.3	4.33 4.24P2
	- 1	95.1	- 91.4	3.7052h 2.4843h	---		- 1	95.1	- 91.4	3.5515h 2.3880h	---
	- 2	27.6	-146.1	2.3728h	---		- 2	27.6	-146.1	2.2728h	---
2	- 5	24.2	-266.1	2.2524h	---		- 5	24.2	-266.1	2.1524h	---
	-10	27.0	-533.9	2.0420h 2.0 - 1.8	---		-10	27.0	-533.9	1.9527h	---
	- 2	90.4	-713.3	2.5028h 2.5 - 1.67	2.15 2.41P3		- 2	90.4	-713.3	2.4334h 2.4 - 1.61	2.15 2.37P3
	2	239.5	-230.5	2.5-3.484h 4.2-6.0160h	4.0 3.90P4		2	239.5	-230.5	2.0-3.697h 4.4-7.7143h	3.5 2.41P4

Appendix A, (NaFe-19 & NaFe-20).  
Charge/discharge performances of the Na/Nasicon/FeCl<sub>3</sub>:MEICl<sub>3</sub>/Mo or Steel cell system at 125°C.

Na/Nasicon/FeCl <sub>3</sub> :MEICl <sub>3</sub> /AlCl <sub>3</sub> /Mo 0.10 : 0.34: 0.56 NaFe-19						
Cycle no.	mA	Time h	Total Charge mAh	CCV V	Eq. Voltage V	
3	- 2	215.0	-657.5	3.302.5h 2.30167h 2.20-1.77	2.19 2.62P5	
	2	213.0	-228.5	3.1-3.943h 4.5-5.2142hA 5.4-5.928h	4.0 3.90P6 2.91P7	
	- 2	361.5	-945.8	2.25170h 2.19-1.4480h 1.44112h	1.62P8	
4	2	238	-466.5	1.7332h 1.86-2.82655h 3.16-4.2067h p(1h) 2.84 4.20-4.4260h p(1h) 2.82 4.42-4.4823h	4.04p9 3.9p9	
	1	72	-394.0	3.40-4.3272h		
	2	104	-184.5	4.6-5.8104h		

Na/Nasicon/FeCl <sub>3</sub> :MEICl <sub>3</sub> /AlCl <sub>3</sub> /Stainless Steel 0.10 : 0.35: 0.55 NaFe-20						
	mA	Time h	Total Charge mAh	CCV V	Eq. Voltage V	
	- 2	76.4	-382.2	1.6076h	2.18P5	
	2	95.0	-190.7	4.52-8.30	2.48 2.31P6 2.85P7	
	- 2	361.5	-908.0	2.17170h 2.12-1.8059h 1.6881h 1.4852h	1.70P8	
	2	238	-428.7	1.70-1.994h 2.32-3.5081h 4.10-5.4869h p(1h) 2.80 4.67-5.1246h 5.85-5.8515h p(1h) 2.85 5.15-5.9223h	4.10 2.95P9	
	1	72	-356.2	4.56-6.5072h		
	2	24	-307.9	5.9-9.8524h		
	1	80	-227.3	8.3-9.280h		

#### Appendix A.

- A: The voltage oscillated and was very unstable after 75h of charging. This was shown in Figure 3.5.4.2.3.5.
- P1: Measured after 115h.  
P2: Measured after 29h.  
P3: Measured after 6 days.  
P4: Measured after 67h.  
P4 (NaFe-20) : After 5h the OCV suddenly dropped from 3.4 V to 2.5 V, as if the cell was discharged.  
P5: Measured after 32h.  
P5 (NaFe-20) : Measured after 171h.  
P6: Measured after 26h.  
P6 (NaFe-20) : Measured after 168h.  
P7: Measured after 750h (1 month).  
P7 (NaFe-20) : Measured after 888h (1 month and 1 week).  
P8: Measured after 20h.  
P9: Measured after 41h.

Explanations of the columns in the appendix:

#### Charge :

Gives the actually charge/discharge set value in milliamperes. Discharge is denoted with a minus sign.  
The exactly values during charge/discharge are measured to be  
Charge: set value + 0.7%.  
Discharge: set value - 0.8%.

#### Time :

Gives the time in hours corresponding to the charge/discharge action.

#### Total Charge :

Sum up the amount of charge/discharge in milliamperes hours, using the corrected charge/discharge values.

#### CCV :

Gives the mean measured close circuit voltage (volt) during charge/discharge. In superscript are denoted how long time (hours) a certain value was stable.  
The hyphen denotes that the mean voltage value slowly changed in between the written values.

#### Eq. Voltage :

Gives the measured Open Circuit Voltage (OCV) at 'equilibrium'. (Equilibrium means at least 20h after last charge/discharge operation has stopped).  
The upper value is the OCV measured immediately after the charge/discharge operation has stopped.  
The lower value is the actual OCV value after at least 20h.  
The superscript gives reference to the actually elapsed time.

We have succeeded in the preparation of several organic chloride derivative compounds of imidazoles, pyrazoles, triazoles and tetrazoles. The preparations have been simplified and scaled up, to give yields of 50-100 g/synthesis.

Examination of the conductivity for the equimolar 14dm124tcl:AlCl<sub>3</sub> mixture in a wide temperature range (-30°C to 114°C), has shown a specific conductivity comparable to that of the similar MEICl:AlCl<sub>3</sub> system. This makes 14dm124tcl:AlCl<sub>3</sub> a promising candidate for a room temperature electrolyte.

Voltammetric investigations on NaCl:AlCl<sub>3</sub>:14dm124tcl acidic mixtures showed that new high velocity processes were involved, suppressing the aluminum electrooxidation.

Neosepta<sup>R</sup> anion and cation membranes were examined and found to have too high a resistance for battery application. Nasicon was found to have too high a resistance at and below 125°C.

Investigations of sodium in MEICl:AlCl<sub>3</sub> melts have shown a fast surface reaction in acidic melts, and a very slow surface reaction in basic melts. Impedance measurements supported the passivation of sodium electrodes in basic melts, giving high internal cell resistances.

All room temperature batteries with sodium anodes and MEICl:AlCl<sub>3</sub> electrolytes failed due to this passivation.

Middle temperature (125°C) batteries based on Na/Nasicon/FeCl<sub>3</sub>:MEICl:AlCl<sub>3</sub>/Mo were found to be very reversible and thats somewhat promising, but as mentioned above, Nasicon is not a good choice at these temperatures. Furthermore, the FeCl<sub>3</sub> was found to be reduced to FeCl<sub>2</sub> in acidic melts of MEICl:AlCl<sub>3</sub>. However, the FeCl<sub>2</sub> formed was found to be very reversible.

## 5.0

## References

- 1: J.J.P. Stewart,  
Frank J. Seiler Research Laboratory (FJSRL),  
FJSRL-TR-88-0007.  
United States Air Force Academy, Colorado Springs  
CO 80840, U.S.A.
- 2: J.J.P. Stewart,  
J. of Computer-Aided Molecular Design, 4, 1 (1990).
- 3: J.S. Wilkes, C.L. Hussey,  
Selection of cations for ambient temperature chloroaluminate  
molten salts using MNDO molecular orbital calculations,  
Frank J. Seiler Research Laboratory (FJSRL-TR-82-0002),  
United States Air Force Academy, Colorado Springs  
CO 80840, U.S.A.
- 4: R.J. Gale, R.A. Osteryoung,  
Inorg. Chem., 18, 1603 (1979).
- 5: R.J. Gale, R.A. Osteryoung,  
J. Electrochem. Soc., 127, 2167 (1980).
- 6: K.M. Dieter, C.J. Dymek, Jr., S.W. Lander, H.A. Øye,  
J.W. Rovang, J.R. Stuff, J.S. Wilkes,  
J. Electrochem. Soc. Extended Abs. 87-1,  
Abs nr. 474, 681 (1987).
- 7: C.-L. Yu, J. Winnick and P.A. Kohl,  
J. Electrochem. Soc., 138, 339 (1991).
- 8: B. Vestergaard,  
Status report, October 28<sup>th</sup> (1990).  
The Technical University of Denmark,  
Chemistry Department A, Dk 2800 Lyngby.
- 9: J.S. Wilkes, J.S. Frye, G.F. Reynolds,  
Inorg. Chem. 22, 3870 (1983).
- 10: A.A. Fannin, Jr., L.A. King, J.A. Levisky, J.S. Wilkes,  
J. Phys. Chem. 88, 2609 (1984).
- 11: A.A. Fannin, Jr., D.A. Floreani, J.L. Williams, J.S. Landers,  
B.J. Piersma, D.J. Stech, R.L. Vaughn, J.S. Wilkes, L.A. King,  
J. Phys. Chem. 88, 2614 (1984).
- 12: C.J. Dymek, Jr., G.E. Godec,  
Viscosity and Conductance of  $\text{MEICl}/\text{AlCl}_3$  Melts  
Containing Nonaqueous Solvents.  
FJSRL-TR-88-0003 (May 1988).



- 13: C.J. Dymek, Jr., J.J.P. Stewart,  
Inorg. Chem. 28, 1472 (1989).
- 14: C.L. Hussey,  
'Advances in Molten salt Chemistry',  
Editors: G. Mamantov, C. Mamantov,  
Elsevier, NY, 5, 185 (1983).
- 15: J.J. Auborn, Y.L. Barberio,  
J. Electrochem. Soc., 132, 598 (1985).
- 16: K.M. Dieter, C.J. Dymek, Jr., S.W. Lander, H.A. Øye,  
J.W. Rovang, J.R. Stuff, J.S. Wilkes,  
Irreversibility of the aluminum electrode in  
basic room-temperature chloroaluminate molten salts.  
FJSRL-TR-87-0003 (June 1987).
- 17: G.F. Reynolds, C.J. Dymek, Jr.,  
J. Electrochem. Soc. Extended Abs. 85-2,  
Abs nr. 473, 705 (1985).
- 18: F.M. Donahue, L. Simonsen, R. Moy, S. Borns,  
Chemical and Electrochemical Properties of Potential  
Battery Systems in Room Temperature Molten Salts.  
AFOSR-TR-88-1256 (October 1988).
- 19: M.J.S. Dewar, W. Thiel,  
J. Am. Chem. Soc., 99, 4899 (1977).
- 20: R.C. Bingham, M.J.S. Dewar, D.H. Lo,  
J. Am. Chem. Soc., 97, 1294 (1975).
- 21: M.J.S. Dewar, E.G. Zoebisch, E.F. Healy, J.J.P. Stewart,  
J. Am. Chem. Soc., 107, 3902 (1985).
- 22: D.L. Beveridge, P.A. Dobosh,  
J. Chem. Phys., 47, 2026 (1967).
- 23: Norio Takami and Nobuyuki Koura,  
J. Electrochem. Soc., 136, 730 (1989).
- 24: P.R. Gifford and J.B. Palmisano,  
J. Electrochem. Soc., 135, 650 (1988).
- 25: Chenniah Nanjundiah, Kunio Shimizu and R.A. Osteryoung,  
J. Electrochem. Soc. 129, 2474 (1982).
- 26: C.L. Hussey, L.A. King, J.S. Wilkes,  
J. Electroanal. Chem. 102, 321 (1979).

- 27: Francis M. Donahue, S.E. Mancini, Leif Simonsen,  
J. Appl. Electrochem. 22, 230 (1992).
- 28: R.J. Bones, J. Coetzer, R.C. Galloway, D.A. Teagle,  
J. Electrochem. Soc. 134, 2379 (1987).
- 29: R.J. Bones, D.A. Teagle, S.D. Brooker, F.L. Cullen and  
J. Lumsdon,  
Proceedings of the Second Symposium on  
Electrode Materials and Processes for Energy  
Conversion and Storage, 12, 537 (1987).
- 30: J. Coetzer,  
6<sup>th</sup> International Conference on  
Solid State Ionics in Garmisch.  
Extended Abstracts A1-II, p 609 (1987).
- 31: Organic Syntheses, 51, 142.  
Editor: R.E. Benson, Wiley & Sons, NY (1971).
- 32: Morten Jentzsch Seeberg,  
Danish report (1991),  
'Synthesis of 1,4-dimethyl-tetrazolium chloride.  
The Technical University of Denmark,  
Chemistry Department A, Dk 2800 Lyngby.
- 33: Skoog, West and Holler,  
5th ed.  
Fundamental of Analytical chemistry.  
Saunders College Publishing, NY (1988).
- 34: M. Begtrup, P. Larsen,  
Acta Chem. Scan. 44, 1050 (1990).
- 35: Anne Marie Horneman,  
Danish Report (1991),  
'Synthesis of 1,4-dimethyl-1,2,4-triazolium chloride and  
1-ethyl-4-methyl-1,2,4-triazolium chloride'.  
The Technical University of Denmark,  
Chemistry Department A, Dk 2800 Lyngby.
- 36: Corning Labware and Scientific Equipment catalogue,  
Staffordshire, England (1981).
- 37: Handbook of Chemistry and Physics, 62 ed.
- 38: M. Begtrup, H.P. Nytoft,  
Acta Chem. Scand. 40, 262 (1986).
- 39: Professor M. Begtrup and F. Sløk,  
Private communication.

- 40: M. Begtrup,  
Bull. Soc. Chim. 97, 573 (1988).
- 41: K. Thomas Finley,  
Triazoles: 1,2,3.  
Wiley & Sons NY (1980).
- 42: Frank A. Sløk,  
Danish Report (1990),  
'Synthesis of 1,2-dimethyl-1,2,3-triazolium chloride'.  
The Technical University of Denmark,  
Chemistry Department A, Dk 2800 Lyngby.
- 43: M. Begtrup, J. Holm,  
J. Chem. Soc., Perkin Trans. 1, 503 (1981).
- 44: M. Begtrup, H.P. Nytoft,  
Acta Chem. Scand. 40, 262 (1986).
- 45: Tina M. Jespersen,  
Danish Report (1990),  
'Synthesis of Heterocyclic Quaternary Salts'.  
The Technical University of Denmark,  
Chemistry Department A, Dk 2800 Lyngby.
- 46: R.T. Morrison, R.N. Boyd,  
Organic Chemistry, 4.ed.  
Allyn and Bacon Inc., Massachusetts, p.760 (1983).
- 47: Claus Christophersen,  
Danish Report (1991),  
'Synthesis of 3-methyl-thiazolium chloride'.  
The Technical University of Denmark,  
Chemistry Department A, Dk 2800 Lyngby.
- 48: L. Brandsma, R.L.P. de Jong, H.D. Ver Kruijsse,  
Synthesis, No. 10, 948 (1985).  
ISSN: 0039-7881.
- 49: J.S. Wilkes, J.A. Levisky, R.A. Wilson, C.L. Hussey,  
Inorg. Chem. 21, 1263 (1982).
- 50: J.A. Boon, J.S. Wilkes, J.A. Lanning,  
A Fundamental Electrochemical Investigation of Bromoaluminate  
and Mixed Chloro-Bromoaluminate Room Temperature Molten  
Salt Systems.  
FJSRL-TR-89-0004 Report (March 1989).
- 51: J.S. Mihina, R.M. Herbst,  
J. Org. Chem. 15, 1082 (1950).

- 52: A.R. Katritzky, C.W. Rees,  
Comprehensive Heterocyclic Chemistry,  
The structure, Reactions, Synthesis, and Uses of  
Heterocyclic Compounds. 5, 818-828 (1984).  
Pergamon Press NY (1984).
- 53: R.W. Berg, N.J. Bjerrum, H.A. Hjuler,  
Inorg. Chem. 23, 557 (1984).
- 54: J.H. von Barner, N.J. Bjerrum,  
Inorg. Chem. 12, 1891 (1973).
- 55: G. Jones, B.C. Bradshaw,  
J. am. Chem. Soc. 55, 1780 (1933).
- 56: B. Vestergaard, N.J. Bjerrum, I. Petrushina, H.A. Hjuler,  
R.W. Berg, M. Begtrup,  
Molten Triazolium Chloride Systems as new Aluminum  
Battery Electrolytes (to be published).
- 57: R.W. Berg, S. von Winbush, N.J. Bjerrum,  
Inorg. Chem. 19, 2688 (1980).
- 58: B. Vestergaard,  
Danish report (1989),  
'Sodium Batteries'  
The Technical University of Denmark,  
Chemistry Department A, Dk 2800 Lyngby.
- 59: N.J. Bjerrum, J.E. Engell, J. Høj, H.A. Hjuler,  
Proceedings of the Seventh Australian Electrochemistry  
Conference, February 15<sup>th</sup>-19<sup>th</sup>, 73 (1988).
- 60: M.J.S. Dewar, H. Kollmar, S. Suck,  
Theoret. Chim. Acta, 36, 237 (1975).
- 61: F.A. Cotton and G. Wilkinson,  
Basic Inorganic Chemistry,  
Wiley & Sons, Singapore 1976.
- 62: B. Case, N.S. Hush, R. Parsons and M.E. Peover,  
J. Electroanal. Chem. 10, 360 (1965).
- 63: P.W. Atkins,  
Physical Chemistry, 2<sup>nd</sup>. ed.,  
Oxford University Press (1982).
- 64: B.J. Piersma, J.S. Wilkes,  
Electrochemical Survey of Selected Cations and  
Electrode Materials in Dialkylimidazolium  
Chloroaluminate Melts.  
FJSRL-TR-82-0004  
September 1982.

- 65: T.A. Riechel, J.S. Wilkes,  
J. Electrochem Soc. 139, 977 (1992).
- 66: M. Matsunaga, T. Miwa, Y. Inoue, K. Hosokawa,  
Materials Sciencs Forum, 70-75, 473 (1991).
- 67: R.A.Carpio, L.A.King, R.E.Lindstrøm, J.C.Nardi, C.L.Hussey.  
J. Electrochem. Soc. 138, 1644 (1979).
- 68: H.L. Jones, R.A. Osteryoung,  
J. Electroanal. Chem. 49, 281 (1974).
- 69: A.J. Calandra, N.R. de Tacconi, R. Pereiro, A.J. Arvia,  
Electrochim. Acta, 19, 901 (1974).
- 70: D. Tromans, R. Sun,  
J. Electrochem. Soc. 138, 3235 (1991).
- 71: H. Y-P Hong,  
Mat. Res. Bull. 11, 173 (1976).
- 72: J.W. Høj,  
'Fremstilling og karakterisering af Nasicon-keramik'  
The Technical University of Denmark,  
Institute of Mineral Industry (1988).
- 73: Y. Mizutani, W.Teshima, S. Akiyama, H. Ihara,  
U.S. patent 3.451.951 (1969).
- 74: S. Atlung, T. Jacobsen,  
'Elektrokemi',  
The Technical University of Denmark,  
Institute of Physical Chemistry (1986).
- 75: Torben Lapp,  
Solid State Ionic Conductors  
Ph.D dissertation,  
The Technical University of Denmark  
Physical Laboratory III, (1980).
- 76: F.A. Cotton and G. Wilkinson,  
Advanced Inorganic Chemistry, 5. ed.  
Wiley & Sons, New York (1988).
- 77: D.E. Paul, D. Lipkin, S.I. Weissman,  
J. Am. Chem. Soc. 78, 116 (1956).
- 78: F.J. Tehan, B.L. Barnett, J.L. Dye,  
J. Am. Chem. Soc. 96, 7203 (1974).

- 79: Torben S. Sørensen and Jørgen B. Jensen,  
'Lærebog i elektrokemi' (1983),  
The Technical University of Denmark  
Dk 2800 Lyngby.
- 80: C.L. Hussey, L.A. King, R.A. Carpio,  
J. Electrochem. Soc. 126, 1029 (1979).
- 81: C. Nanjundiah, R.A. Osteryoung,  
J. Electrochem. Soc. 130, 1312 (1983).
- 82: T.J. Melton, J.T. Maloy, J.S. Wilkes,  
175<sup>th</sup> Electrochem. Soc. Meet.  
Extended Abs. 589, 89-1 (1989).
- 83: B.J. Piersma, J.S. Wilkes,  
FJSRL-TR-86-0009.
- 84: D. Floreani, D. Stech, J. Wilkes, J. Williams, B. Piersma,  
L. King and R. Vaughn,  
Proceedings of the 30<sup>th</sup> Power Source Symposium,  
7-10 June, 1982 p.84.
- 85: P.A. Nelson,  
Proceedings of the 24<sup>th</sup> Intersociety Energy  
Conversion Engineering Conference,  
Vol 3, 1363 (1989).